

Université Mohamed Khider – Biskra
Faculté des Sciences et de la technologie
Département : Génie Electrique
Ref :



جامعة محمد خيضر بسكرة
كلية العلوم و التكنولوجيا
قسم: الهندسة الكهربائية
المرجع:

Thèse présentée en vue de l'obtention
Du diplôme de
Doctorat en sciences en : Electrotechnique

Spécialité (Option) : Electrotechnique

Intitulé

**Modélisation D'un Isolateur Dans Les Conditions De
Pollution Sous Tension Alternative 50Hz.**

Présentée par :

Hani BENGUESMIA

Soutenue publiquement le : 11/10/2018

Devant le jury composé de :

Dr. ZOUZOU Salah Eddine	Professeur	Président	Université de Biskra
Dr. M'ZIOU Nassima	Professeur	Rapporteur	Université de Boumerdès
Dr. BOUBAKEUR Ahmed	Professeur	Co-rapporteur	ENP, Alger
Dr. MOKHNACHE Leïla	Professeur	Examineur	Université de Batna 2
Dr. MEGHERBI Ahmed Chouaki	Maitre de Conférences 'A'	Examineur	Université de Biskra
Dr. MAHDAD Belkacem	Maitre de Conférences 'A'	Examineur	Université de Biskra

Université Mohamed Khider – Biskra
Faculté des Sciences et de la technologie
Département : Génie Electrique
Ref :



جامعة محمد خيضر بسكرة
كلية العلوم و التكنولوجيا
قسم: الهندسة الكهربائية
المرجع:

Thèse présentée en vue de l'obtention
Du diplôme de
Doctorat en sciences en : Electrotechnique

Spécialité (Option) : Electrotechnique

Intitulé

**Modélisation D'un Isolateur Dans Les Conditions De
Pollution Sous Tension Alternative 50Hz.**

Présentée par :

Hani BENGUESMIA

Soutenue publiquement le : 11/10/2018

Devant le jury composé de :

Dr. ZOUZOU Salah Eddine	Professeur	Président	Université de Biskra
Dr. M'ZIOU Nassima	Professeur	Rapporteur	Université de Boumerdès
Dr. BOUBAKEUR Ahmed	Professeur	Co-rapporteur	ENP, Alger
Dr. MOKHNACHE Leïla	Professeur	Examineur	Université de Batna 2
Dr. MEGHERBI Ahmed Chouaki	Maitre de Conférences 'A'	Examineur	Université de Biskra
Dr. MAHDAD Belkacem	Maitre de Conférences 'A'	Examineur	Université de Biskra

University Mohamed Khider - Biskra -

Faculty of Sciences and Technology

Department of Electrical Engineering

Ref :.....



جامعة محمد خيضر - بسكرة -

كلية العلوم و التكنولوجيا

قسم الهندسة الكهربائية

المرجع:.....

A thesis submitted for the fulfillement of
the degree of
Doctorate in science: Electrical Engineering

Specialty (Option): Electrical Engineering

Entitled

**Modeling an Insulator Under Pollution Conditions
Under Alternative Voltage 50 Hz.**

Presented by:

Hani BENGUESMIA

Defended on: 11/10/2018

In front of the jury composed of:

Dr. ZOUZOU Salah Eddine	Professor	President	University of Biskra
Dr. M'ZIOU Nassima	Professor	Supervisor	University of Boumerdes
Dr. BOUBAKEUR Ahmed	Professor	Co-supervisor	ENP, Algiers
Dr. MOKHNACHE Leïla	Professor	Examiner	University of Batna 2
Dr. MEGHERBI Ahmed Chouaki	Associate Professor 'A'	Examiner	University of Biskra
Dr. MAHDAD Belkacem	Associate Professor 'A'	Examiner	University of Biskra

Dedication

From the deepest of my heart, I devote this work

To my father, for his support and his love,

To my mother, for her support and her love,

*To my future lovely wife, for her perpetual
encouragement,*

*For the uninterrupted encouragements and the great
love they gave me,*

*That God reserves for them long happy life and good
health.*

*To all my friends, their names are beyond the capacity
to be cited in a page, for their fraternities and their
continuous support.*

They will be filled with happiness and joy.

Acknowledgement

In the first place, we thank God Allah, who gave us the courage, patience, strength and serenity and the will to do this modest work during all these years of study .

The success of any project depends largely on the encouragement and guidelines of many others. We take this opportunity to express our gratitude to the people who have been instrumental in the successful completion of this project.

*In the second place, we would like to show our greatest appreciation to my supervisor **Pr. Nassima M'ziou** Professor at the University of Boumerdes, and **Pr. Ahmed Boubakeur** ,^ض Professor at the National Polytechnic School of Algiers (ENP). We can't say thank you enough for his tremendous support and help. We feel motivated and encouraged every time we attend his meeting. Without her encouragement and guidance this PhD theses would not be materialized.*

*I would like to thank the president of the jury, **Mr. Salah Eddine Zouzou**, Professor at the University of Biskra, and the members of the jury: **Mr. Ahmed Chouaki Megherbi**, Associate Professor at the University of Biskra, **Mr. Belkacem Mehdad**, Associate Professor at the University of Biskra and **Mrs. Leïla Mokhnache**, Professor at the University of Batna2, for having participated in the jury and for taking the time to examine my thesis.*

*Finally, I thank all those who contributed directly or indirectly to the development of this work especially **Mr. Zied Driss**, Professor at the University of sfax (ENIS), **Mrs. Habiba Dahmani**, Associate Professor at the University of M'sila and **Mr. Yacine Bourek**, Associate Professor at the University of ouargla.*

تَوْطَى

إني رأيت أنه لا يكتب إنسان كتابا في يومه

إلا قال في غده
لو زيد هذا لكان أحسن.
ولو قدم هذا لكان أفضل.
ولو ترك هذا لكان أجمل.

و هذا من أعظم العبر وهو دليل على
ض إستلاء النقص على جملة البشر.

إبن خلدون

ملخص

تتعرض خطوط النقل وتوزيع الطاقة الكهربائية (الهوائية) لمضادات مختلفة. من بين هذه، تلوث العوازل. وجود التلوث يسبب تدهور الخصائص الكهربائية لعوازل خطوط النقل، ويشجع على ظهور قوس الإحاطة. وقد تم هذا العمل في هذا السياق، يتم دراسة سلوك النموذج الحقيقي والتجريبي للعازل. أولاً دراسة تأثير الموصلية (الناقلية) وتوزيع التلوث على سلوك العازل ذي قبعة و دبوس، الملوث اصطناعياً. بالإضافة إلى ذلك، يتم دراسة تأثير التلوث على جهد توتر الإحاطة، تيار التسرب و فرق الطور بين الجهد المطبق و التيار. وأخيراً، يتم دراسة سلوك النموذج الحقيقي والتجريبي للعازل. تظهر النتائج التي تم الحصول عليها أن وجود طبقة التلوث على سطح العازل، يغير تماماً من سلوك العازل ذو الجهد العالي.

في الخطوة الثانية، اقترحنا مفهومًا جديدًا للمحاكاة الرقمية يعتمد على المنطق الغامض والشبكات العصبية كتنقيتين للذكاء الاصطناعي للتنبؤ بالتوتر الإحاطي للعازل، حيث يتم إخضاع العازل لتوتر متناوب 50 هرتز. أظهرت النتائج التي تم الحصول عليها القدرة، الكفاءة والسهولة في استخدام المنطق الغامض والشبكات العصبية الاصطناعية في مثل هذه الدراسات.

في الخطوة الأخيرة، التنبؤ بأداء العازل الحقيقي تحت التلوث. للقيام بذلك، يتم دراسة توزيع الجهد والحقل الكهربائي على طول عازل الجهد العالي باستخدام طريقة العناصر المتناهية. النتائج المتحصل عليها جيدة وواعدة.

الكلمات المفتاحية:عازل ذي قبعة و دبوس، نموذج دائري، توتر الإحاطة، تيار التسرب، التلوث الغير المستمر، جهد عالي، ذكاء اصطناعي، محاكاة، تنبؤ، جهد كهربائي، مجال كهربائي، طريقه العناصر المتناهية.

Résumé

Les lignes aériennes de transport et de distribution d'énergie électrique sont exposées à diverses contraintes. Parmi celles-ci, la pollution des isolateurs. La présence de pollution entraîne la dégradation des propriétés électriques de l'isolateur des lignes de transport, et favorise l'apparition de l'arc de contournement.

Ce travail a été réalisé dans ce cadre, dans un premier temps, nous examinons l'impact de la conductivité ainsi que la répartition de la pollution sur le comportement de l'isolateur capot et tige 1512L, artificiellement pollué. De plus, l'influence de la pollution sur la tension de contournement, le courant de fuite ainsi que le déphasage (tension-courant) sont étudiés. Enfin, le comportement du modèle réel et expérimental de l'isolant est étudié. Les résultats obtenus montrent que la présence d'une couche de pollution sur la surface d'un isolateur modifie complètement le comportement de l'isolateur de haute tension.

Dans un second temps, nous avons proposé un nouveau concept de simulation numérique basé sur la logique floue et les réseaux de neurones artificiels comme deux techniques d'intelligence artificielle pour prédire la tension de contournement, où l'isolateur est soumis à une tension Alternative 50Hz. Les résultats obtenus ont montré la capacité et la facilité d'utiliser la logique floue et les réseaux de neurones artificiels dans de telles études.

Dans la dernière étape, la prédiction des performances de l'isolateur réel sous pollution. Pour ce faire, la distribution du potentiel et du champ électrique le long de l'isolateur de haute tension est étudiée à l'aide d'une méthode numérique. Les résultats sont favorables et prometteurs.

Mot clé : Isolateur 1512L, Modèle circulaire, contournement, courant de fuite, pollution discontinue, haute tension, Intelligences artificielles (LF, RNA), Prédiction, Simulation, potentiel électrique, champ électrique, MEF.

Abstract

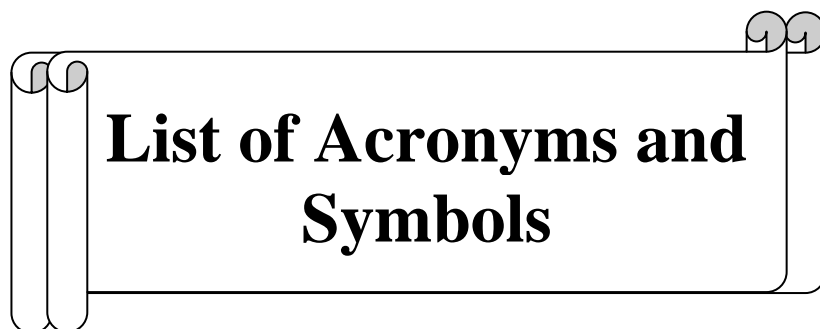
Overhead power transmission and distribution lines are exposed to various constraints. Among these, the pollution of insulators. The presence of pollution causes degradation of the electrical properties of the insulator of the transmission lines, and promotes the appearance of the flashover arc.

This work was done in this context; the behavior of the real and experimental model of the insulation is studied. First we examine the impact of conductivity and the distribution of pollution on the behavior of the cap and pin insulator, artificially polluted. In addition, the influence of pollution on the flashover voltage, the leakage current and the angle phase (voltage-current) are studied. The results obtained show that the presence of a pollution layer on the surface of an insulator completely modifies the behavior of the high voltage insulator.

In a second step, we proposed a new concept of numerical simulation based on fuzzy logic and artificial neural networks as two techniques of artificial intelligence to predict the flashover voltage, where the insulator is subjected to AC voltage (50 Hz). The obtained results have shown the ability and ease of use of fuzzy logic and artificial neural networks in such studies.

In the last step, the prediction of the performance of the actual insulator under pollution has been presented. To do this, the distribution of the potential and the electric field along the high voltage insulator is studied using a numerical method. The results are auspicious and promising.

Keyword: Isolator1512L, Circular model, flashover, leakage current, discontinuous pollution, high voltage, Artificial Intelligences (FL, ANN), Prediction, Simulation, electric potential, electric field, MEF.

A decorative graphic of a scroll with a black outline and a light gray shadow. The scroll is unrolled in the center, with the ends of the scroll visible on the left and right sides. The text is centered within the unrolled portion.

**List of Acronyms and
Symbols**

List of Acronyms and Symbols

AC	Alternative current
DC	Direct current
AI	Artificial intelligence
ANN	Artificial Neural Networks
FL	Fuzzy Logic
1512L	Type cap and pin insulator
CSM	Charge Simulation Method
FDM	Finite Difference Method
BEM	Boundary Element Method
FEM	Finite Element Method
2D	Two dimensions
FEMM	Finite Element Magnetism Method
Hz	Hertz

Chapter I

LC	Leakage current (mA)
1512L	Insulator profile
NaCl	Sodium chloride
AC	Alternative current
e	Thickness (mm)
r_i	Radius (mm)
Z_i	Polluted area (zones)
L_i	Level of pollution
P_i	Polluted area (mm)
C_i	Cleaned area (mm)
V	Volts
L_i	Level of pollution (ml)
HV	High voltage
mS	Milli-siemens
mm	Millimeter
cm	Centimeter
kV	Kilovolts
kVA	Kilovolt-amperes
CH1	Channel 01
CH2	Channel 02
I.T	Isolating transformer
T.O	Test object (insulator 1512L)
R.T	Regulating transformer
H.T	High voltage transformer
V.C	Video, Camera
C_m	A capacitive for measuring the applied tension

Chapter II

AI	Artificial Intelligence
FL	Fuzzy Logic
1512 L	Real high voltage insulator model

A	The fuzzy set
X	Point space (universe)
x	Generating element
$\mu_A(x)$	Function
FLC	Fuzzy Logic Controller
FIS	Fuzzy Inference System
V	Flashover Voltage (kV)
δ	Conductivities (mS/cm)
Z_i ($Z_1, Z_2,$ Z_3, Z_4)	Pollution zones (ml)
L_i ($L_1, L_2,$ $L_3, L_4, L_5,$ L_6, L_7, L_8)	Level of pollution
V_cal	Calculated voltage (predict)(kV)
V_exp	Experimental voltage (Flashover Voltage) (kV)
Error	Absolute error (kV)
Error	Error (%)

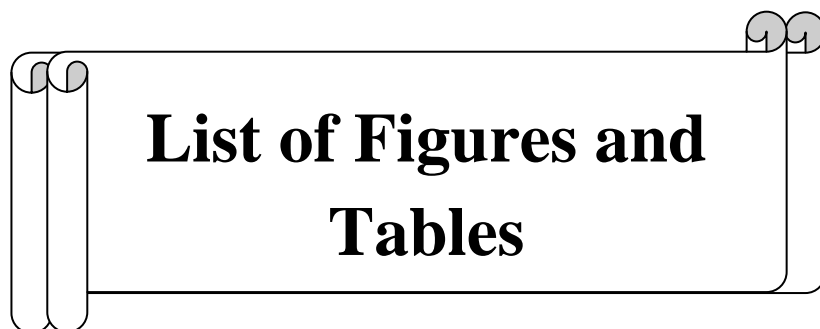
Chapter III

ANN	Artificial Neural Network
In_i	i^{th} input of the neuron
w_i	Weight of connections with the inputs
s	The output of the neuron
i and j	Neurons
NNTOOL	Neural network tool
MSE	The mean squared error
J	The jacobian matrix
Δw	The adaptation rate of the network weight matrix
μ	An adaptive coefficient
e	The error vector
$e_k(n)$	The learning error
$\frac{1}{2} e_k^2$	Quadratic error value
$\xi(n)$	The squared sum of the instantaneous
$MSE(n)$	The sum of the quadratic error
N	The number of examples representing the learning base

Chapter IV

PDEs	Partial differential equations
1512L	Insulator profile
2D	Two-dimensional
AC	Alternative Current
BEM	Boundary Element Method
CSM	Charge Simulation Method
cm	Centimeter
DC	Direct Current
D	The normal component of the electric induction (C/m^2) \Leftrightarrow ($A.s/m^2$) Electric Flux Density

<i>div</i>	Divergence
<i>E</i>	Electric field (V/cm) the magnitude of Electric Field Intensity
EFVD	Electric Field and Voltage (Potential) Distribution
FDM	Finite Difference Method
FEM	Finite Element Method
FEMM	Finite Element Magnetism Method
<i>grad</i>	Gradient
HV	High Voltage
<i>j</i>	Current density (A/m ²)
kV	Kilovolts
mm	Millimeter
V	Volts
<i>V</i>	Electric potential (V)
μS	Micro-siemens
ϵ	Permittivity
ϵ_r	Relative Permittivitie
ϵ_0	The constant dielectric of the air (F/m)
ρ	Charge density
σ	Electrical conductivities
R	Radius (cm).
$x_{1,2,3,4}$	Width of the ribs

A decorative graphic of a scroll with a black outline and a light gray shadow. The scroll is unrolled in the center, with the ends of the scroll visible on the left and right sides. The text is centered within the unrolled portion.

**List of Figures and
Tables**

List of Figures and Tables

N°	Figures Chapter I	Page
Fig. I.1	1512L insulator profile	8
Fig. I.2	Cap and pin1512L insulator dimension (Table 1)	8
Fig. I.3	1512L Proposed model	8
Fig. I.4	Distribution of polluted zones on the 1512L high voltage insulator	9
Fig. I.5	Determination of different levels of pollution for 1512L insulator	10
Fig. I.6	Experimental model verses real model of 1512L insulator	11
Fig. I.7	Determination of clean and polluted area insulator (Tab I.2)	12
Fig. I.8	Test circuit. (a) Real model, (b) Experimental model	13
Fig. I.9	Schematic diagram of the experimental setup	13
Fig. I.10	Flashover process observed in laboratory for 1512L polluted insulator (a)Initialization of the arc; (b) evolution of the arc; (c) total flashover	14
Fig. I.11	Flashover process observed in laboratory for experimental model polluted insulator (a) Initialization of the arc; (b) evolution of the arc; (c) total flashover	15
Fig. I.12	Flashover voltage-level of pollution for different conductivities(δ)	16
Fig. I.13	Flashover voltage-conductivity for different levels of pollution(L_i)	16
Fig. I.14	Visualizations of leakage current waves for applied voltage 10kV.	17
Fig. I.15	Leakage current-level of pollution for different conductivities for an applied voltage of 5kV	18
Fig. I.16	Leakage current-level of pollution for different conductivities for an applied voltage of 10kV	18
Fig. I.17	Leakage current-level of pollution for different conductivities for an applied voltage of 15kV	18
Fig. I.18	Leakage current-level of pollution for different conductivities for an applied voltage of 20kV	19
Fig. I.19	Leakage current-level of pollution for different conductivities for an applied voltage of 25kV	19
Fig. I.20	Leakage current-conductivity for various applied voltages for level L_1 of pollution (Table 2)	21
Fig. I.21	Leakage current-conductivity for various applied voltages for level L_2 of pollution (Table 2)	21
Fig. I.22	Leakage current-conductivity for various applied voltages for level L_3 of pollution (Table 2)	21
Fig. I.23	Leakage current-conductivity for various applied voltages for level L_4 of pollution (Table 2)	22
Fig. I.24	Leakage current-conductivity for various applied voltages for level L_5 of pollution (Table 2)	22
Fig. I.25	Leakage current-conductivity for various applied voltages for level L_6 of pollution (Table 2)	22
Fig. I.26	Leakage current-conductivity for various applied voltages for level L_7 of pollution (Table 2)	23

Fig. I.27	Leakage current-conductivity for various applied voltages for level L_8 of pollution (Table 2)	23
Fig. I.28	Leakage current- applied voltage for various level of pollution 1.823 mS/cm (Table I.1)	24
Fig. I.29	Leakage current- applied voltage for various level of pollution 3.33 mS/cm (Table I.1)	24
Fig. I.30	Leakage current- applied voltage for various level of pollution 8.02 mS/cm (Table I.1)	24
Fig. I.31	Leakage current- applied voltage for various level of pollution 12.61 mS/cm (Table I.1)	25
Fig. I.32	Leakage current- applied voltage for various level of pollution 16.32 mS/cm (Table I.1)	25
Fig. I.33	Leakage current- applied voltage for various level of pollution 30.50 mS/cm (Table I.1)	25
Fig. I.34	Leakage current- applied voltage for various level of pollution 50.4 mS/cm (Table I.1)	26
Fig. I.35	Leakage current- applied voltage for various level of pollution 93.7 mS/cm (Table I.1)	26
Fig. I.36	Displays of the angle phase for different values of the applied voltage	27
Fig. I.37	Angle phase -applied voltage for different conductivities, $L_5 = Cste$	28
Fig. I.38	Angle phase -level of pollution, for different conductivities, $5kV = Cste$	28

N°	Chapter II	Page
Fig. II.1	Linguistic variable	34
Fig. II.2	General structure of a system based on fuzzy logic (FL)	37
Fig. II.3	Architecture of a fuzzy inference system (FIS) studied	39
Fig. II.4	Membership function of the output (V)	41
Fig. II.5	Membership function of the conductivities (δ)	41
Fig. II.6	Membership function of zone 1 (Z1)	41
Fig. II.7	Membership function of zone 2 (Z2)	41
Fig. II.8	Membership function of zone 3 (Z3)	41
Fig. II.9	Membership function of zone 4 (Z4)	41
Fig.II.10	Principal window of fuzzy inference system "FIS Editor" under MATLAB	47
Fig. II.11	Inputs and output under the interface FIS a,b,c,d: Inputs, e: Output	48
Fig. II.12	Window for visualization fuzzy rules	49
Fig. II.13	Window for visualization fuzzy rules (a) 25 Rules, (b) 135 Rules	50

N°	Chapter III	Page
Fig. III.1	Structure of a neuron network	56
Fig. III.2	General diagram of an artificial neuron	57
Fig. III.3	General architecture of a neuron network	59
Fig. III.4	Perceptron monolayer type of network: Structure	60
Fig. III.5	Multi-layer perceptron network: Structure	60

Fig. III.6	Structure of our neural network	64
Fig. III.7	Graphical interface "nntool"	65
Fig. III.8	Data import window	66
Fig. III.9	Network creation window	69
Fig.III.10	Neural network used for the experiment	69
Fig. III.11	Design flowchart of a neural network	70
Fig. III.12	Learning window and network simulation	71
Fig. III.13	Window of the train network in the case: (a) two hidden layers and two neurons per layer with a thousand iteration number, (b) two hidden layers and six neurons per layer with a thousand iteration number.	73
Fig. III.14	Regression curves	75

N°	Chapter IV	Page
Fig. IV.1	Basic structure of the software Comsol multiphysics	81
Fig. IV.2	Parameters of cap and pin insulator 1512L	83
Fig. IV.3	FEM model in the software of 220kV insulator (a) Clean model, (b) Discontinuous uniformly polluted model	83
Fig. IV.4	Resolution Steps in COMSOL	85
Fig. IV.5	Discretization in finite elements and determination of mesh elements of the insulator 1512L.Multiphysics	86
Fig. IV.6	Potential distribution and equipotential lines (clean model)	88
Fig. IV.7	Electrical potential distribution for different conductivities	88
Fig. IV.8	Electric potential-leakage distance for different conductivities	89
Fig. IV.9	Electrical potential distribution for different applied voltage of the line	90
Fig. IV.10	Electric potential-leakage distance for different applied voltage of the line.	91
Fig.IV.11	Electrical (electric) field distribution for a clean model	92
Fig. IV.12	Electric field-leakage distance for different conductivities	92
Fig. IV.13	Electric field distribution for different conductivities	93
Fig. IV.14	Electric field-leakage distance for different applied voltage (a)Simple scale (b) Logarithmic scale	94
Fig. IV.15	Electric field distribution for different applied voltage	95
Fig. IV.16	Dimensioning of the ribs of the insulator 1512L, (a)Real Model, (b) Model_02, (c) Model_01	96
Fig. IV.17	Electric field-leakage distance for three studied cases (real model, model_01, model_02). (a)Simple scale, (b)Logarithmic scale	97
Fig. IV.18	Insulator destroyed for two cases, (a) Real model, (b) Broken ribs x _{1,2,3,4} (c) Partially broken (the two internal ribs x _{2,3})	98
Fig. IV.19	Electric field-leakage distance for three studied cases (real model, broken ribs, partial broken ribs). (a)Simple scale, (b)Logarithmic scale	99

N°	Tables	Page
Chapter I		
Tab. I.1	Dimension of 1512L.	9
Tab. I.2	Dimensions of polluted area and clean area for experimental	9
Chapter II		
Tab. II.1	Principal membership functions.	33
Tab. II.2	Variable of inputs and output.	40
Tab. II.3	Decomposition of input and output variables.	40
Tab. II.4	Inference matrix	43
Tab. II.5	Number of fuzzy intervals, number and type of membership function of the inputs and the output.	45
Tab. II.6	Results of tests conducted in the laboratory vs calculated (predicted) our proposed model using FIS.	52-53
Tab. II.7	Error results upper than 10%.	53
Chapter III		
Tab. III.1	ANN activation function. [7]	58
Tab. III.2	Characteristic of the established neuron network.	68
Tab. III.3	Different ANN parameters tested to optimize the number of hidden layers, neurons per layer so the number of iterations.	71
Tab. III.4	Choice of neuron number per hidden layer.	72
Tab. III.5	Choice of hidden layer number.	72
Tab. III.6	Choice of the number of iteration.	73
Tab. III.7	Final parameter of the ANN structure.	73
Tab. III.8	Demonstration of the value of "R" of each curve.	75
Tab. III.9	Experimental (practical) data collected and prediction results by "ANN" and "FL".	77
Chapter IV		
Tab. IV.1	Geometrical parameter of cap and pin 1512L insulator	83
Tab. IV.2	Material properties of FEM model of cap and pin 1512L.	84
Tab. IV.3	Characteristic of the meshing	87
Tab. IV.4	Sizing of proposed HV insulator.	96

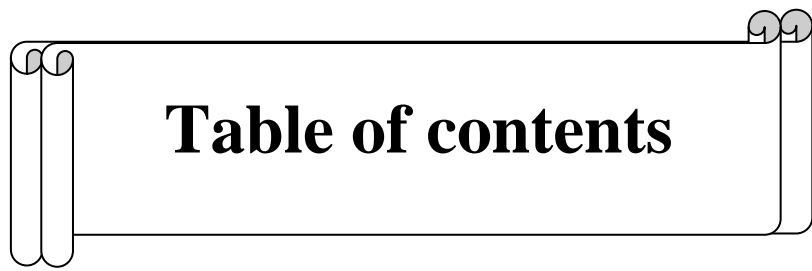
A decorative border resembling a scroll, with a central rectangular area containing the text. The border has rounded corners and a slight shadow effect.

Table of contents

Table of contents

List of Acronyms and Symbols	i
List of Figures and Tables	iv
Table of contents	viii
General introduction	1
Chapter I: Experimental Study	
I.1. Introduction	7
I.2. General description of real and experimental model	7
I.3. Experimental study	10
I.3.1. Flashover process	10
I.3.1.1. Laboratory observations	12
I.3.1.2. Effect of pollution on the flashover voltage	15
I.3.1.3. Effect of pollution severity on the flashover voltage	16
I.3.2. Leakage current	17
I.3.3. Angle phase (Leakage current_Applied voltage)	26
I.4. Conclusion	28
Chapter II: Prediction of Flashover Voltage Using Fuzzy Logic (FL)	
II.1. Introduction	30
II.2. Fuzzy Logic (FL)	30
II.3. Fuzzy logic vs. classical logic	31
II.4. Basic concept of fuzzy sets	32
II.4.1. The membership functions	32
II.4.2. Reasoning in Fuzzy Logic	33
II.5. The Fuzzy logic controller	34
II.5.1. The linguistic variables	34
II.5.2. Fuzzification	34
II.5.3. Fuzzy rules	35
II.5.4. Fuzzy inference	35
II.5.4.1. Mamdani's fuzzy inference	35
II.5.4.2. Takagi-Sugeno-Kang's fuzzy inference	36
II.5.5. Defuzzification	36

II.5.6. The fuzzy knowledge base	37
II.5.7. Diagram of the fuzzy control	37
II.6. Prediction of flashover voltage using Artificial Intelligence (AI)	38
II.6.1. Prediction of the flashover voltage by the Fuzzy Logic (FL)	39
II.6.1.1. The inputs and outputs of the SIF (Fuzzy Inference System)	40
II.6.1.2. The fuzzy characteristics	40
II.6.1.3. The membership functions of the input and output variables	42
II.6.1.4. The fuzzy inference rules	42
II.6.1.5. Fuzzification	44
a. The linguistic variable and the fuzzy interval	45
b. The membership function	45
II.6.2. The fuzzy rules	45
II.6.3. Implementation of the fuzzy inference system	46
II.6.3.1. Implementation of the Fuzzy Inference System "FIS" under MATLAB	47
a. Fuzzification of the input and output variables	48
b. Inference rules	49
c. Defuzzification	49
II.6.3.2. Tests and validation	51
II.7. Conclusion	54

Chapter III: Prediction of Flashover Voltage Using the Artificial Neural Network (ANN)

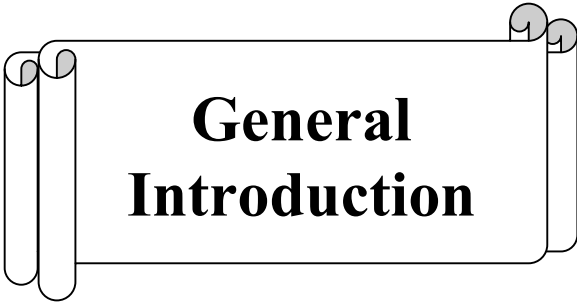
III.1. Introduction	55
III.2. Artificial neural networks	55
III.2.1. Mathematical model of a "Formal" or an "Artificial" neuron	57
III.2.2. Characteristics of the ANN	58
III.2.2.1. The input layer	58
III.2.2.2. The hidden layer	58
III.2.2.3. The output layer	59
III.2.3. Feed-Forward propagation networks	59
III.2.3.1. Mono-layer perceptron	59
III.2.3.2. Multi-layer Perceptron	60
III.2.4. Learning	61
III.2.4.1. Supervised learning	61

III.2.4.2. Strengthening (The reinforcement)	61
III.2.4.3. Unsupervised (or self-organizing) mode	61
III.2.4.4. Hybrid mode	61
III.2.5. Learning rules	61
III.2.5.1. Error correction rule	62
III.2.5.2. Boltzmann learning	62
III.2.5.3. The Hebbian theory	62
III.2.5.4. Competitive learning rule	62
III.3. The back-propagation algorithm	62
III.4. Validation	63
III.5. The strategy followed in this work	63
III.5.1. Step of neural network design	64
III.5.1.1. Determination of the neural network inputs/outputs	64
III.5.1.2. Elaboration of the network structure	64
III.5.1.3. Network Learning	64
III.5.1.4. Test and validation	65
III.5.2. Implementation and simulation	65
III.5.2.1. Software presentation	65
III.5.2.2. Data normalization	66
III.5.2.3. Data creation	66
III.5.2.4. Performance function	66
III.5.2.5. Levenberg–Marquardt algorithm	67
III.5.2.6. Mean Squared Error (MSE)	67
III.5.3. Application of the ANN in the prediction of the flashover voltage	68
III.5.3.1. Neuron network model (Structure of the elaborated ANN)	68
III.5.3.2. Creation of the network	69
III.5.3.3. Determination of the number of hidden layers, number of neurons per hidden layer and number of iteration	70
III.5.3.4. Implementation of the network	71
III.5.3.5. Choice of the number of neurons per hidden layer/ number of hidden layer and number of iterations	72

III.5.3.6. Result of the number of number of neurons per hidden layer, hidden layer and that of iterations	73
III.5.3.7. Network performance	74
III.5.3.8. Results and comparison "ANN" & "FL	76
III.6. Discussion of the results obtained	78
III.7. Conclusion	78

Chapter IV: Numerical Simulation

IV.1. Introduction	80
IV.2. Modeling on the comsol software	81
IV.3. Method of the simulation	82
IV.4. Mathematical Model	84
IV.5. Results and Discussion	86
IV.5.1. Electric potential distribution	87
IV.5.1.1. Influence of the conductivities	87
IV.5.1.2. Influence of the applied voltage of the line	89
IV.5.2. Electric field distribution	91
IV.5.2.1. Influence of the conductivities	92
IV.5.2.2. Influence of the applied voltage of the line	94
IV.5.3. Influence of the rib width of the insulator	95
IV.5.4. Performance of a destroyed insulator	98
IV.6. Conclusion	99
General Conclusion	101
References	105



**General
Introduction**

General Introduction

The transport and the reliability of the electric power delivery networks used by an insulator string which provides the function of insulation. So, transmission lines used in electric power delivery are subject to various constraints; such as insulator pollutions, which is of prime interest regarding power quality issues. [1-2]

Insulator pollution phenomena are considered as a continuous or intermittent accumulation of impurities coming from various sources. This can resulting from a cloud of smokes to industrial and urban pollution [3], small particles of salt in coast regions (marine pollution) [4-5] or fine particles coming from sandstorm in the desert regions. [6-7]

The investigation of pollution insulator illuminates the reader on how far relevant concepts have been researched and what particular fields and topics need further investigation and study. Lots of researchers and engineers have done some great work to investigate the mechanisms involved in contamination flashover [8].

The modeling of polluted insulator flashover started from a mathematical pollution flashover model put forward by Obneuas [9], In 1958, is proposed an electric circuit model of a partial arc in series with a residual resistance to represent the wet, polluted surface of an insulator [9]. Based on this model, many researchers improved and developed the pollution flashover model under various conditions, and built up both static and dynamic models [10-13].

Several researchers have worked to make useful contributions to this subject and have been summarized in [10].

Such particles, often made up by a combination of several kinds of pollution (mixed pollution) [14-15], brought by the wind and accumulated on the insulator for a long time may cause a number of malfunctions in the presence of high humidity.

Actually, the accumulated pollution causes a remarkable and a persistent leakage current in the insulator, depending on the severity of the pollution in the considered site. In such situation, flashover will occur, when critical leakage current as reached [16], and then transmission line will be broken.

Site comments have shown that the accumulated pollution made of sand layers on the cap and pin insulator, are concentrated on the most protected parts against self-cleaning factors. The discontinuous distribution of the accumulated pollution depends mainly on the insulator profile,

wind direction, sandstorms, rain fall rating and the location of insulator chains and the relative distance to the ground.

Several experimental and theoretical studies have investigated DC and AC models where outdoor and laboratory tests for different voltage shapes (forms) (DC, AC, and impulse voltage [17-19]) have been carried out in order to assess their effectiveness. In fact, most of the research studies have been devoted to highlight the flashover mechanism taking place in insulators under pollution and to study the main parameters that govern flashover voltage such as the degree of the agent on the polluted surface [20], chemical constitution of polluted layer covering the insulator[21], and its width, ...etc [22]. Good theoretical and experimental models for calculating the flashover voltage are valuable as they can permit engineers to make reasonable predictions over a wide range of operating conditions, insulator shapes and materials, thereby enhancing the value of information obtained from laboratory tests and field experience [23].

Practical tests, under natural pollution, have the advantage for accounting of all constrains with their related complexity, in a given site. The main disadvantage of this natural test is the required number of years to assess the behavior of the tested insulator. Hence, artificial reproduction in a laboratory test of natural pollution conditions, has attracted many researchers in different laboratories in order to get results and carry out fast comparisons, in a easy way and cost effective rather than in outdoor tests.

The aim is the evaluation of the behavior of a high voltage insulator (real and model) such as the flashover voltage, leakage current and the phase angle (between applied voltage-leakage current) for different surface conductivity. The experimental results of our laboratory will be presented and compared under AC voltage.

In recent years, Artificial Intelligence (AI) methods such as Artificial Neural Networks (ANN) [24-25] and Fuzzy Logic (FL) [26] have been used in high voltage applications, such as prediction for flashover voltage.

The use of (AI) in the study of insulators flashover can provide simplicity in prediction of the flashover voltage for different insulators types. These techniques can be classified into four groups: techniques based on neuronal networks, fuzzy logic, genetic algorithms and expert systems [27-36]. Among the existing artificial intelligence techniques, we have applied the fuzzy logic (FL) and artificial neuronal networks (ANN) techniques to predict insulator flashover voltage.

Several models and techniques are used to improve the understanding insulator flashover phenomenon. Among these models and techniques, we have interested to use fuzzy logic (FL) and artificial neuronal networks (ANN) as two artificial techniques to study polluted insulators flashover. Some authors have already applied these two techniques in similar area of research. [35-37, 27].

Neural network and fuzzy logic algorithms and their hybridization have been successfully used in insulator flashover studies. The application of these two techniques requires a collection of database numerically or practically. The consideration of diverse types of inputs/outputs in the FL and ANN applications can lead to different and new studies of insulator flashover. In cited works [25,29,35-38].and others works, the ANN and FL are used for studding insulator flashover considering different parameters as leakage current, acoustics signal, different insulator parameters and pollution characteristic...etc., which gives an originality to each work carried using artificial intelligence technique.

The use of FL and ANN for prediction of flashover voltage of high voltage insulator remains one of subjects rarely studied. Most authors used in their published works the leakage current as the most important parameters for studding insulator flashover phenomenon. In our work we considered other parameters different from those used in cited works. We have considered the high applied voltage, artificial pollution conductivity and artificial pollution quantity in insulator as essential parameters influencing insulator flashover.

In our study we used this technique to predict insulator flashover voltage which gives another advantage to our study. The determination of internal parameters of FL and ANN for our application is an essential step during their implementation. The utilization of MATLAB interface graphic can help to determinate their parameters as we have explained during our study.

In this part, we propose a new concept for the prediction of flashover voltage of outdoor insulator of type cap and pin insulator (1512L) largely used by the Algerian company of electricity and gas (SONELGAZ).

The flashover effects in insulators can cause the breakdown of a transmission system. Furthermore, the knowledge of the electric field is helpful for the detection of defects in insulators. Recently, the electrical (electric) field and potential distribution can be estimated using various numerical techniques, such as Charge Simulation Method (CSM), Finite Difference Method (FDM), Boundary Element Method (BEM) and Finite Element Method (FEM).

A numerical simulation is an approach that gives researchers the possibility to analyze the behavior of several phenomena which, because of their complexity, are beyond the scope of classical calculus [39]. Consequently, it is important to model the electric fields and potentials in the study of the characteristics and the behavior of the polluted insulators. For this reason, Comsol Multiphysics can serve as a powerful and interactive way to solve complex problems using the finite element method.

In the field of high voltage transmission line applications, the published results of the numerical simulation of the potential distribution and the electric field of some studies are all for simple geometries [40-45]. The numerical models based on the finite element method [39,49], give better results in the modeling of the flashover phenomenon of the insulators polluted compared to the static and dynamic models. This peculiarity encouraged us to use the finite element method to study the performance of a real insulator.

Comsol Multiphysics is a widely used tool in various fields of scientific research. It amply facilitates the modeling steps. The Finite Element Method (FEM) is most well-situated for calculate the electric field and potential distribution in high voltage insulator, because it is one of the more successful numerical methods to solve electrostatic problems (using the discretization of the domain) [47]. Hence, it is a method flexible and led to relatively simple techniques allowing to estimate the fields at the surface of the electrode thin and highly curve with various dielectric materials, which is well adapted to problems of complicated geometry [42-45].

Electric field and potential distribution along a cap and pin insulator (1512L) has been calculated in Comsol Multiphysics. Electric currents formulation has been used to study the effect of pollution conductivity on the electric field distribution. Level of pollution has been fixed (L1: Level of discontinuous pollution) with various conductivities and influence of the destroyed ribs and their widths to investigate effect of pollution on electric field and potential distribution.

To do so, we opted to use the following software:

- **G**rapher is used to make 2D graphics, very easy to use, both useful for students and teachers, we can better understand and understand a mathematical problem by visualizing it in its 2D form.
- **F**EMM and **A**UTOCAD are used for the construction of the geometry of the components of the real insulator.

➤ **COMSOL Multiphysics** is numerical simulation software based on the finite element method. Used the AC/DC Module is used to simulate the potential and electric field distribution in static and low frequency applications. Typical applications are capacitors, inductors and insulators.

➤ **MATLAB** is used as an interface for the exploitation and visualization of numerical results. This thesis focuses on the study of the behavior of the insulator of high voltage under AC voltage installed in the regions of Sahara of Algeria. This PhD dissertation is the continuity of work done in the M.Sc thesis.

The thesis is structured into four major chapters.

In the first chapter, presents the experimental study the flashover process, the leakage current and phase angle under 50 Hz applied voltage on real and a circular model witch simulating the 1512 L high voltage insulator largely used by the Algerian company of electricity and gas (SONELGAZ): installed in the electric area in the algerian sahara region. This chapter consists in presenting the impact of conductivity as well as distribution of discontinuous pollution on the behavior of a real and experimental model artificially polluted. This model of laboratory is subjected to a distribution of discontinuous pollution reproducing the surface quality of the cap and pin insulator 1512L. In the present work there are also experimental observations of tests carried in the high voltage laboratory and the various measures of the flashover voltage, leakage current and phase angle between applied voltage and the leakage current under the influence of artificial pollution deposited on the insulator surface to study its behavior under AC voltage.

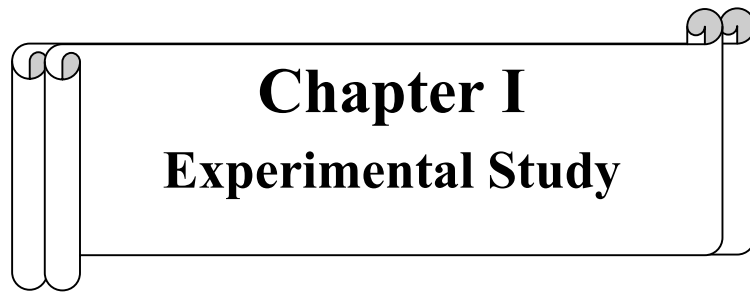
In the second chapter, we have presented the theory of the artificial intelligence technique and the methodology used to predict the flashover voltage of a real model of high voltage insulator 1512 L under different electro-geometric conditions such as conductivity, pollution levels. The technique based on Fuzzy Logic (FL) has been applied. The necessary bases for the understanding of the method are presented in this chapter, such as the use of fuzzy logic concepts, description of the constituents of a fuzzy system, the linguistic variable concept and the fuzzy inference system. The results obtained during our work will be presented and interpreted under normal conditions and with different electro-geometric parameters. We exploited the database of the first chapter to create our model.

In the third chapter, we will use the experimental data in chapter I to construct a model based on ANN architectures that can estimate the flashover voltage on the real model using as inputs some characteristics of the pollution (conductivities (δ) and level of pollution (L_i) or zones

of pollution (Z_i), utilization of interface graphic can help to determinate their parameters as we have applied and explained during our study, and we conclude our chapter with a comparison between the two artificial intelligence methods of Chapter II (FL) and Chapter III (ANN).

In the fourth chapter, we have studied the numerical results using the Comsol Multiphysics based on the finite element method (FEM), for different electro-geometric parameters such as the influence of conductivities, the width of ribs, ribs thus destroys and the influence of the applied voltage of the high-voltage line under AC voltage, a brief description of the real model of insulator, parameters and material properties in the Finite Element Method (FEM) to estimate the electric field, electric potential, electric field and potential distribution artificially polluted of cap and pin insulator (1512L), our work based on the real model. Numerical results using Comsol Multiphysics are presented and discussed.

Finally, we present a general conclusion of this work and the outlook suggested by this study.



Chapter I
Experimental Study

I.1. Introduction

Outdoor insulators are exposed of experienced different atmospheric condition (pollutions) at different geographic area of a country. These pollutants are also known as contaminants. Contamination caused insulator flashover has been studied by many researchers in the recent years [1-9].

Insulator pollution research is usually performed in areas of medium to heavy pollution severity, [10] (for example Algerian Sahara). It is a phenomenon that acts negatively on the high voltage insulators "behavior". Into investigations of the flashover voltage mechanism have been studied by many researchers. The behavior is studied by analyzing the evolution of the main parameters such as flashover voltage, leakage current (LC), and phase angle between leakage current-Applied voltage.

The aim of this chapter is the experimental study of the flashover process and the leakage current under 50 Hz applied voltage on real and a circular model witch simulating the 1512 L high voltage insulator largely used by the Algerian company of electricity and gas (SONELGAZ): installed in the electric area in the Algerian Sahara region. The previous knowledge of pollution severity in these regions this work consists in presenting the impact of conductivity as well as distribution of discontinuous pollution on the behavior of an real and experimental model artificially polluted. This model of laboratory is subjected to a distribution of discontinuous pollution reproducing the surface quality of the cap and pin insulator 1512L. In the present work there are also experimental observations of tests carried in the high voltage laboratory and the various measures of the flashover voltage and leakage current under the influence of artificial pollution deposited on the insulator surface to study its behavior under AC voltage.

I.2. General description of real and experimental model

The impact of the conductivity as well as the distribution of pollution on the behavior of the 1512L cap and pin insulator (Figures I.1 and 2) and its experimental model proposed (figure I.3) under AC voltage then due a comparison has been examined.

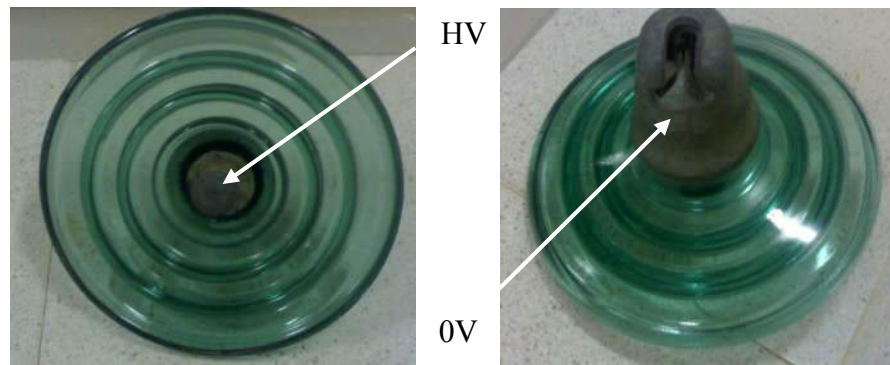


Fig. I.1. 1512L insulator profile.

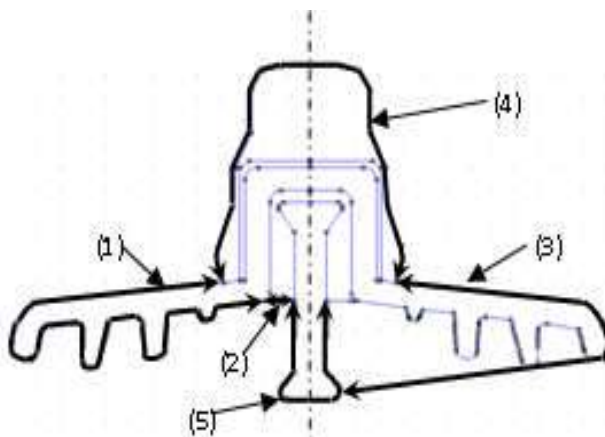


Fig. I.2. Cap and pin 1512L insulator dimension (Table 1)

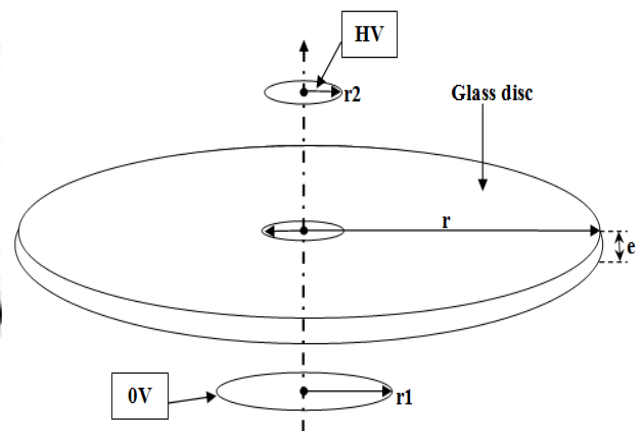


Fig. I.3. 1512L Proposed model

The dimensions of the 1512L experimental model proposed in this paper are obtained from the dimensions of the insulator (table I.1). The proposed model has a shape of a glass disc with a radius (r) of 200 mm (figure I.3) and thickness (e) of 5 mm, having the property of resisting heat due to electrical discharge. The proposed model is provided with two electrodes in aluminum paper. The first one is circular (radius $r_1 = 86$ mm) represented the cap and connected to the ground. The second one is circular too (radius $r_2 = 13$ mm) represented the pin related to high voltage supply. The pollution is supposed distributed in the form of circular bands on the surface of the proposed experimental model which reproduces the surface condition of the 1512L insulator. For both the 1512L insulator and its proposed experimental model, the artificial pollution is realized by a salt solution (NaCl + distilled water), having various conductivities. The artificial pollution is applied by pulverizing the surface of the experimental model (figure I.3), and filling the 1512 L (zones (figure I.4, table I.2)) insulator.

Tab. I.1. Dimension of 1512L.

	Dimensions	Values
1	Leakage distance	292 mm
2	Cement	14 mm
3	Air flashover distance	230 mm
4	Insulator cap	488 mm
5	Insulator pin	250 mm
Net weight of the insulator		3.75 Kg

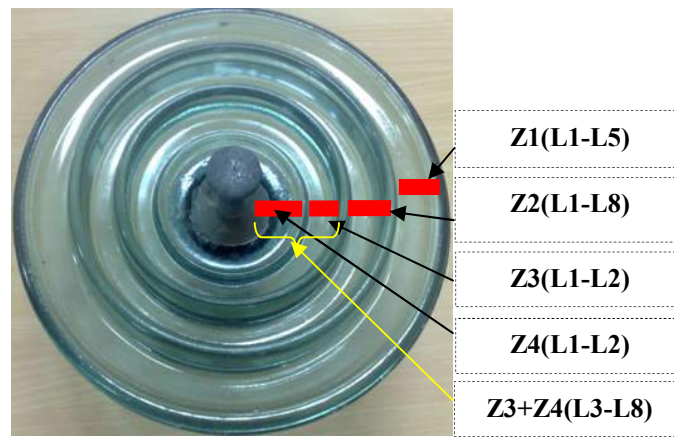


Fig. I.4. Distribution of polluted zones on the 1512L high voltage.

Tab. I.2. Dimensions of polluted area and clean area for experimental

Level of pollution	Experimental model								Real model			
	Polluted area (mm)				Cleaned area (mm)				Polluted area (ml)			
	P1	P2	P3	P4	C1	C2	C3	C4	Z1	Z2	Z3	Z4
L1	51	19	17	18	9	38	40	8	30	15	11	15
L2	53	23	21	22	5	34	36	6	60	30	22	30
L3	83	0	25	26	0	30	32	4	90	45	87,5	87,5
L4	85	0	29	30	0	26	28	2	120	60	123	123
L5	87	0	33	34	0	22	24	0	150	75	158,5	158,5
L6	89	0	37	34	0	18	22	0	-	90	194	194
L7	91	0	41	34	0	14	20	0	-	105	229,5	229,5
L8	93	0	45	34	0	10	18	0	-	120	265	265

I.3. Experimental study

The test voltage is measured using a capacitive divider, connected to the secondary of a transformer test (220 V/140 kV, 5 kVA), whose primary winding is connected to a regulating transformer in order to adjust the voltage with the desired value. It can deliver a secondary voltage ranging from 0 to 140 kV. An average of 10 tests is performed in each case. Different conductivities of the pollution are used by varying the salt concentration of the salt solution, eight conductivities (1.823 mS/cm, 3.33 mS/cm, 8.02 mS/cm, 12.61 mS/cm, 16.32 mS/cm, 30.5 mS/cm, 50.4 mS/cm, 93.7 mS/cm) are obtained.

The pollution is applied on the 1512L insulator by filling the different zones (figure I.4) by the salt solution with different conductivities to obtain different levels of pollution (figure I.4, table I.2).

I.3.1. Flashover process

To observe the effect of the pollution on the behavior of the insulator (real model), one value of conductivities is prepared and to measure the flashover voltage corresponding, the following steps must be complied:

- تنظيف العازل: The insulator is cleaned at first with distilled water and dried with papers. Then it is cleaned with 70° alcohol.
- إعداد مستوى التلوث L_1 (figure I.5) من خلال ملء المناطق ($Z_1+Z_2+Z_3+Z_4$) من العازل (figure I.4) كما هو مذكور في الجدول I.2 بحل ملحي.
- تطبيق جهد عالٍ حتى يتم الحصول على قوس كهربائي.
- أخذ القياسات لجهد القوس الكهربائي. لكل مستوى، يتم تكرار جميع الخطوات حتى يتم الوصول إلى المستوى L_8 .

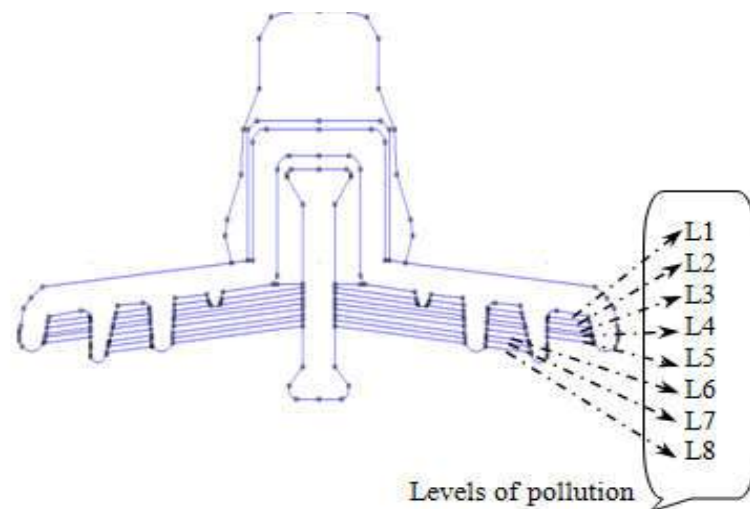


Fig. I.5. Determination of different levels of pollution for 1512L insulator.

In order to study the effect of the pollution severity, another value of conductivities is chosen with respect to all precedent steps and taking measurement.

In order to study the effect of the pollution on the behavior of the experimental model (figures I.6 and 7), at first, one value of conductivities is prepared, and to measure the flashover voltage corresponding, the following steps must be complied:

- Cleaning the experimental model. The insulator is cleaned first with distilled water and dried with papers. Then it is cleaned with 70° alcohol.
- Preparing the level L_1 (figures I.6 and 7) of pollution by pulverizing the surface of the experimental model as is referred to in table I.2 by salt solution.
- Applying a high voltage until a flashover is obtained.
- Taking the measurement of flashover voltage.

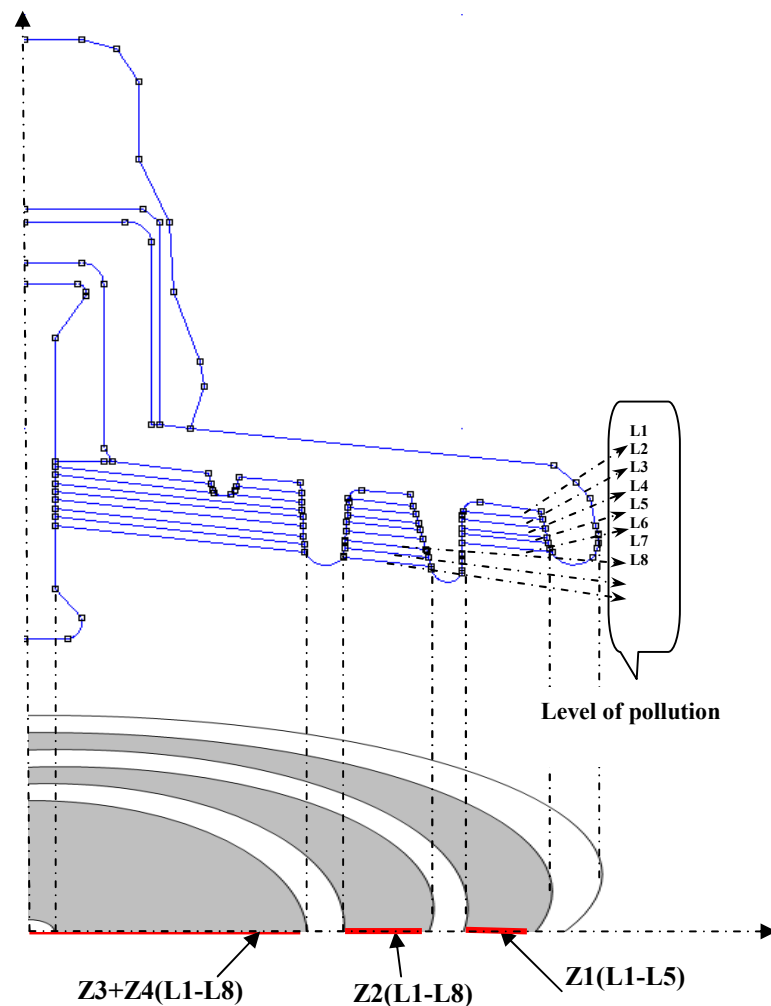


Fig. I.6. Experimental model versus real model of 1512L insulator.

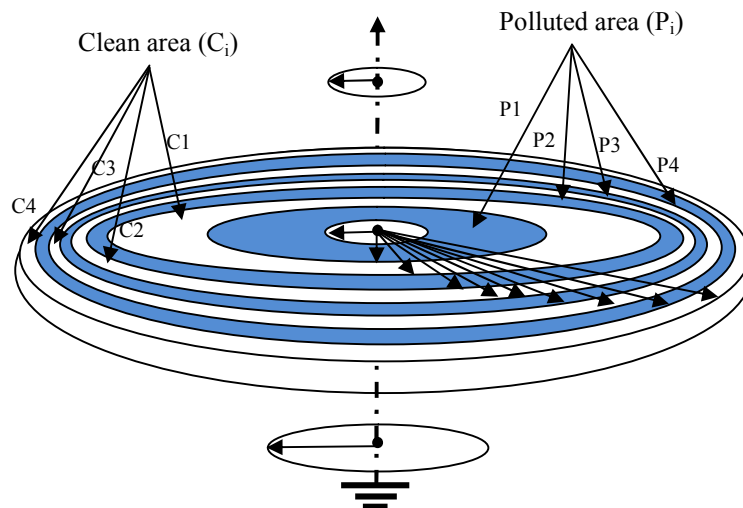


Fig. I.7. Determination of clean and polluted area insulator (Tab. I.2).

I.3.1.1. Laboratory observations

The work presented in this study has been carried out in the laboratory of high voltage of the Mohamed kheider University of Biskra. (figure I.8).

We have carried out an experimental work which consists mainly of the study of the impact of pollution on the behavior of a real insulator and of an artificially polluted laboratory model on certain parameters such as: the level of pollution & surface conductivity.

Experimental studies have been carried out using experimental test bench shown in figure I.9, at High Voltage Laboratory (University of Biskra, Algeria), the flashover voltage is measured using a capacitive voltage divider connected to the secondary of a high-voltage transformer. The alternating measuring devices are respectively shown in figure I.9, where the following elements are found:

- ض High voltage transformer, 140kV/5kVA/50Hz,
- ض Regulating transformer, $U_1=220V$, $U_2=0$ a $250V$, 5500 VA,
- ض Isolating transformer, $U_1=220V$, $U_2=220V$,
- ض A capacitor to measure the applied voltage $C_m=100$ pF,
- ض A digital scope meter. (25 Mhz, 250M Sa/s)
- ض Control panel, powered by 220V, not presented in the figure,
- ض A PC used for data acquisition, and a video camera to record the evolution of electrical discharge behavior.

The figure I.9 corresponds to the assembly is carried out in the laboratory of high voltage.

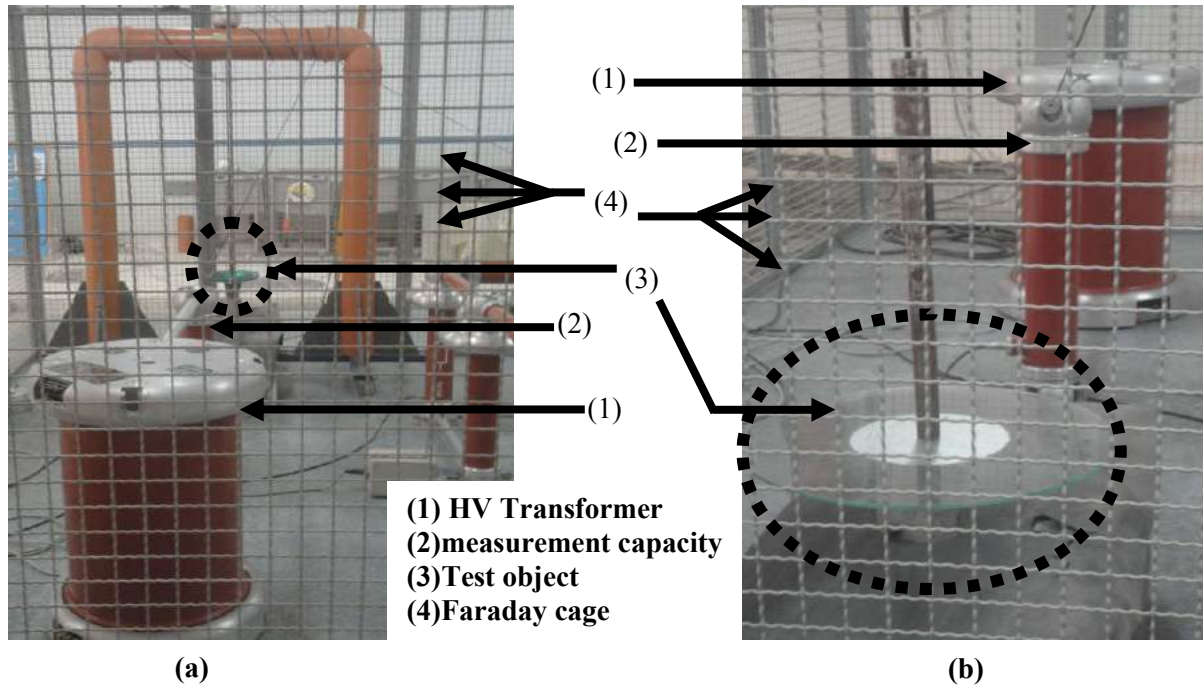


Fig. I.8. Test circuit. (a) Real model, (b) Experimental model.

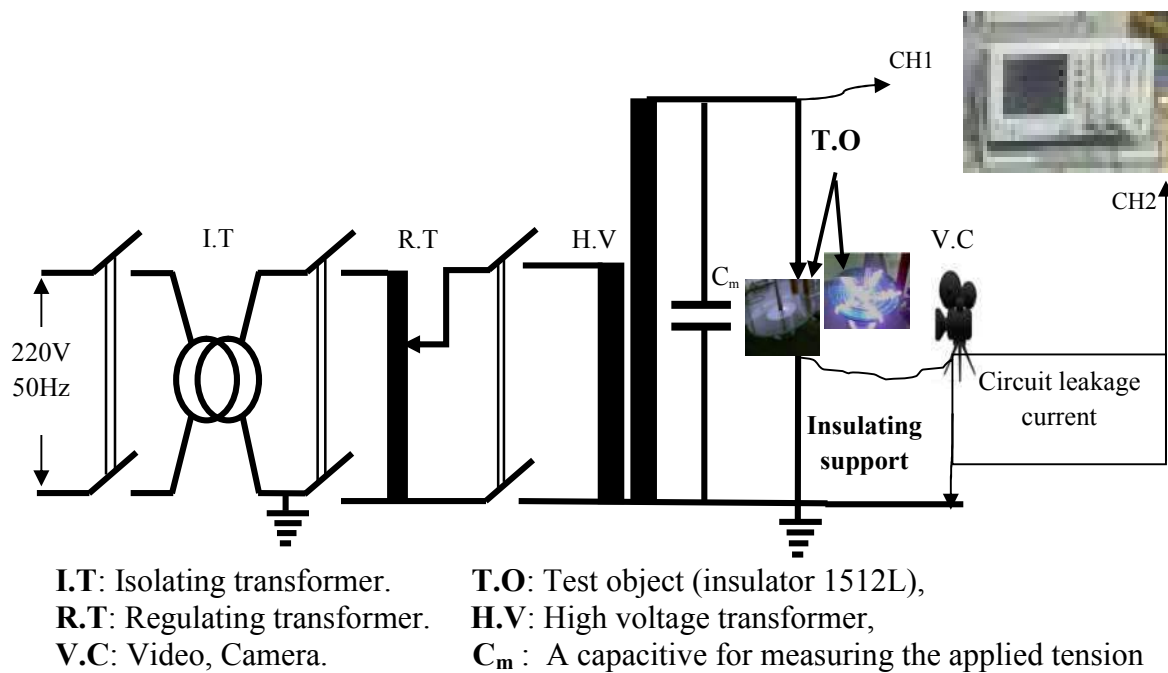


Fig. I.9. Schematic diagram of the experimental setup.

The AC voltage whose maximum up to 140 kV in our laboratory. The flashover voltage has been obtained by the "voltage increase" method, that is to say any voltage is applied to the insulator (real or model) for a sometime, if the flashover does not occur on increases this applied voltage. We continue until we get flashover. During the development of the flashover the applied voltage is kept constant.

It has been observed that the application of a few kilovolts between the electrodes generates a leakage current (initiation of arcs figure I.10(a) and figure I.11(a)). The high current density in the vicinity of the HV (High Voltage) electrode causes an evaporation of the salt solution, by the Joule effect, and a dry area appears. The increase in the applied voltage causes the lengthening of the arcs in the direction of the opposite electrode (figure I.10(b), figure I.11(b)). By increasing the voltage, a critical state is reached, beyond which further increases in voltage causes a total flashover by development of the random arcs (figure I.10(c), figure I.11(c)).

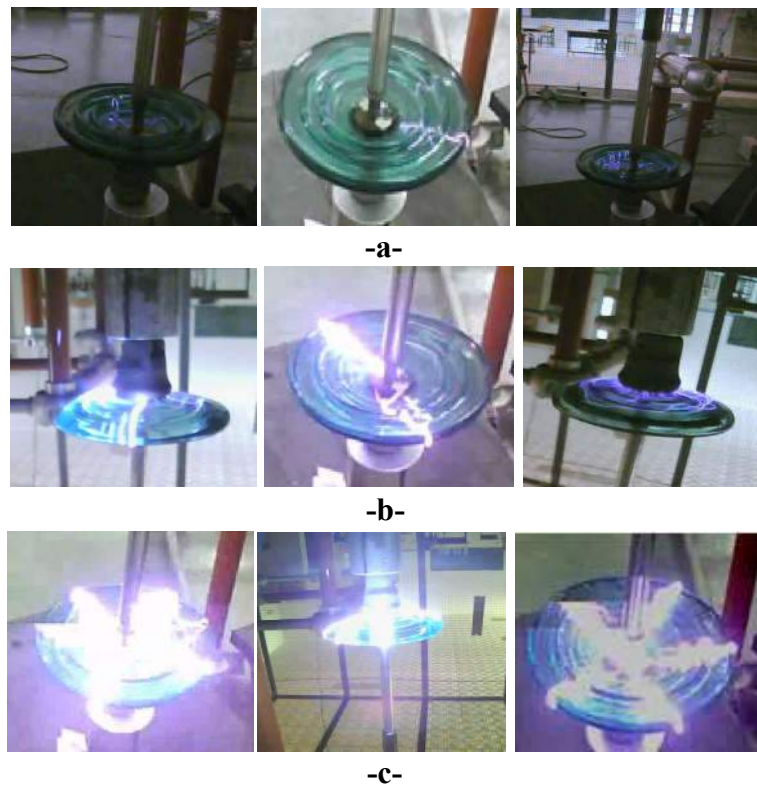


Fig. I.10. Flashover process observed in laboratory for 1512L polluted insulator
(a) Initialization of the arc; (b) evolution of the arc; (c) total flashover.

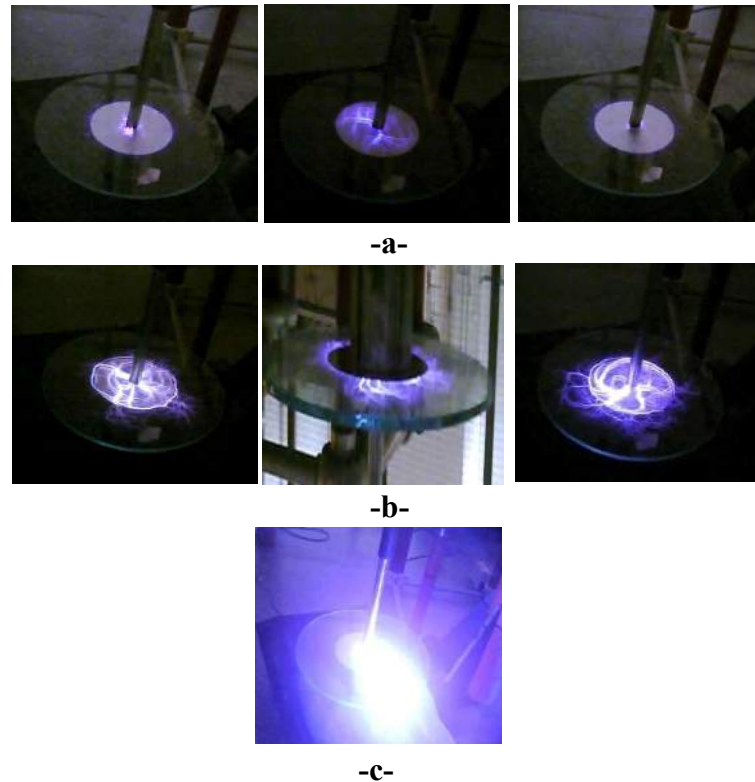


Fig. I.11. Flashover process observed in laboratory for experimental model polluted insulator
 (a) Initialization of the arc; (b) evolution of the arc; (c) total flashover.

I.3.1.2. Effect of pollution on the flashover voltage

In this section, the variation of flashover voltage according to the conductivity figure I.12 (a) (real model) and figure I.12 (b) (experimental model) is investigated. This phenomenon, characterized by the no generation of partial arcs, is due at the same time to the nature of the pollution used and the fact that the overall length of the equivalent clean band exceeds the breaking value from which no stable discharge is propagated [11–19].

Figure I.12 present the variation of the flashover voltage according to different levels of pollution for real model and experimental model respectively. An increase in flashover voltage following the reduction in the level of pollution is expected. However, this increase is unimportant and does not exceed in the extreme case 30% of the initial flashover voltage in real model and the value of 21% in experimental model. In these conditions, the average gap calculated between the experimental results (real and model) is equal to 18%.

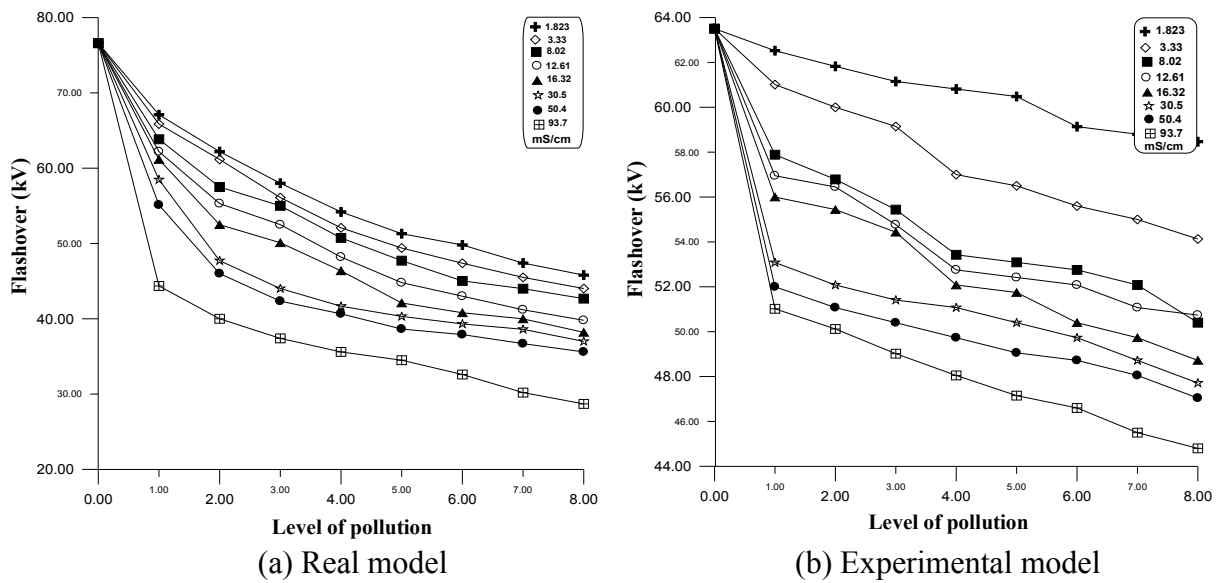


Fig. I.12. Flashover voltage-level of pollution for different conductivities(δ).

I.3.1.3. Effect of pollution severity on the flashover voltage

The variation of flashover voltage according to different conductivities is presented in figure I.13. It is noted that the flashover voltage reveals a clear reduction for conductivities lower than 30.5 mS/cm and more slowly beyond this conductivity. On the other hand, the reduction in the flashover voltage becomes less accentuated when conductivity is higher. It could be deduced that the isolating system (insulator) is more rigid when the conductivity is weak.

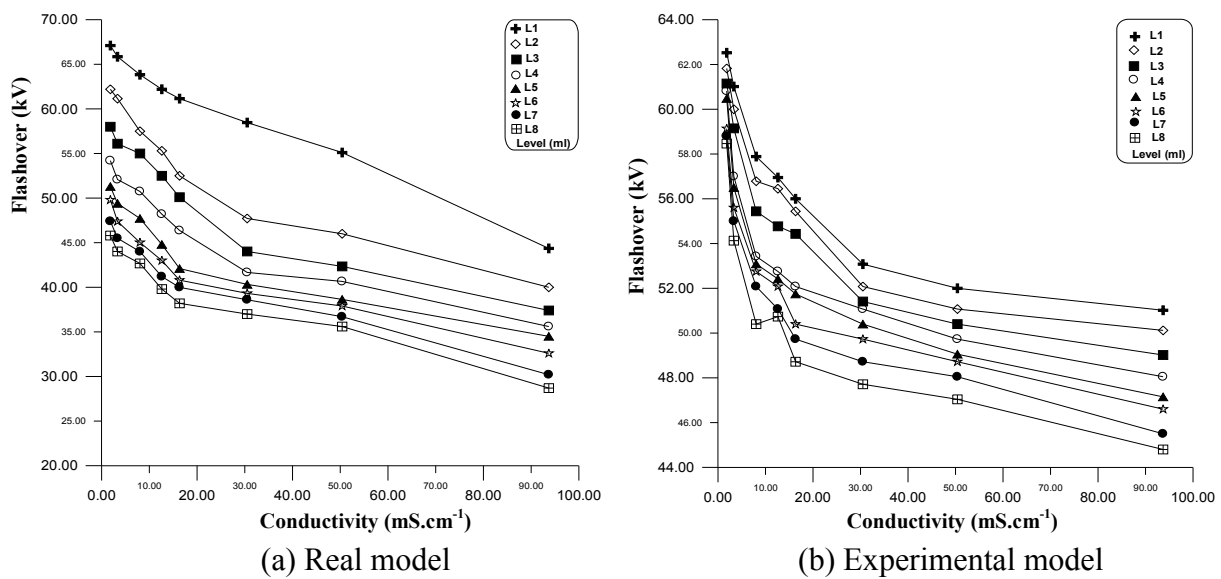


Fig. I.13. Flashover voltage-conductivity for different levels of pollution(L_i).

I.3.2. Leakage current

In this section, we interested to measure and visualized the leakage current forms for the different pollution layers under different voltage levels using a digital oscilloscope. The leakage current wave is reported using a coaxial cable, allowing the voltage (leakage current image) to be displayed on a digital oscilloscope (DSO 25MHz). In order to fully collect the current signal, we used an adapter at the input of the oscilloscope. (figure I.14).

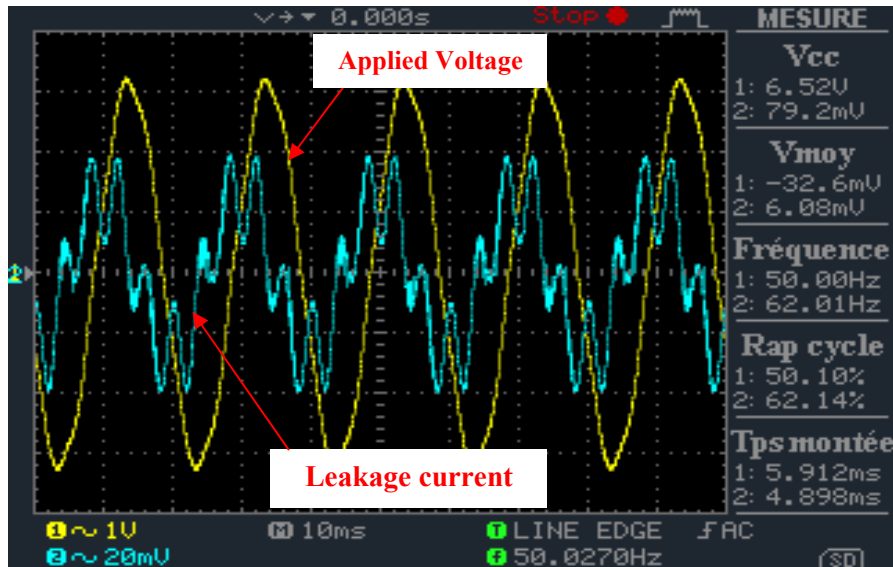
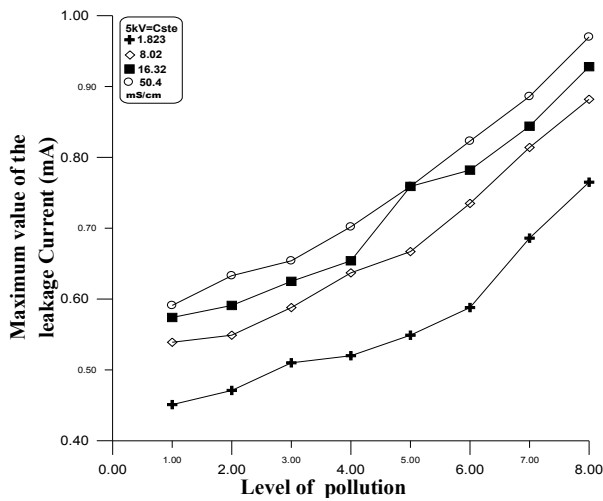
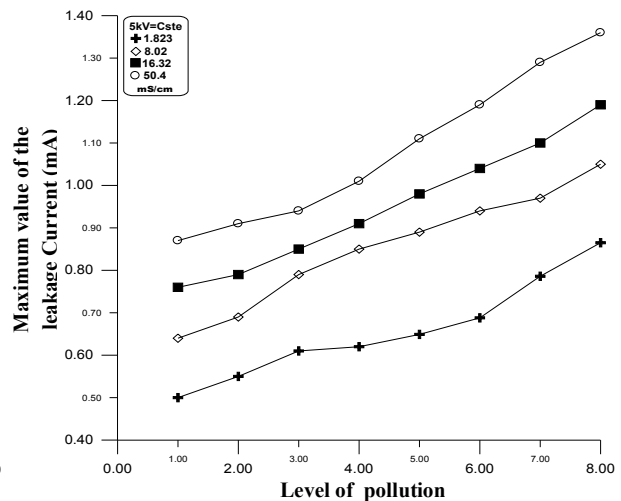


Fig. I.14. Visualizations of leakage current waves for applied voltage 10kV.

Figure I.15 to figure I.19 present the variation of leakage current according to the level of pollution for each conductivity studied and applied voltage, (a) for real model & (b) for experimental model. An increase in current is noted. This is explained by the reduction in the surface resistivity of the clean zones which depends on their temperature. A reduction in the leakage current length caused by the level of pollution is also confirmed.

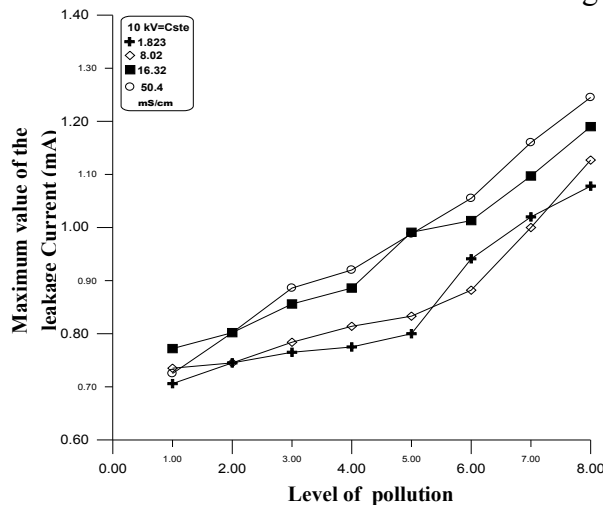


(a) Real model

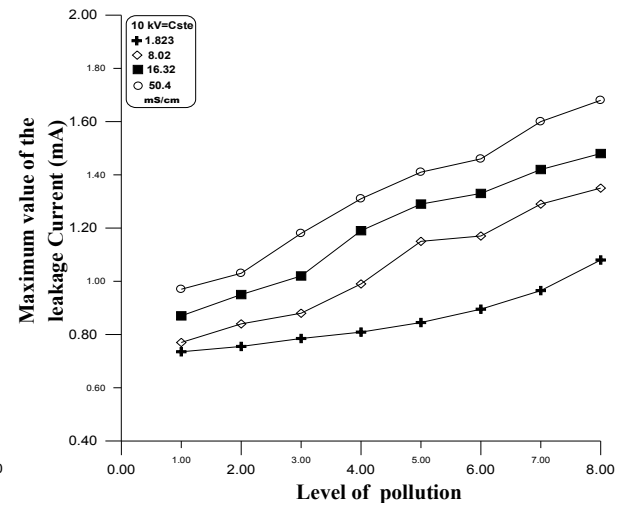


(b) Experimental model

Fig. I.15. Leakage current-level of pollution for different conductivities for an applied voltage of 5kV.

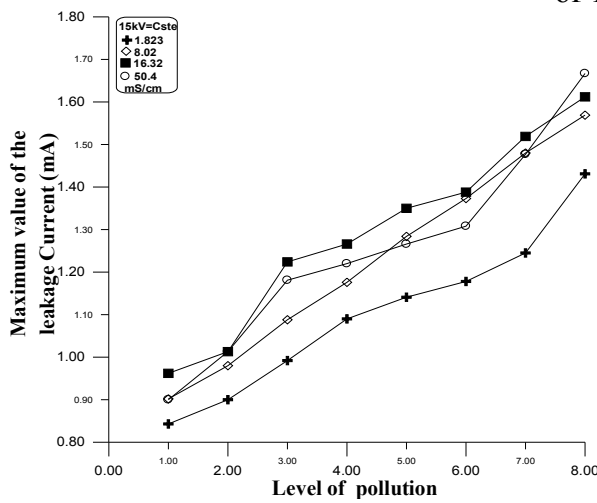


(a) Real model

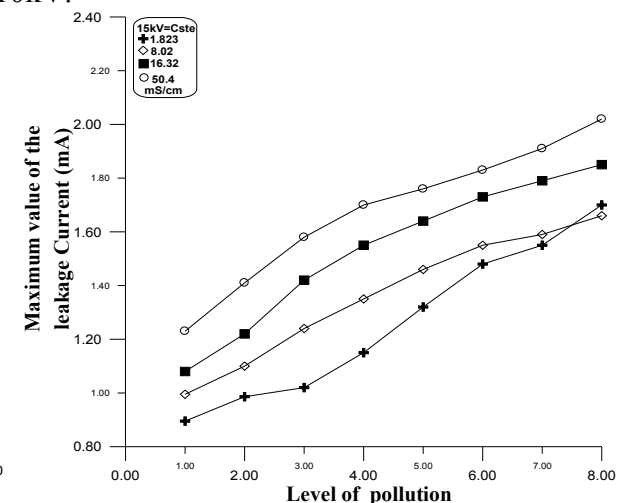


(b) Experimental model

Fig. I.16. Leakage current-level of pollution for different conductivities for an applied voltage of 10kV.



(a) Real model



(b) Experimental model

Fig. I.17. Leakage current-level of pollution for different conductivities for an applied voltage of 15kV.

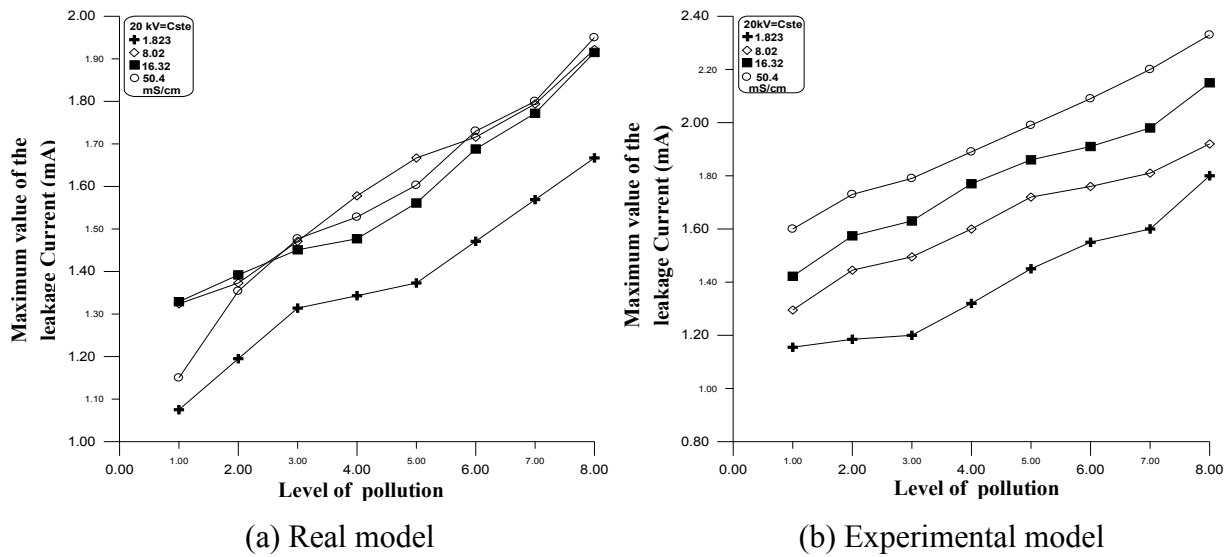


Fig. I.18. Leakage current-level of pollution for different conductivities for an applied voltage of 20kV.

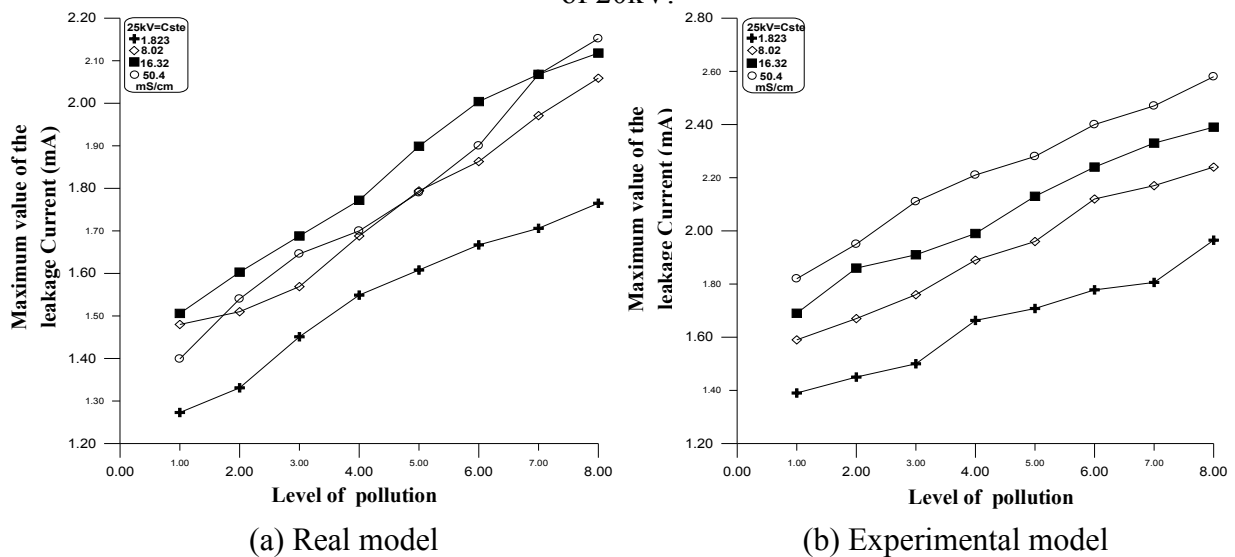


Fig. I.19. Leakage current-level of pollution for different conductivities for an applied voltage of 25kV.

Figure I.20 to figure I.27 illustrate the variation of the leakage current as a function of the conductivity and the applied voltage, (a) for real model & (b) for experimental model.

For low conductivities, it is noted that the increase in leakage current is relatively low for the lower voltage levels applied to 15 kV (lower 25% of the flashover voltage), and discharges at the active electrode are not yet intense, which can explain the low values of leakage currents.

For important conductivity, values of the leakage current are significantly greater with respect to other conductivities, once the voltage level of $U = 25$ kV (greater than 50% of flashover voltage) is attained.

This is due to the activity of discharges that becomes intense when they exceed 50% of the flashover voltage, which may explain the sudden increase in the leakage current. In addition, the rigidity of the insulation system decreases when conductivity pollution increases.

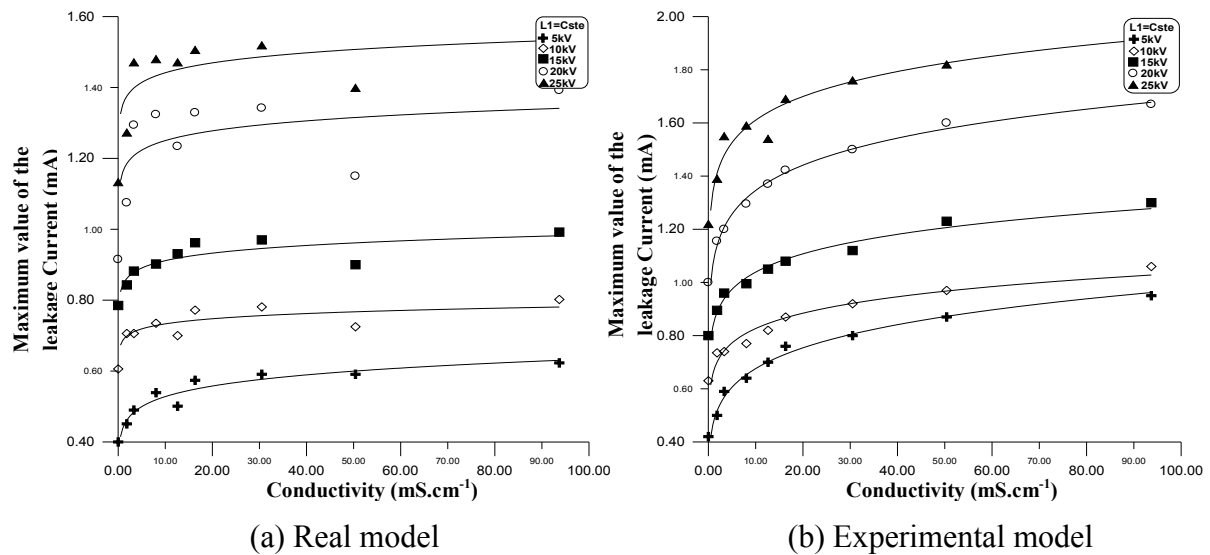


Fig. I.20. Leakage current-conductivity for various applied voltages for level L₁ of pollution (Tab. I.2).

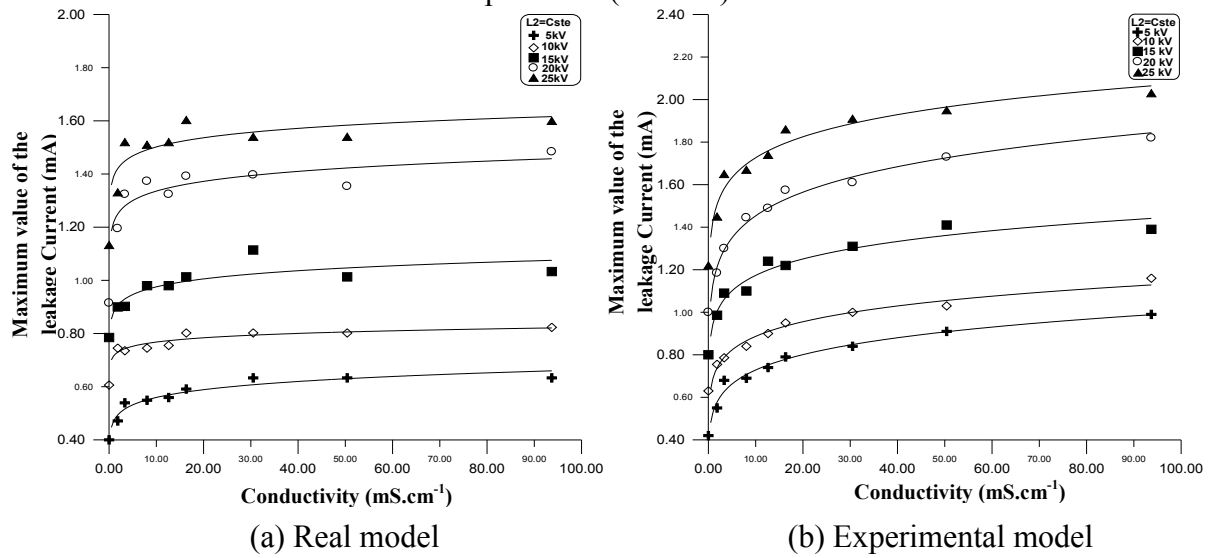


Fig. I.21. Leakage current-conductivity for various applied voltages for level L₂ of pollution (Tab. I.2).

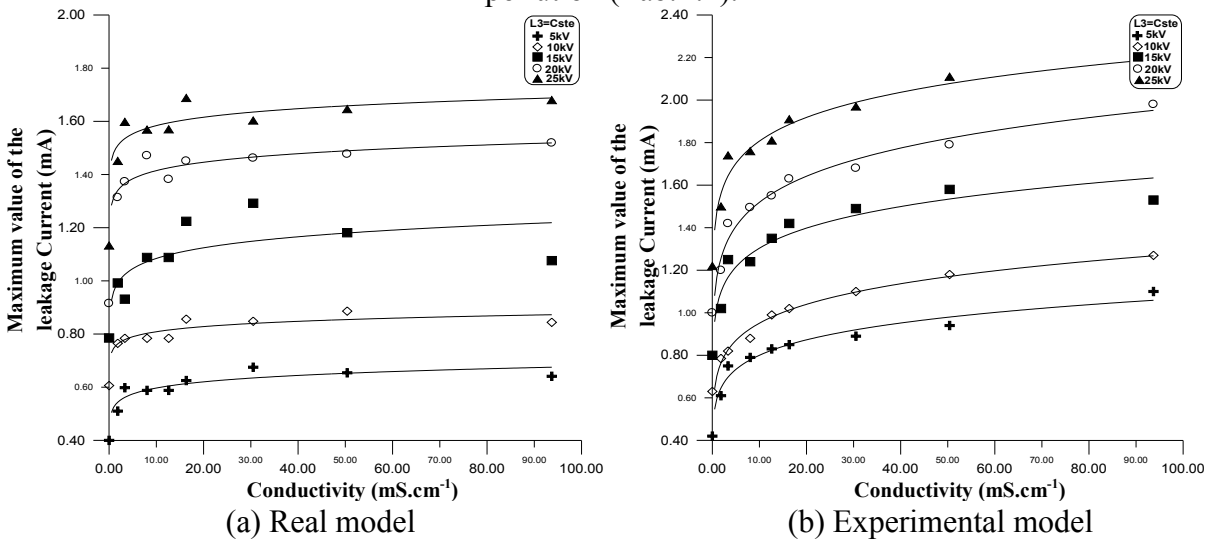


Fig. I.22. Leakage current-conductivity for various applied voltages for level L₃ of pollution (Tab. I.2).

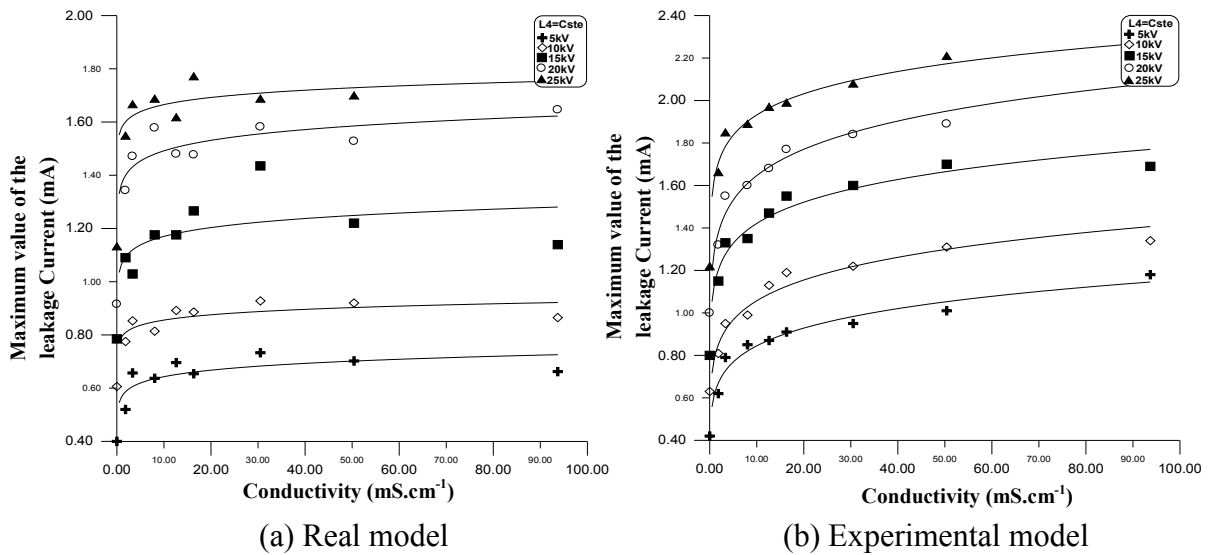


Fig. I.23. Leakage current-conductivity for various applied voltages for level L₄ of pollution (Tab. I.2).

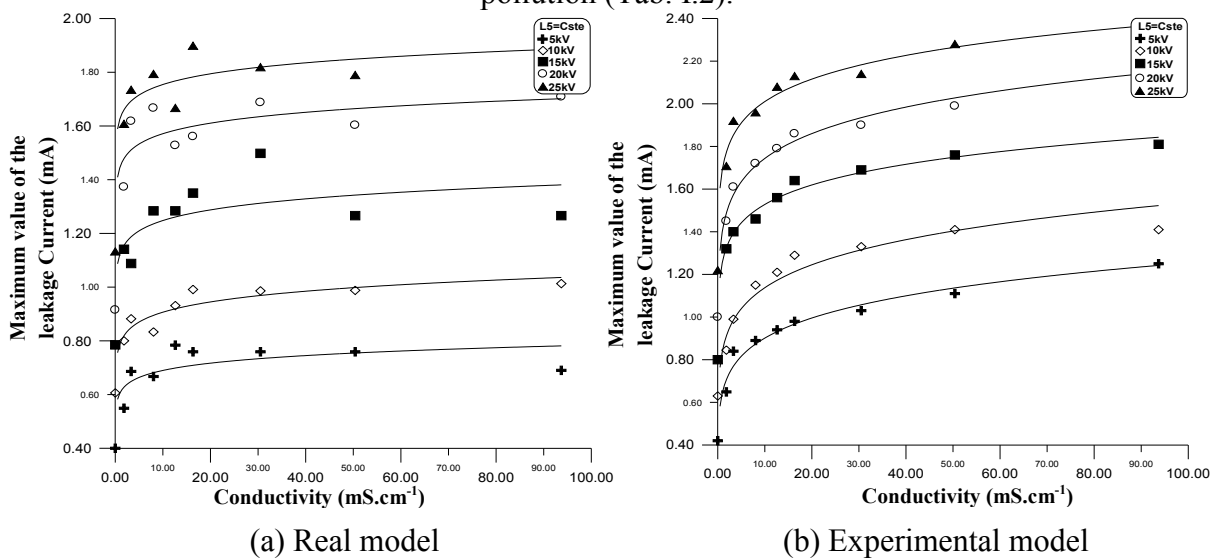


Fig. I.24. Leakage current-conductivity for various applied voltages for level L₅ of pollution (Tab. I.2).

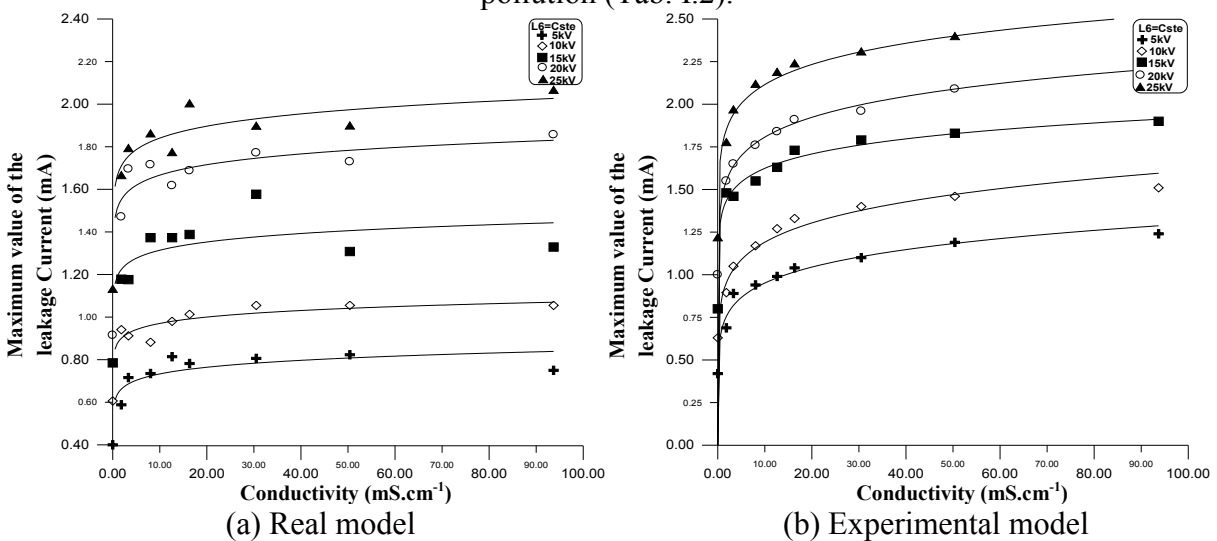


Fig. I.25. Leakage current-conductivity for various applied voltages for level L₆ of pollution (Tab. I.2).

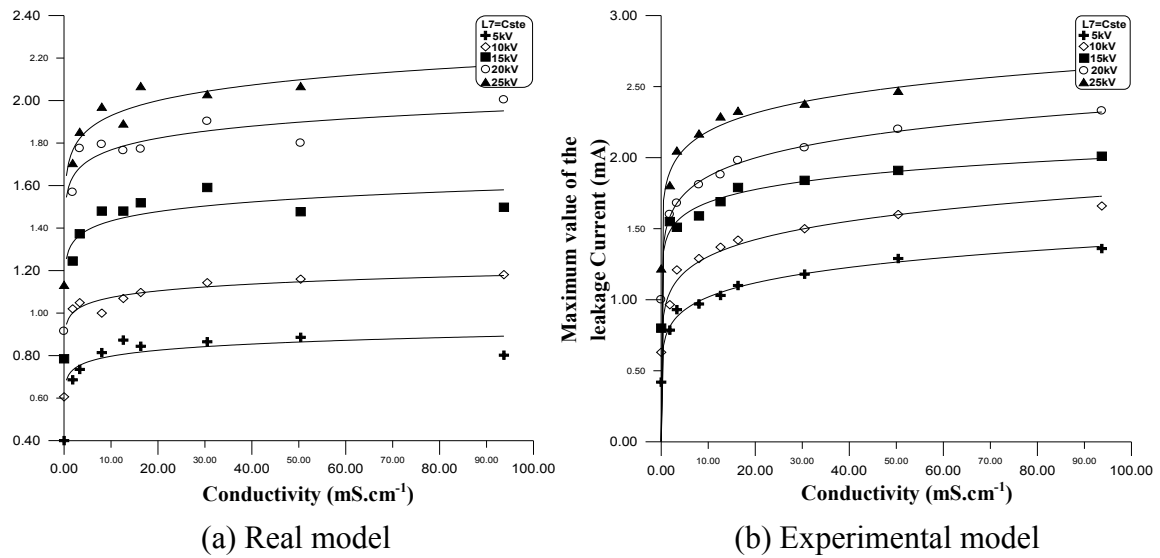


Fig. I.26. Leakage current-conductivity for various applied voltages for level L_7 of pollution (Tab. I.2).

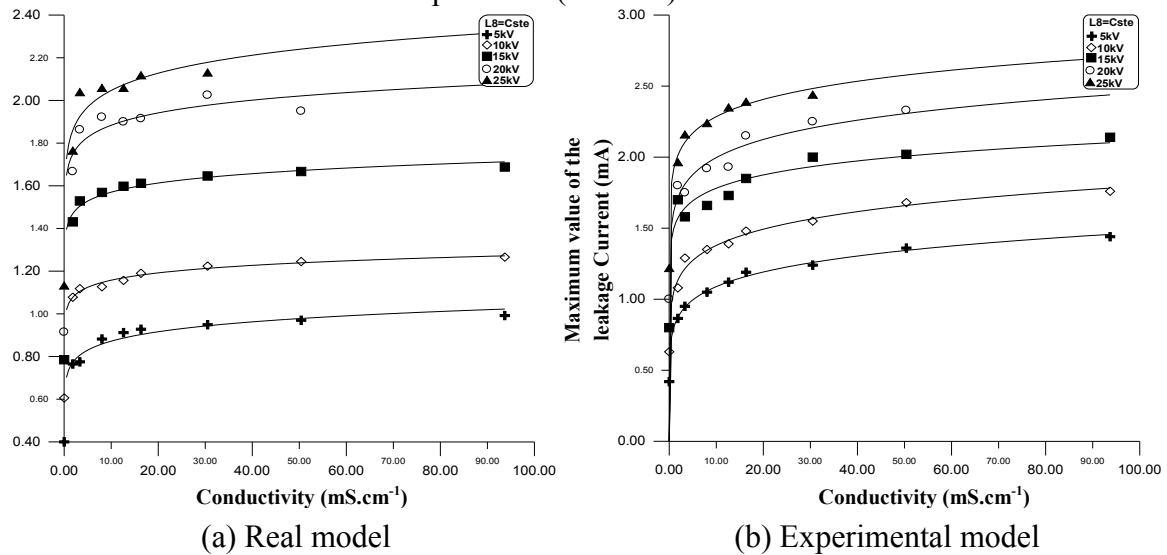


Fig. I.27. Leakage current-conductivity for various applied voltages for level L_8 of pollution (Tab. I.2).

In the figure I.28 to figure I.35 we show the variation of the leakage current as a function of the applied voltage, (a) for real model and (b) for experimental model, and this for all the conductivities studied. We find that the leakage current varies almost linearly as long as the applied voltage increases for all pollution levels.

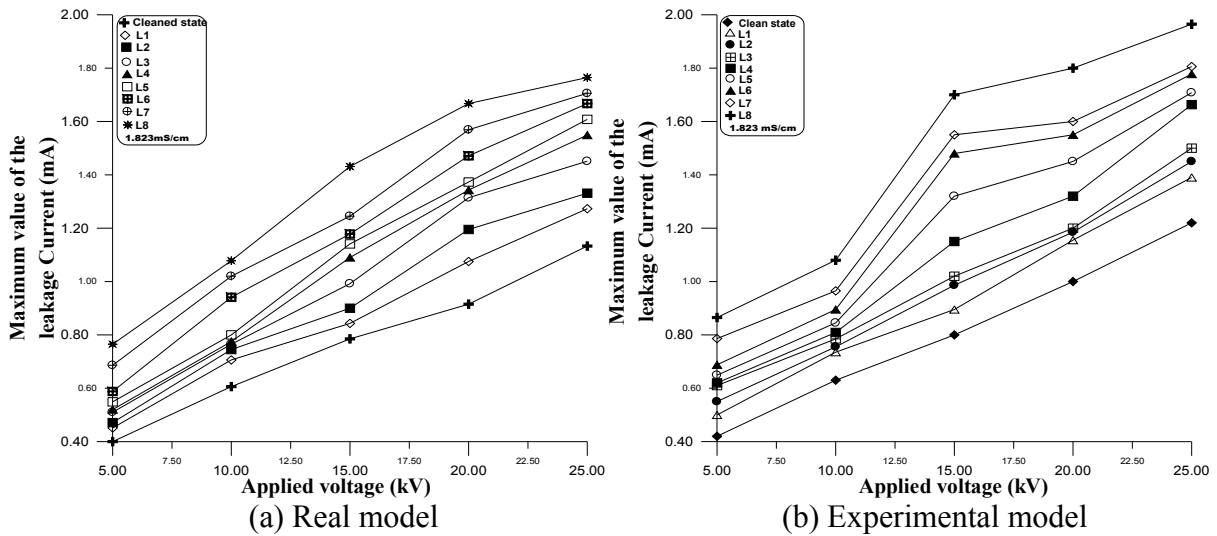


Fig. I.28. Leakage current- applied voltage for various level of pollution 1.823mS/cm (Tab. I.1).

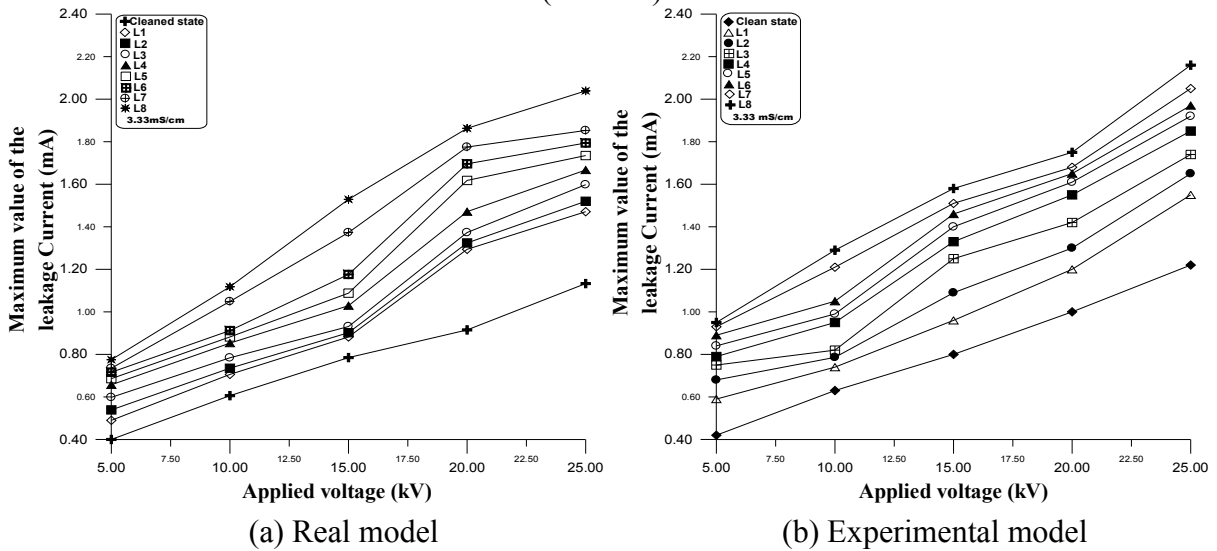


Fig. I.29. Leakage current- applied voltage for various level of pollution 3.33 mS/cm (Tab I.1).

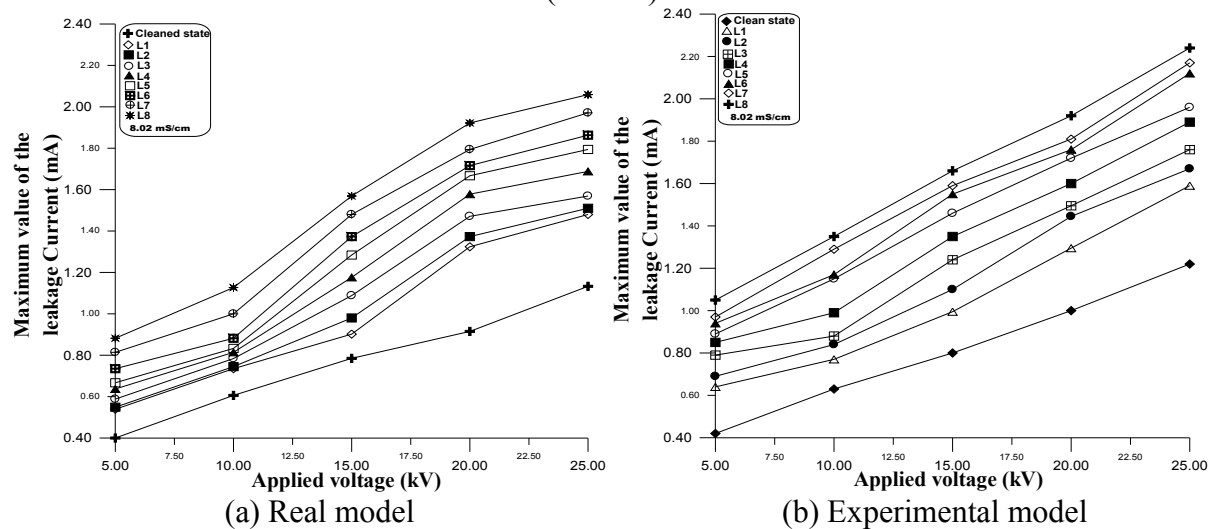


Fig. I.30. Leakage current- applied voltage for various level of pollution 8.02 mS/cm (Tab. I.1).

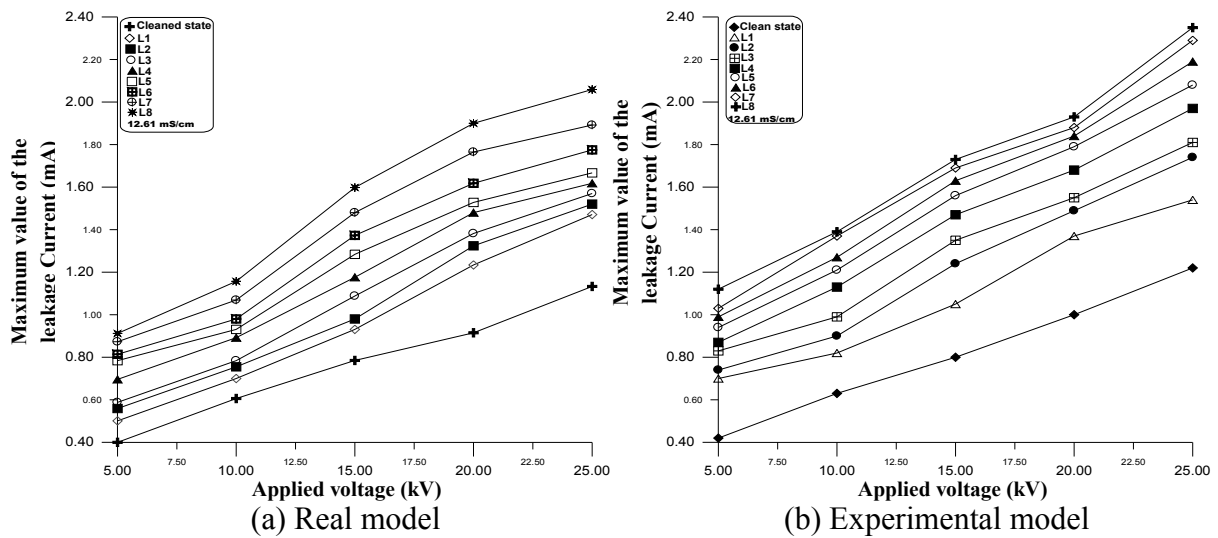


Fig. I.31. Leakage current- applied voltage for various level of pollution 12.61 mS/cm (Tab. I.1).

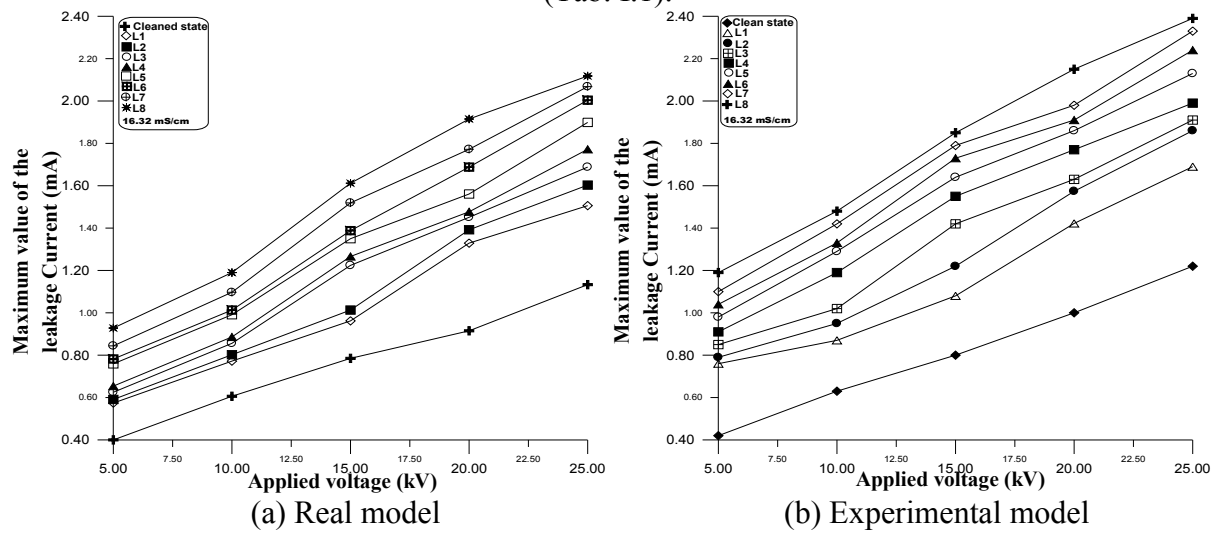


Fig. I.32. Leakage current- applied voltage for various level of pollution 16.32 mS/cm (Tab. I.1).

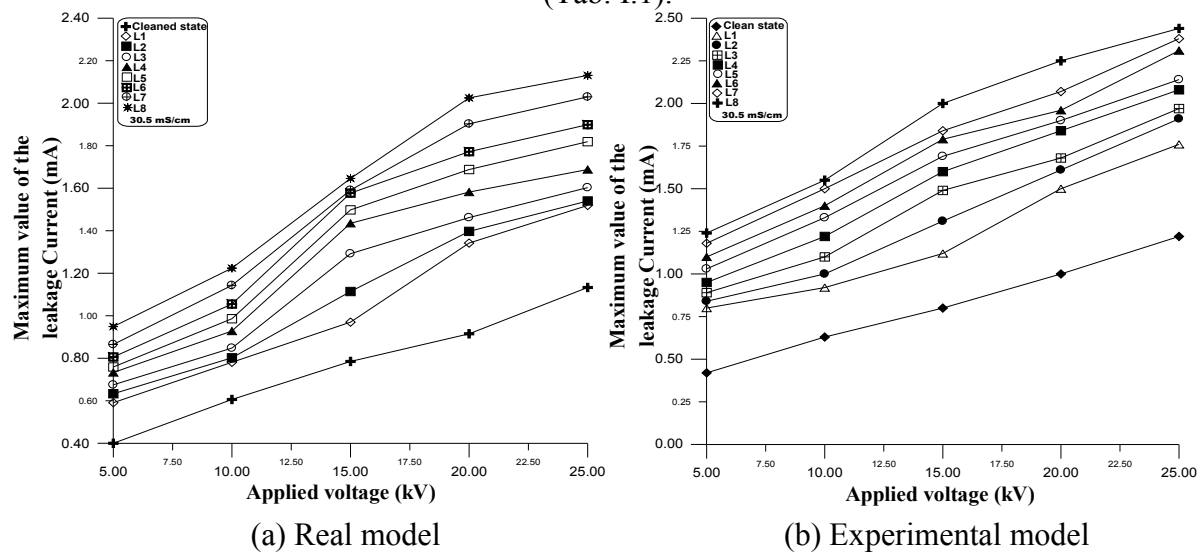


Fig. I.33. Leakage current- applied voltage for various level of pollution 30.50 mS/cm (Tab. I.1).

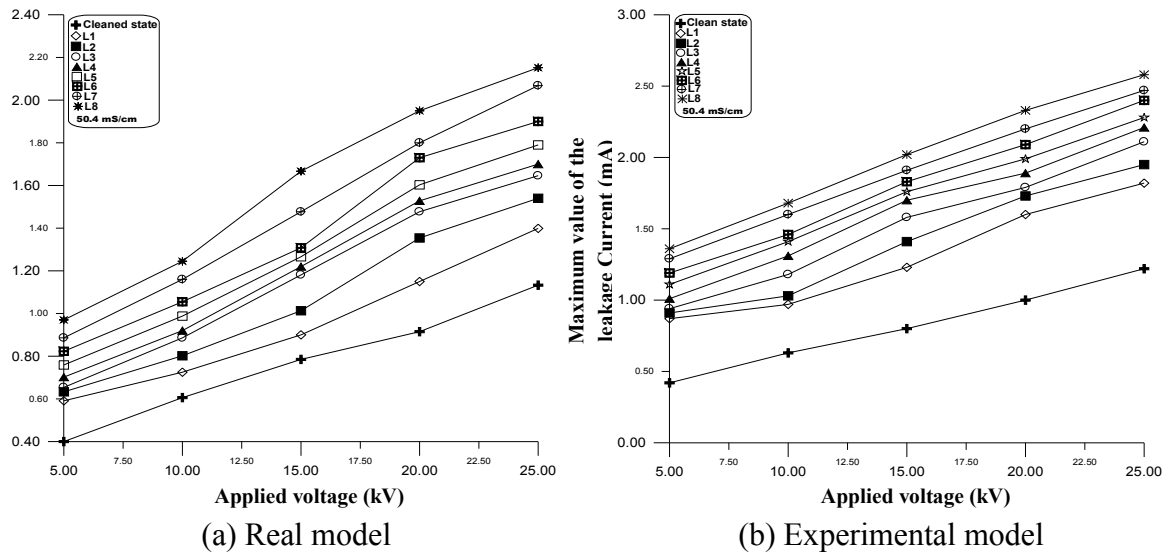


Fig. I.34. Leakage current- applied voltage for various level of pollution 50.4 mS/cm (Tab. I.1).

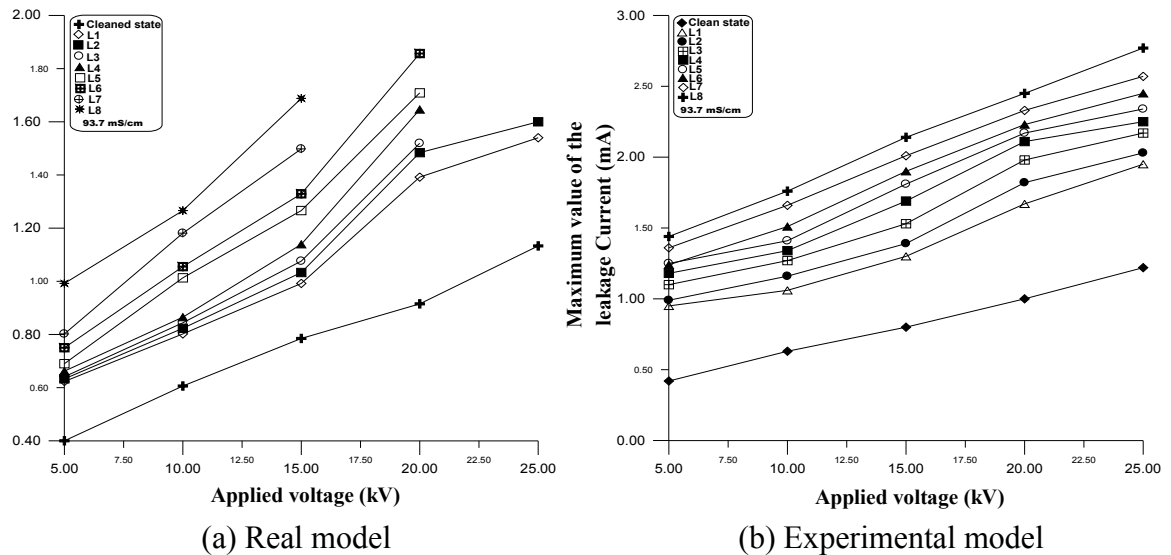


Fig. I.35. Leakage current- applied voltage for various level of pollution 93.7 mS/cm (Tab. I.1).

I.3.3. Angle phase (Leakage current_Applied voltage)

Figure I.36 shows the visualizations of the angle phase for different values of the applied voltage. By using the digital oscilloscope, the simultaneous recording of the leakage current wave and that of the applied voltage makes it possible to obtain the phase angle. This phase angle displayed on the oscilloscope screen and saved on our PC.

The recording of the two signals shows that there is a fluctuation at the applied voltage (figure I.36), this fluctuation is probably due to the non-linear magnetic characteristics of the

high-voltage transformer. This study shows that the angle phase is always of a capacitive nature.

Figure I.37 shows the leakage current-voltage angle phase as a function of the applied voltage for different conductivities. The phase angle is not affected by the applied voltage for two models (real and experimental model) (figure I.37).

Figure I.38 shows the (leakage current-applied voltage) angle phase as a function of the level of the pollution, for different conductivities. The phase angle is evolved irregularly according to the width of the pollution layer for a given surface conductivity. For experimental and real model, these observations illustrate that the capacitive character is dominant, so the increase in surface conductivity causes a slight reduction of the capacitive character, tending to make it more resistive. The maximum phase angle is obtained in the clean case and is equal to an average of 80° for the real model and 72° for the experimental model.



Fig. I.36. Displays of the angle phase for different values of the applied voltage.

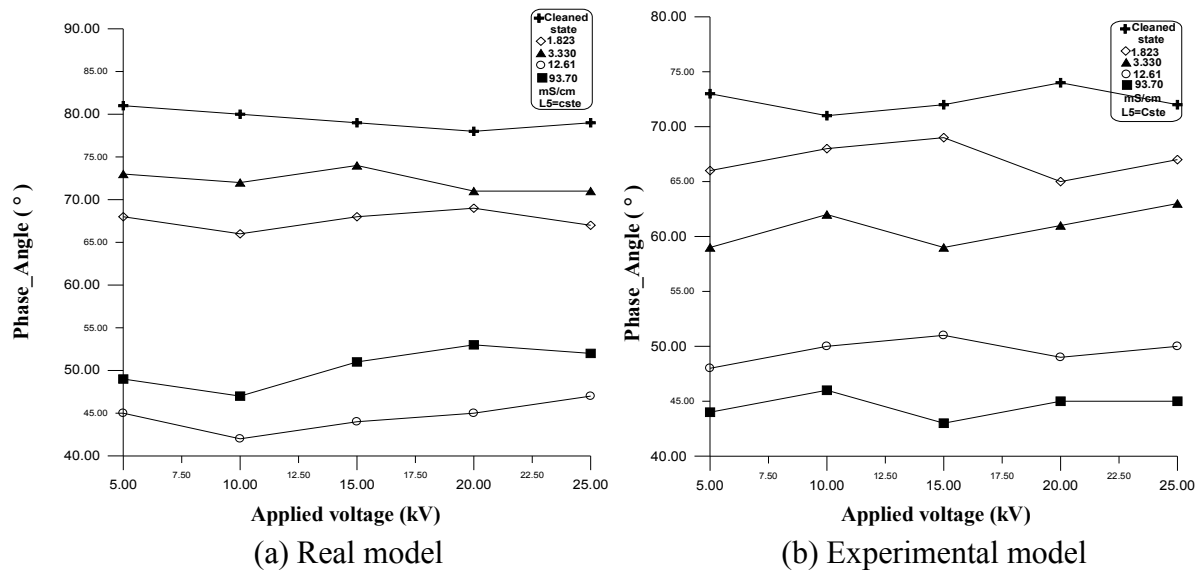


Fig. I.37. Angle phase -applied voltage for different conductivities, $L_5 = Cste$.

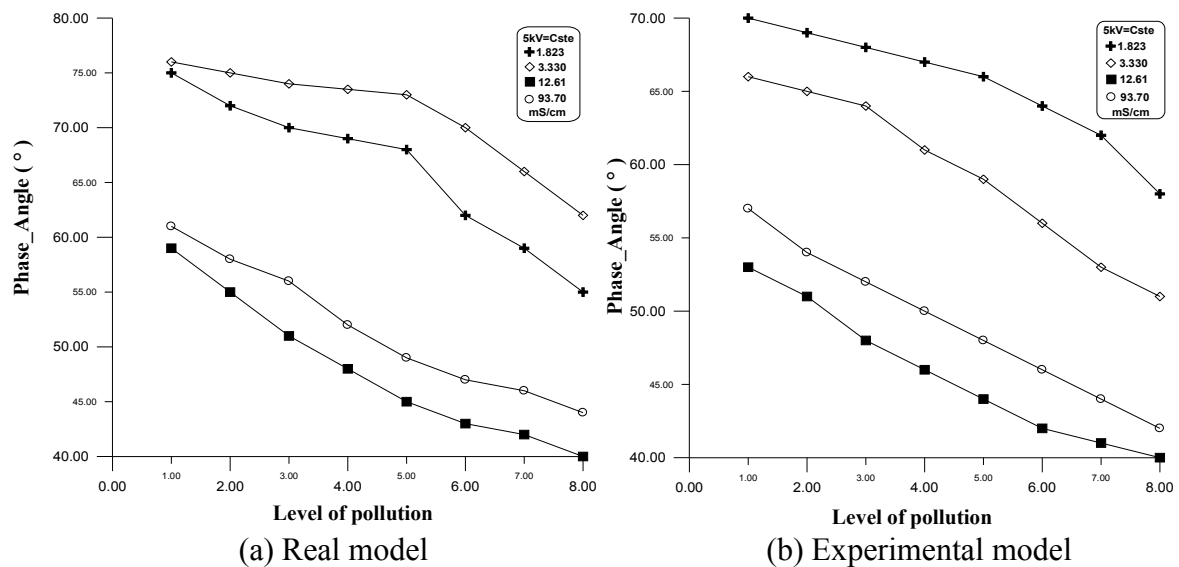


Fig. I.38. Angle phase -level of pollution, for different conductivities, $5kV = Cste$.

I.4.Conclusion

The aim of this work is to determine the leakage current, the flashover voltage, the phase angle as well as the influences of the level and the conductivity of pollution on the performance of the polluted insulators.

In our chapter, the tests carried out at the High Voltage Laboratory of the University of BISKRA were aimed at studying the behavior of the artificially polluted cap and pin insulator type 1512L, and the proposed model when an AC voltage is applied.

In this present work we exposed the principal experimental results relating to the influence of the discontinuity of the polluting layer on the behavior of a model of the insulator of high voltage cap and pin of the 1512L type and its proposed experimental model tested

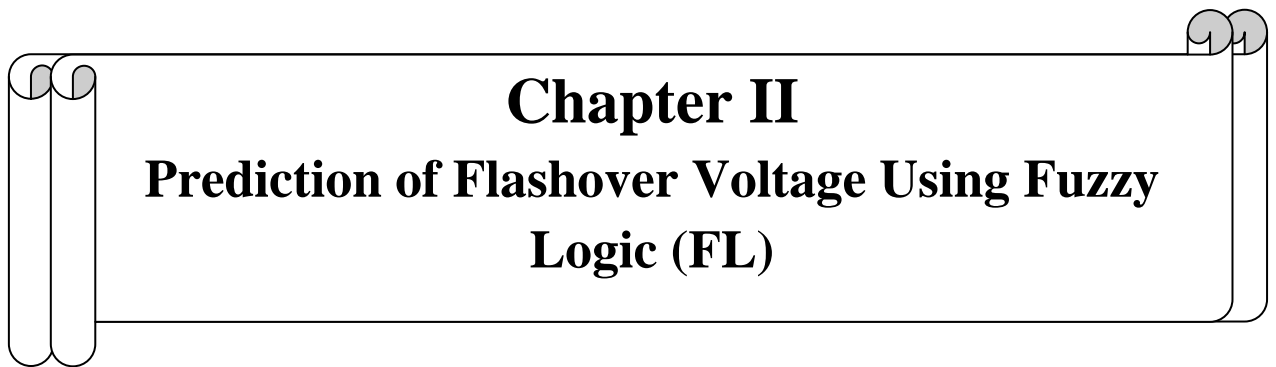
under an alternating voltage. We carried out many tests in the laboratory for the two models (real one and the proposed model). Several solutions of various conductivities (1.823mS/cm, 3.33mS/cm, 8.02mS/cm, 12.61mS/cm, 16.32mS/cm, 30.5mS/cm, 50.4mS/cm, 3.7mS/cm) and a distribution of pollution (discontinuous by pulverizing the surface of the experimental model and filling different zones of the real one) were applied.

During the experimental tests, we followed the variations of the voltage flashover as well as the leakage current. We concluded that the flashover and the leakage current change according to the conductivity and the width of the polluting layer.

Indeed, the flashover decreases with the increase in the surface conductivity of pollution. Consequently, the insulator is less rigid when it is applied a polluting layer. It is obvious that the flashover voltage is affected by the surface quality of the insulator. The flashover is more important in the case of the dry state than in the polluted case. According to the width and the conductivity of pollution, the low voltage of the flashover has been obtained for the level of pollution 8 and conductivity 93,7 mS/cm.

It is clear that the isolator in the dry and clean state is characterized by a capacitive effect. The humidification or filling of the insulator generates, in general, a decrease in this capacitive character by making it more resistive.

In the next parts we apply the methods of artificial intelligence to make the validation of the experimental results for our real model.



Chapter II
Prediction of Flashover Voltage Using Fuzzy
Logic (FL)

II.1. Introduction

Today, fuzzy logic is an important research focus of many scientists. Technological spin-offs are already available, both in the field of the general public (cameras, washing machines,...) and in the industrial field (regulation and control of complex processes related to energy, transport, the transformation of matter, robotics and machine tools).

The difficulty of obtaining a full mathematical model to study the phenomenon of pollution in the field of high voltage has prompted several researchers to introduce different analyzes, models and methods to study such a subject. In what follows, we will use the artificial intelligence (AI) technique to predict the flashover voltage of a real model of the 1512L high voltage insulator.

The objective in this part is to predict the flashover voltage under different electro-geometric conditions, such as conductivity, pollution levels where the fuzzy logic technique has been applied.

In this chapter, we will present the theory of the artificial intelligence technique (Fuzzy Logic (FL)) as well as the methodology followed to predict the flashover voltage of a real 1512 L high voltage insulator model. Therefore, the exploitation of the results obtained during our work will be presented and interpreted under the normal conditions and with different electro-geometric configurations.

II.2. Fuzzy Logic (FL)

For a long time, man has sought to master the uncertainties and imperfections that are peculiar to his nature. The first real manifestation of the desire to formalize the taking into account of uncertain knowledge has been the development of the theory of probability from the XVII century. However, the probabilities cannot control psychological and linguistic uncertainties. Therefore, subjective probability theories were developed (in the 1950s), obviously (in the 1960s) [1-2], and later the Logic.

This is an extension of Boolean algebra by Lofti Zadeh in 1965 based on his mathematical theory of fuzzy sets, which is a generalization of the classical set theory. [3-4] By introducing the level concept in the checking of a condition which can be in a state other than true or false, the fuzzy logic provides a very appreciable flexibility for the reasoning it uses it, which the consideration of inaccuracies and uncertainties very possible. One of the major interests of the fuzzy logic in the formalization of human reasoning is that the rules are spelled out in a natural language.[5]



In 1970: First experiences in Europe.

1980's: Applications in Decision Making and Data Analysis. [6]



1980's: Fuzzy logic has been introduced in Japan by researcher M. Sugeno. Japanese companies quickly realized its technical and commercial advantage. The research has been not only theoretical but also applied. Application for industrial control, strong growth in the use of fuzzy systems. [6]



Mid-1990's: Appear in many applications in Germany and on a smaller scale in the United States of America. First US applications (competition requires), combination with neural networks. [6]

The fuzzy logic is a very powerful problem-solving technique with a wide applicability in the control and decision-making process [7-8]. It is very useful when the mathematical model of the problem to be treated does not exist or exists but difficult to implement, or it is too complex to be relatively quickly evaluated for real-time operations (our case) [7-10], or when human experts are available to provide subjective descriptions of the system behavior with terms in a natural language. The fuzzy logic is also meant to work in situations where there is a broad uncertainty and unknown variations in the system parameters and structure.

II.3. Fuzzy logic vs. classical logic

The fuzzy logic is an extension of the classical logic capable of modeling of the data weaknesses and to some extent gets close to the flexibility of human reasoning .[6-10] In the classical logic, the managed variables are Boolean, that is to say, they take only two values 0 or 1. However, the fuzzy logic aims at reasoning on the basis of the imperfect knowledge that shows resistance to the classical logic. For this reason, the fuzzy logic suggests replacing the Boolean variables with fuzzy ones [11]. In fact, the fuzzy logic, which is based on fuzzy sets, uses a natural language besides; it is characterized by its generalization. Actually, it is considered as an alternative through the experience of an expert when the deterministic model is difficult to obtain. Moreover, it is used in several fields, such as in control and regulation, in signal processing, and in robot control. .[8,12]

II.4. Basic concept of fuzzy sets

The concept of a set is one of the fundamental mathematical concepts, however, it cannot reflect the simple and quite frequent situations because in the theory of classical sets, an element belongs or does not belong to a given set. For example, it is easy to define all the men among people, however, it is impossible to define all older men who do not become old overnight but they gradually age. For the purpose of taking into account such situations, L. Zadeh introduced the notion of a vague set based on the concept of partial membership. [13-14]

II.4.1. The membership functions

The fuzzy set A can be defined by a set of pairs 'membership degree element' [3]:

$$A = \int_x \mu_A(x) / x \quad (\text{II.1})$$

Such as :

X is a point space with a generating element x , therefore $X = \{x\}$. A fuzzy set A in X is a set defined by its function $\mu_A(x)$ which, with each point in X , associates a real number belonging to interval [0 1].

$$\mu_A(x) : x \rightarrow [0 \ 1] \quad (\text{II.2})$$

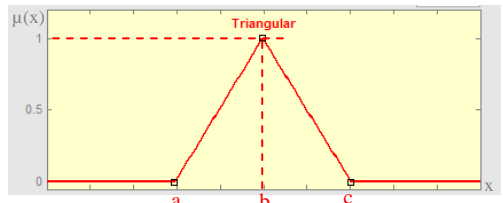
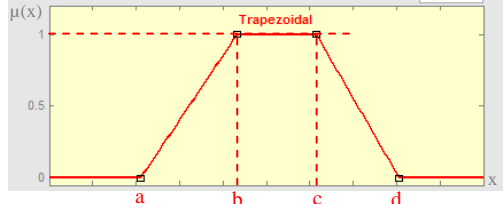
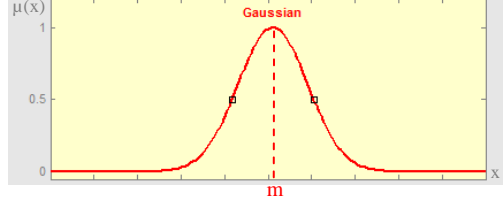
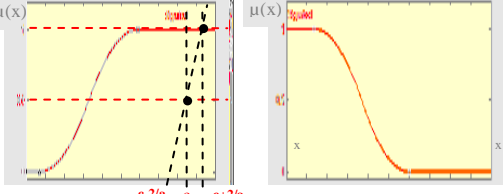
This real number represents the membership degree of x in A:

$$\mu_A(x) \begin{cases} = 1 & x \text{ is a full element of } A \\ \in]0 \ 1[& x \text{ is a full element of } A \\ = 0 & x \text{ is not a full element of } A \end{cases} \quad (\text{II.3})$$

Each fuzzy subset can be represented by its membership function.

Hence, the main membership functions presented in table II.1 are summarized in the following table:

Tab. II.1. Principal membership functions.

Name	Form	Equation
Triangular membership function		$\mu(x) = \begin{cases} \frac{x-a}{b-a} & \text{if } x \in [a, b] \\ \frac{c-x}{c-b} & \text{if } x \in [b, c] \\ 0 & \text{if } x \text{ is elsewhere} \end{cases}$
Trapezoidal membership function		$\mu(x) = \begin{cases} \frac{x-a}{b-a} & \text{if } x \in [a, b] \\ 1 & \text{if } x \in [b, c] \\ \frac{d-x}{d-c} & \text{if } x \in [c, d] \\ 0 & \text{if } x \text{ is elsewhere} \end{cases}$
Gaussian membership function		$\mu(x) = e^{-\frac{1}{2}\left(\frac{x-m}{\sigma}\right)^2}$ <p>where : σ, m: the variance, Average of the Gaussian.</p>
Sigmoid membership function		$\mu(x) = \frac{1}{1 + \exp(-a(x-c))}$

II.4.2. Reasoning in Fuzzy Logic

Reasoning is the most important sub-part and the essence of the fuzzy logic. [7,12] In the classical logic, the arguments are of the form:

$$\left\{ \begin{array}{l} \text{If } p \text{ then } q \\ \text{If } p \text{ is true, then } q \text{ is true} \end{array} \right\}$$

In the fuzzy logic, the fuzzy reasoning, which is called approximate reasoning, is based on fuzzy rules expressed in a following natural language using the language variables of the form:
If [premises] then [conclusion].

The result of the application of a fuzzy rule depends on two factors:

- The definition of the membership function of the fuzzy set of the proposal provided in the conclusion of the fuzzy rule.
- The degree of the proposal validity located in the premise.

II.5. The Fuzzy logic controller

Management of the traffic road, air traffic control, the environment, medicine, and many others. It has been introduced into the world of systems control for the first time by Mamdani and Assilian in 1974 [5], in the Fuzzy Logic Controller (FLC). [15] A fuzzy controller has the following elements:

II.5.1. The linguistic variables

A linguistic variable is characterized by a quintuple $(V, T(V), X, G, M)$ in which:

- V is the name of the variable defined on the speech universe X .
- $T(V) = A_1, A_2, \dots, A_n$ is a set of linguistic terms which are fuzzy numbers that define the restrictions on the values that V takes in X . [16-17]
- G a set of syntactic rules which help form other linguistic words using $T(V)$. These rules are called linguistic modifiers. For instance, in order to define the membership function of the linguistic term «pas A », we use the expression:

$$\mu_{pas(A)} = 1 - \mu_A \quad (\text{II.4})$$

- M is the set of semantic rules that define the linguistic terms. [16-17]

Figure II.1 shows an example of the "speed" linguistic variable using three linguistic terms: small, medium and large.

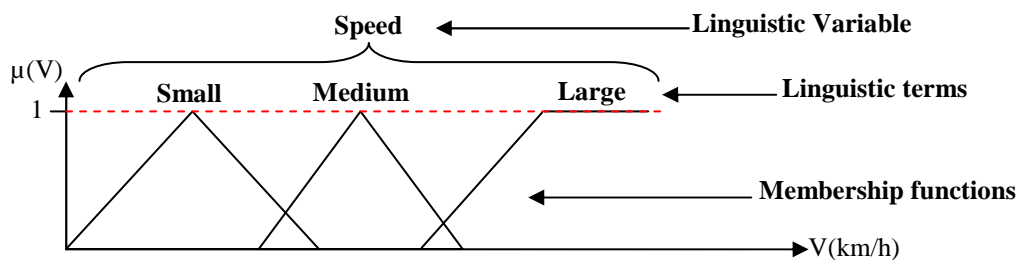


Fig. II.1. Linguistic variable.

II.5.2. Fuzzification

Fuzzification is carried out in the input interface of the fuzzy controller. [18] During this phase, information from the system is first standardized and then transformed into language skills using semantic rules defined by an expert. During the normalization phase, each measurement from the system is modified to provide a value belonging to a relatively simple speech universe.

The discourse universe is then represented by a linguistic variable containing a relatively small number of terms (usually three, five or seven) in order to reduce the one of the rules. Finally, the normalized values deduced from each of the entries are transformed into linguistic qualifications using the corresponding linguistic variables.

During the fuzzification stage, each input and output variable is associated with fuzzy subsets. [12,15]

II.5.3. Fuzzy rules

The fuzzy rules make us deduce knowledge about the state of the system according to the linguistic qualifications provided by the fuzzification stage. This knowledge is also a language qualification. Usually, the fuzzy rules are deduced from the experience acquired by the operators or experts. This type of knowledge is translated into simple rules that can be used in a fuzzy inference process. For example, if an expert expresses the rule, "if the water temperature is warm, cold water should be added", the system will use a rule of the type, "if p, then q". This kind of expressions forms what is called linguistic variables of the fuzzy logic.[19] This strategy will be described in more detail later in this thesis.

II.5.4. Fuzzy inference

A Fuzzy Inference System (FIS) is designed to transform input data into output data based on the evaluation of a set of rules. The inputs come from the process of fuzzification and the set of rules normally are defined by the expert's skills. [20]

An FIS consists of four steps:

- Fuzzing (fuzzification);
- Inference;
- Defuzzification;
- The fuzzy knowledge base. [20-21]

Fuzzy inference is a fuzzy relationship defined between two subsets. The definition of this relationship can theoretically involve any combination operator. However, the fuzzy inferences defined by Mamdani and Takagi-Sugeno are often used.

II.5.4.1. Mamdani's fuzzy inference

Let us suppose that the knowledge base consists of n inference rules each of which contains premises and a conclusion. The inference process can be described by the following schema: [19,22-23]

Rule 1: Si (x_1 is A_{11}) and... and (x_m is A_{1m}); then (Y is B_1)

Rule 2: Si (x_1 is A_{21}) and... and (x_m is A_{2m}); then (Y is B_2)

Rule n: Si (x_1 is A_{n1}) and... and (x_m is A_{nm}); then (Y is B_n)

In which x_1, \dots, x_m are elements of the discourse universe X_1, \dots, X_m and $A_{ij}, (j = 1, \dots, m)$, are fuzzy quantities on the discourse universe X_i , and $B_j, (j = 1, \dots, m)$, are also vague quantities on the discourse universe Y . In order to define a single premise for a rule i , the propositions « x_j is A_{ij} », ($j = 1, \dots, m$), are combined by the minimum operator. The membership function of this unique premise is therefore given by:

$$\mu_{R_{A_i}}(x_1, \dots, x_m) = \mu_{A_{i1}}(x_1) \wedge \dots \wedge \mu_{A_{im}}(x_m) \quad (\text{II.5})$$

II.5.4.2. Takagi-Sugeno-Kang's fuzzy inference

This topic discusses the Sugeno, or Takagi-Sugeno-Kang, method of fuzzy inference. Introduced in 1985 [24], this method is similar to the Mamdani method in many respects. The first two parts of the fuzzy inference process, fuzzifying the inputs and applying the fuzzy operator, are the same. The main difference between Mamdani and Sugeno is that the Sugeno output membership functions are either linear or constant. A typical rule in a Sugeno fuzzy model has the form:

If Input 1 is x and Input 2 is y , then Output is:

$$z = ax + by + c \quad (\text{II.6})$$

Takagi-Sugeno proposed a fuzzy inference method that guarantees the continuity of the output. This method of inference is very effective in applications involving both linear and adaptive optimization techniques.[23] In Sugeno's inference, the fuzzy rules are expressed as follows:

Rule i : if (x_1 is A_{i1}) and.... and (x_m is A_{im}); then $y = f_i(x_1, \dots, x_m)$

in which x_1, \dots, x_m and y are elements of the discourse universe X_1, \dots, X_m and A_{i1}, \dots, A_{im} are linguistic terms on these same universes of discourse. y is a function of x_1, \dots, x_m . Compared to Sugeno's inference, Mamdani's inference is more intuitive, more general, and is particularly suited to the use of knowledge derived from human expertise.[19,21,25-26]

II.5.5. Defuzzification

Defuzzification consists of characterizing the linguistic variables used in the system. It is therefore a transformation of the real inputs into a fuzzy part defined on a representation space

linked to the input. This representation space is normally a fuzzy subset. During the fuzzification stage, each input and output variable is associated with fuzzy subsets. [27,28]

II.5.6. The fuzzy knowledge base

It contains the set of the fuzzy rules describing the system behavior.

II.5.7. Diagram of the fuzzy control

Figure II.2 Shows a general structure of a fuzzy logic-based system (FL). The implementation of a fuzzy control revealed three large modules.[29]

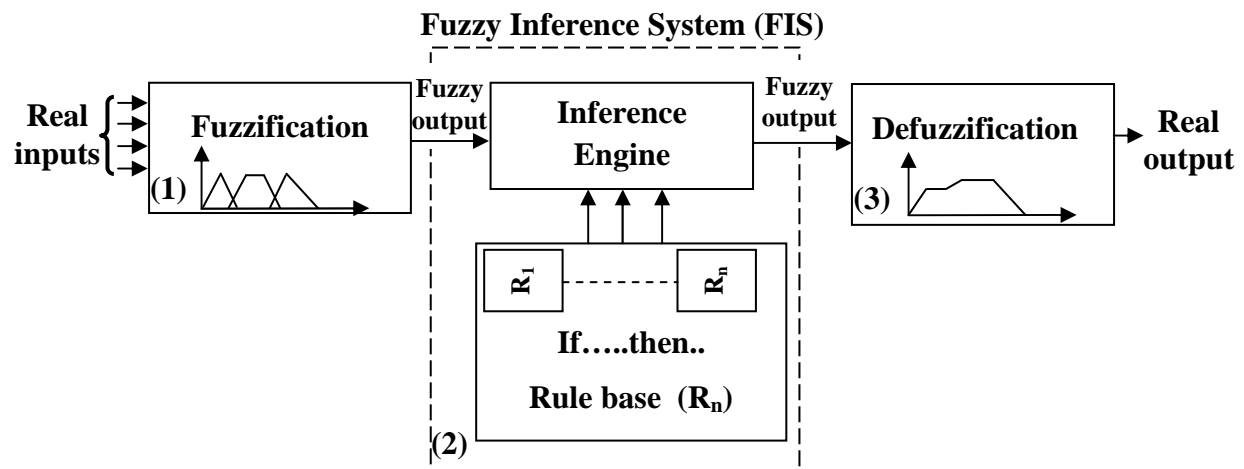


Fig. II.2. General structure of a system based on fuzzy logic (FL).

- **The first module (1)** deals with the system inputs (setting values). First, we define a discourse universe, a partitioning of this universe into classes for each input, and membership functions for each of these inputs (for example, large, small, weak pressure, and change of the measurement deviation from the material flow from a very high, high, medium, negative, and very negative hopper). The first step, which is called fuzzification, consists in attributing to the real value of each entry, at time t , its function of belonging to each of the previously defined classes, which transforms the actual entry into a fuzzy subset.
- **The second module (2)** is the set of rules and the choice of fuzzy operators. It transforms the fuzzy part resulting from the fuzzification phase into a new fuzzy part in accordance with the fuzzy rules, and associates each rule with an output value. This module is composed of a rule base and an inference engine that helps with the calculation.

- **The third module (3)** and the last one describe the defuzzification step, which is the inverse transformation of the first one. It makes it possible to pass from a control belonging degree to the determination of the value to assign to this control.

II.6. Prediction of flashover voltage using Artificial Intelligence (AI)

Experimental (practical) tests can help us determine the flashover voltage of a high voltage insulator. These tests are performed under very specific conditions of temperature, pressure, humidity, type of voltage applied to the insulator ... etc.

The study of the flashover of insulators under AC voltage can be carried out by practical tests or by studies of mathematical modeling of the insulator behavior under the effect of the different constraints applied to it.

The artificial intelligence techniques can also be used in the study of the insulator behavior under the effect of different constraints, in particular, in the prediction of the insulator flashover voltage. In our study, we will use one of the artificial intelligence techniques, which is the fuzzy logic to predict (calculate) the flashover voltage of a high-voltage insulator. The application of this technique in such a study requires the definition of the various parameters necessary for its implementation, such as, the inputs, the outputs, the inference engine,.... etc.

The objective of this chapter is to arrive at the determination of the inference table, which is an essential element in our study by fuzzy logic based on the practical tests carried out in the first chapter that can help us to collect a base of data that will allow us to create this inference table.

In this work, we will present the experimental tests carried out and used in the creation of our fuzzy inference system (FIS) proposed for the prediction of the flashover voltage to be studied and the results obtained with the absolute error and the value of the voltage calculated in the prediction. These tests are performed in the high voltage laboratory of the University of Biskra.

It should be noted that the experimental tests presented in this part were conducted by Hani et al [30]. In fact, we used the results they obtained for the creation of our FIS. The purpose of the fuzzy inference system (FIS) is to predict the flashover voltage of the 1512L cap and pin insulator, which is used by the Algerian Electricity and Gas Company (SONELGAZ).

II.6.1. Prediction of the flashover voltage by the Fuzzy Logic (FL)

Flashover modeling by fuzzy logic has been a topic of interest for many researchers [29-31]. A major problem in all those investigations is the definition of the numbers and values of terms linguistic (variable linguistic) of the inputs. In this part of our study, we use the FIS (Fuzzy Inference System) for the prediction of the flashover voltage (V) of a high voltage insulator subjected to various pollution constraints, such as (conductivity (δ (mS/cm)) and the pollution zones Z_i (ml), given that ' δ ' is the conductivity of the applied pollution, " Z_i " and the areas of the insulator which were mentioned in the previous chapter and [32].

The aim of the fuzzy logic is to formulate and implement human reasoning. It is well known that the latter, in most studies, involves the opinion of an expert in different fields, especially for the creation of the inference table, which is the most difficult element to be identified in the literature by means of the fuzzy logic analysis.

A fuzzy logic system takes, as an input, inaccurate data and vague expressions (such as small, medium, large) and provides decisions on the output variables which are themselves fuzzy [33-34].

The advantage of the use of fuzzy logic is to include the observation and analysis of human expert when this observation is difficult to expressed mathematically. The proposed fuzzy concept, is formed by a fuzzy inference system "FIS" shown in figure II.3.

During tests we have noticed that the electrical discharge develops by increasing the applied voltage. It occupies some percentage of the insulator surface at the beginning of its development.

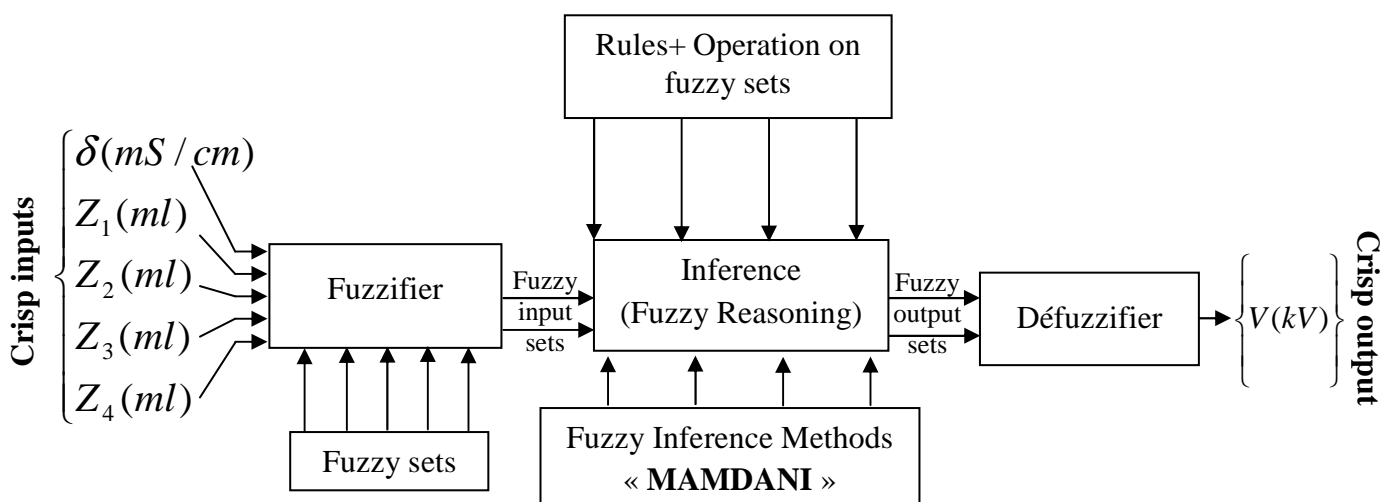


Fig. II.3. Architecture of a fuzzy inference system (FIS) studied.

Our problem formulation in the fuzzy logic requires the definition of:

II.6.1.1. The inputs and outputs of the FIS (Fuzzy Inference System)

The inputs and outputs chosen for our study are given in table II.2.

Tab. II.2. Variable of inputs and output.

Input		Output	
Symbol	Designation	Symbol	Designation
δ (mS/cm)	Conductivities	V(kV)	Flashover Voltage
Z_i (Z_1, Z_2, Z_3, Z_4) (ml)	Pollution zones in the HV insulator		

II.6.1.2. The fuzzy characteristics

The truth values are mentioned in the following table II.3. The discourse universes or intervals of these values are shown in figure II.4 to figure II.9.

Tab. II.3. Decomposition of input and output variables.

Input										Output	
Linguistic Variable of Inputs and Outputs											
Conductivities δ (mS/cm) [0 – 94]		Zone Z_1 (ml) [0 - 150]		Zone Z_2 (ml) [0 - 120]		Zone Z_3 (ml) [0 - 270]		Zone Z_4 (ml) [0 - 270]		Flashover Voltage V(kV) [20 - 80]	
TL	S	TL	S	TL	S	TL	S	TL	S	TL	S
VSC	Very small conductivity [0–2]	SQ1	Small Quantity [0–57]	SQ2	Small Quantity [0–39]	SQ3	Small Quantity [0–20]	SQ4	Small Quantity [0–30]	VSV	Very small Voltage [20 – 44]
SC	Small conductivity [2–15]	AQ1	Average Quantity [40–101]	AQ2	Average Quantity [27–75]	AQ3	Average Quantity [14–215]	AQ4	Average Quantity [18–228]	SV	Small Voltage [39 – 49]
AC	Average conductivity [13–29]	HQ1	High Quantity [84 -150]	HQ2	High Quantity [64-120]	HQ3	High Quantity [196-270]	HQ4	High Quantity [211-270]	AV	Average Voltage [47 – 67]
HC	High conductivity [27–59]	TL : Language Term S : Meaning								HV	High Voltage [51–78]
VHC	Very high conductivity [60–94]									VHV	Very high Voltage [56-80]

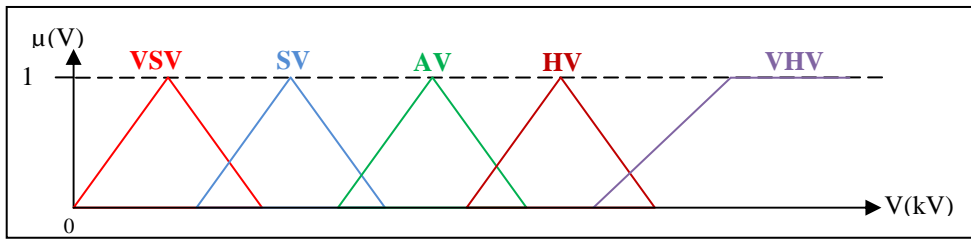


Fig. II.4. Membership function of the output (V).

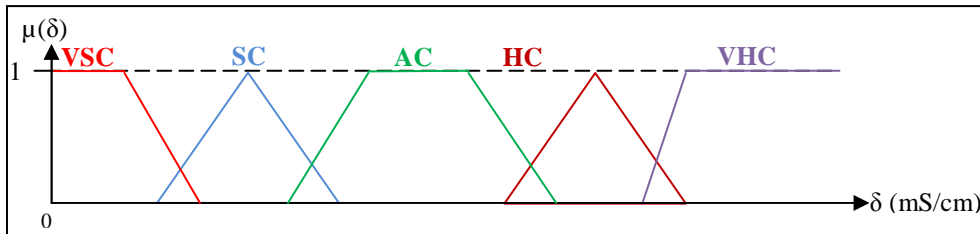


Fig. II.5. Membership function of the conductivities (δ).

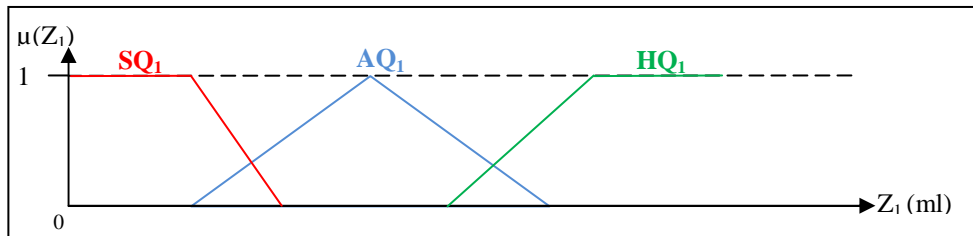


Fig. II.6. Membership function of zone 1 (Z1).

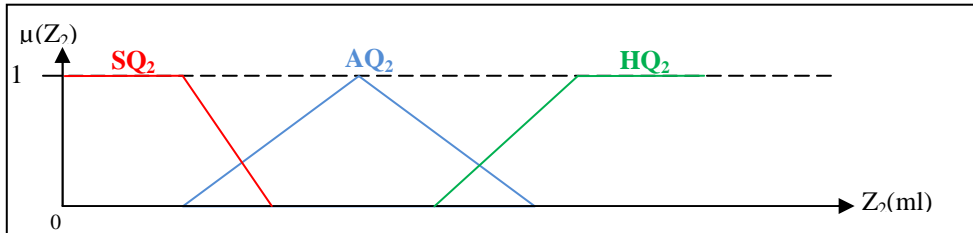


Fig. II.7. Membership function of zone 2 (Z2).

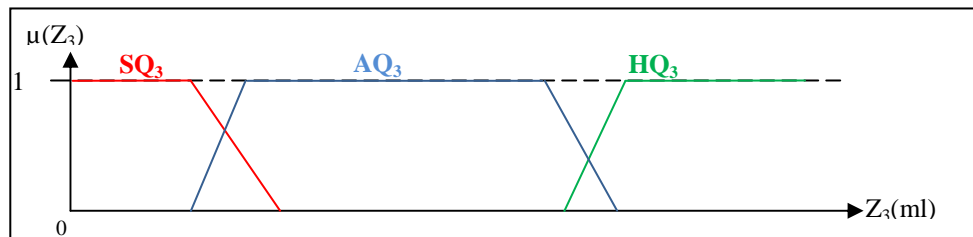


Fig. II.8. Membership function of zone 3 (Z3).

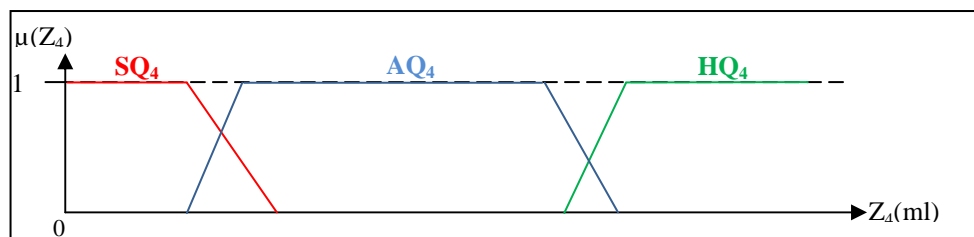


Fig. II.9. Membership function of zone 4 (Z4).

The fuzzy intervals for each language variable in the previous table are chosen to include all values that may indicate one of the flashover steps. Voltage values "V" below "20 kV" mean that no step is reached.

II.6.1.3. The membership functions of the input and output variables

They are shown in figures (II.4 to II.9) and the discourse universes (intervals of these truth values) of the Inputs and output variables, which are defined in the figures.

II.6.1.4. The fuzzy inference rules

In this section the fuzzy rules connecting the sub-sets of inputs and outputs have been entered. This stage consists in identifying the relations between the input and output set based on what has been obtained as results in practice. The following table shows the relationships between inputs and output in linguistic terms.

			VSC			SC			AC			HC			VHC			
			SQ1	AQ1	HQ1	SQ1	AQ1	HQ1	SQ1	AQ1	HQ1	SQ1	AQ1	HQ1	SQ1	AQ1	HQ1	
SQ4	SQ3	SQ2	VHV	HV	HV	HV	HV	AV	HV	HV	AV	AV	AV	AV	SV	SV	SV	
		AQ2	HV	HV	HV	HV	HV	AV	HV	AV	AV	AV	AV	AV	SV	SV	SV	
		HQ2	HV	HV	HV	HV	AV	AV	HV	AV	AV	AV	AV	AV	SV	SV	SV	
	AQ3	SQ2	X	X	X	X	X	X	X	X	X	X	X	X	X	X	X	X
		AQ2	X	X	X	X	X	X	X	X	X	X	X	X	X	X	X	X
		HQ2	X	X	X	X	X	X	X	X	X	X	X	X	X	X	X	X
	HQ3	SQ2	X	X	X	X	X	X	X	X	X	X	X	X	X	X	X	X
		AQ2	X	X	X	X	X	X	X	X	X	X	X	X	X	X	X	X
		HQ2	X	X	X	X	X	X	X	X	X	X	X	X	X	X	X	X
AQ4	SQ3	SQ2	X	X	X	X	X	X	X	X	X	X	X	X	X	X	X	
		AQ2	X	X	X	X	X	X	X	X	X	X	X	X	X	X	X	
		HQ2	X	X	X	X	X	X	X	X	X	X	X	X	X	X	X	
	AQ3	SQ2	AV	AV	AV	AV	AV	AV	AV	AV	AV	AV	AV	AV	SV	SV	SV	VSV
		AQ2	AV	AV	AV	AV	AV	AV	AV	AV	AV	SV	AV	SV	SV	SV	VSV	VSV
		HQ2	AV	AV	AV	AV	AV	AV	SV	AV	AV	SV	SV	SV	SV	SV	VSV	VSV
HQ3	SQ2	AV	AV	AV	AV	AV	AV	AV	AV	AV	AV	AV	AV	SV	SV	SV	VSV	
	AQ2	AV	AV	AV	AV	AV	AV	AV	AV	AV	SV	AV	SV	SV	SV	VSV	VSV	
	HQ2	AV	AV	AV	AV	AV	AV	SV	AV	AV	SV	SV	SV	SV	SV	VSV	VSV	
HQ4	SQ3	SQ2	X	X	X	X	X	X	X	X	X	X	X	X	X	X	X	
		AQ2	X	X	X	X	X	X	X	X	X	X	X	X	X	X	X	
		HQ2	X	X	X	X	X	X	X	X	X	X	X	X	X	X	X	
	AQ3	SQ2	AV	AV	AV	AV	AV	AV	AV	AV	SV	SV	SV	SV	SV	SV	SV	SV
		AQ2	AV	SV	SV	AV	SV	SV	SV	SV	SV	SV	SV	SV	SV	SV	SV	SV
		HQ2	SV	SV	SV	SV	SV	SV	SV	SV	SV	VSV	VSV	VSV	VSV	VSV	VSV	VSV
	HQ3	SQ2	AV	AV	AV	AV	AV	AV	AV	AV	SV	SV	SV	SV	SV	SV	SV	SV
		AQ2	AV	SV	SV	AV	SV	SV	SV	SV	SV	SV	SV	SV	SV	SV	SV	SV
		HQ2	SV	SV	SV	SV	SV	SV	SV	SV	SV	VSV	VSV	VSV	VSV	VSV	VSV	VSV

Tab. II.4. Inference matrix

- The boxes that contain the symbol "X" are cases that cannot be made in laboratories. (False combination) (Illogical).

II.6.1.5. Fuzzification

This section consists in calculating, for each numerical input value, the membership degrees of the fuzzy sets associated and predefined in the fuzzy system database. This block achieves the conversion of the digital inputs into fuzzy symbolic information which can be used by the inference mechanism. The used experimental database is that of our laboratory cited in [31] about a real insulator.

The database processing, which takes into account all the findings and observations during the tests, helps identify the impact of each input on the flashover voltage.

- The existence of a low conductivity and a low level of pollution implies that the insulator is rigid and the flashover voltage is high.
- An average conductivity and a low pollution level means that the flashover voltage is average and thus the system becomes less rigid.
- The flashover voltage depends on both the conductivity and the level of pollution.
- In general, our experience in the high voltage laboratory helped us deduce how the evolution of the electric arc has a variety of pollution conditions under an AC voltage, This made us suggest the discourse universes and the fuzzy intervals for each input and output variable.
- The input discourse universe is chosen given that each linguistic variable can represent a stage.
- The output discourse universe is selected on the basis that that each "V" value can represent a flashover stage, as has been already explained and detailed in the previous chapter, and that the evolution of the flashover voltage can be presented by means of different values.
- A bibliographic research showed that the choice of the membership function is random. In our case, we have chosen the triangular and trapezoidal membership function, which may be suitable first to represent the fuzzy variables of the input and the output of the FIS since it shows a stable value of the variable on a given interval. This form can be altered to improve the achieved results, in other words, it is the best choice that gives the best result.

a. The linguistic variable and the fuzzy interval

Actually, the input and output fuzzy variables already mentioned in table II.3, and their discourse universes (fuzzy intervals) are shown in figures II.4 to II.9.

The choice of the input and output linguistic terms is made in a random way so as to explain the concept.

b. The membership function

A fuzzy set is defined by its membership function that corresponds to it. All the membership functions are inputs and outputs, which will be presented in the next titles.

The choice of the type of the membership function is based on our expertise. Before introducing the types of membership functions that we have chosen, the fuzzy intervals and variables as well as the discourse universe should be chosen from the start.

Table II.5 gives the number of functions and fuzzy intervals chosen for the inputs and outputs, the number of the input and output variables and the type of the chosen membership function. In fact, there is no rule that should be followed in choosing the number of the variables or the intervals or even the form of the membership function, Therefore, only the results of the prediction of the flashover voltage of the real insulator obtained for each choice can judge the efficiency and reliability of our proposed model.

Tab. II.5. Number of fuzzy intervals, number and type of membership function of the inputs and the output.

		Number of intervals	Number of functions	Type of functions
Inputs	Conductivities δ (mS/cm)	5	5	Trapezoidal & Triangular
	Zone 1 Z1(ml)	3	3	
	Zone 2 Z2(ml)	3	3	
	Zone 3 Z3(ml)	3	3	
	Zone 4 Z4(ml)	3	3	
Output	Flashover voltage (kV)	5	5	

II.6.2. The fuzzy rules

In this stage, the fuzzy rules that connect the input and output subsets have been applied. This step is performed in order to determine the relationship between the input and output set based on what has been obtained as results in practice (in the experimental) in the first chapter. Moreover, the rules are always set by a qualified expert or an operator, which is one of the most used methods.

We used our experimental result to exploit and elaborate the set of fuzzy rules of our used FIS, and validate our FL based prediction system.

To take into account all the cases and the intermediate states, an inference matrix (table II.4) has been used. It contains the best fuzzy rules that gave the best output with a minimum error. This matrix helped illustrate 405 cases ($5*3*3*3*3$) where there are 180 cases identified in table "X", which are cases that can't be achieved in practice because they are false combinations; therefore, we finally have 225 rules to calculate the "V" output.

Other researchers showed that expertise has the right to reduce the number of rules by keeping the same results. We tried to minimize the rules and ultimately reduce them up to 25 while keeping the same achieved results.

Actually, we proposed a first set of the established rules. After that, we adjusted these rules as well as the membership functions to improve the results according to the collected experimental data. The inference table (IV.4) contains the best fuzzy rules that gave the best outputs. The method of collecting these rules is a part of the natural extraction methods of the fuzzy rules by referring to an expert's skills. The adjustment of the membership functions will be detailed in this section.

These are some of the suggested rules:

- If (Conductivities (mS/cm) is VSC) and (Z1(ml) is SQ1) and (Z2(ml) is SQ2) and (Z3(ml) is SQ3) and (Z4(ml) is SQ4) then (flashover (kV) is VHV)
- If (Conductivities (mS/cm) is SC) and (Z1(ml) is SQ1) and (Z2(ml) is SQ2) and (Z3(ml) is SQ3) and (Z4(ml) is SQ4) then (flashover (kV) is HV)
- If (Conductivities (mS/cm) is AC) and (Z1(ml) is SQ1) and (Z2(ml) is SQ2) and (Z3(ml) is SQ3) and (Z4(ml) is SQ4) then (flashover (kV) is HV)

⋮

etc.

The operators used in this case are operators of Min-max type "**Mamdani**". To identify the output of each activated rule and the gravity center method of the "response surface" to predict the numerical value of the "V" output.

II.6.3. Implementation of the fuzzy inference system

Our objective consists in increasing the number of inputs to take into account all the constraints that affect the flashover voltage.

The graphical interface "Fuzzy logic", which is available in Matlab, will operate in this part of the current chapter to implement the fuzzy inference system "FIS" and predict the flashover voltage under an AC voltage and in various pollution conditions. A detailed description of the implementation of our fuzzy inference system "FIS" is presented in the following part.

II.6.3.1. Implementation of the Fuzzy Inference System "FIS" under MATLAB

Figure II.10 shows the used FIS. There are several ways of defining the degrees of membership of the output variable to its fuzzy sub-sets. These methods essentially differ in the way that the "and and or" operators used in the inference rules will be put into effect.

Our current work is based on the so-called "MAMDANI" analysis which is the most used in the prediction studies. The following figure shows its different chosen characteristics (MIN for the "and" operator, Max for "or", MAX for the aggregation and defuzzification per gravity centre), the input and output variables as well as the basis of the rules which are often grouped together to form the knowledge base.

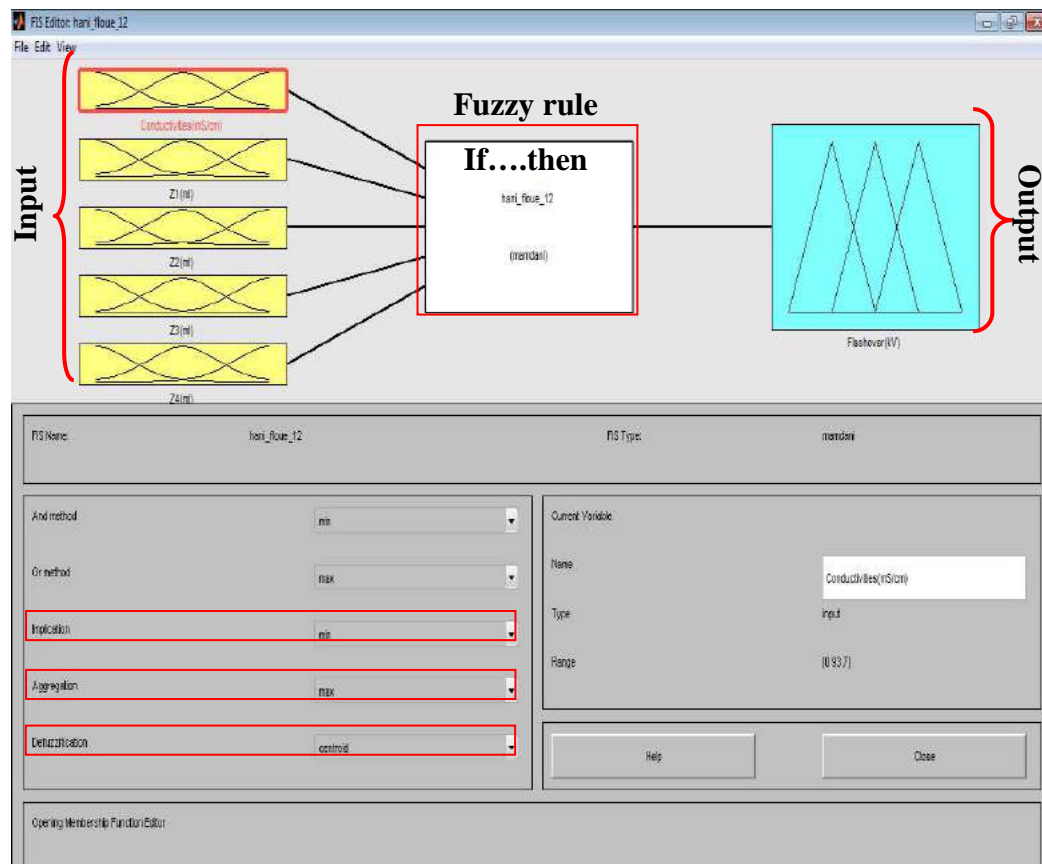


Fig.II.10. Principal window of fuzzy inference system "FIS Editor" under MATLAB

a. Fuzzification of the input and output variables

We chose " δ " conductivity and the zones (areas) " Z_i (Z_1, Z_2, Z_3, Z_4)", as input and a single output, which is the " V " flashover voltage. This choice has been made on the basis of our experiences and analyses of the experimental results. However, other tests may take other inputs and outputs.

The following figure shows the input and output creation using the FIS under MATLAB. To improve the results, we made several adjustments. In fact, we kept the forms (shapes) of the membership functions that give a minimum average error with correct predictions by comparing the experimental data in the previous chapter.

Figure II.11 shows the forms of the implemented input and output membership functions of the FIS using the fuzzy logic under Matlab in the final phase.

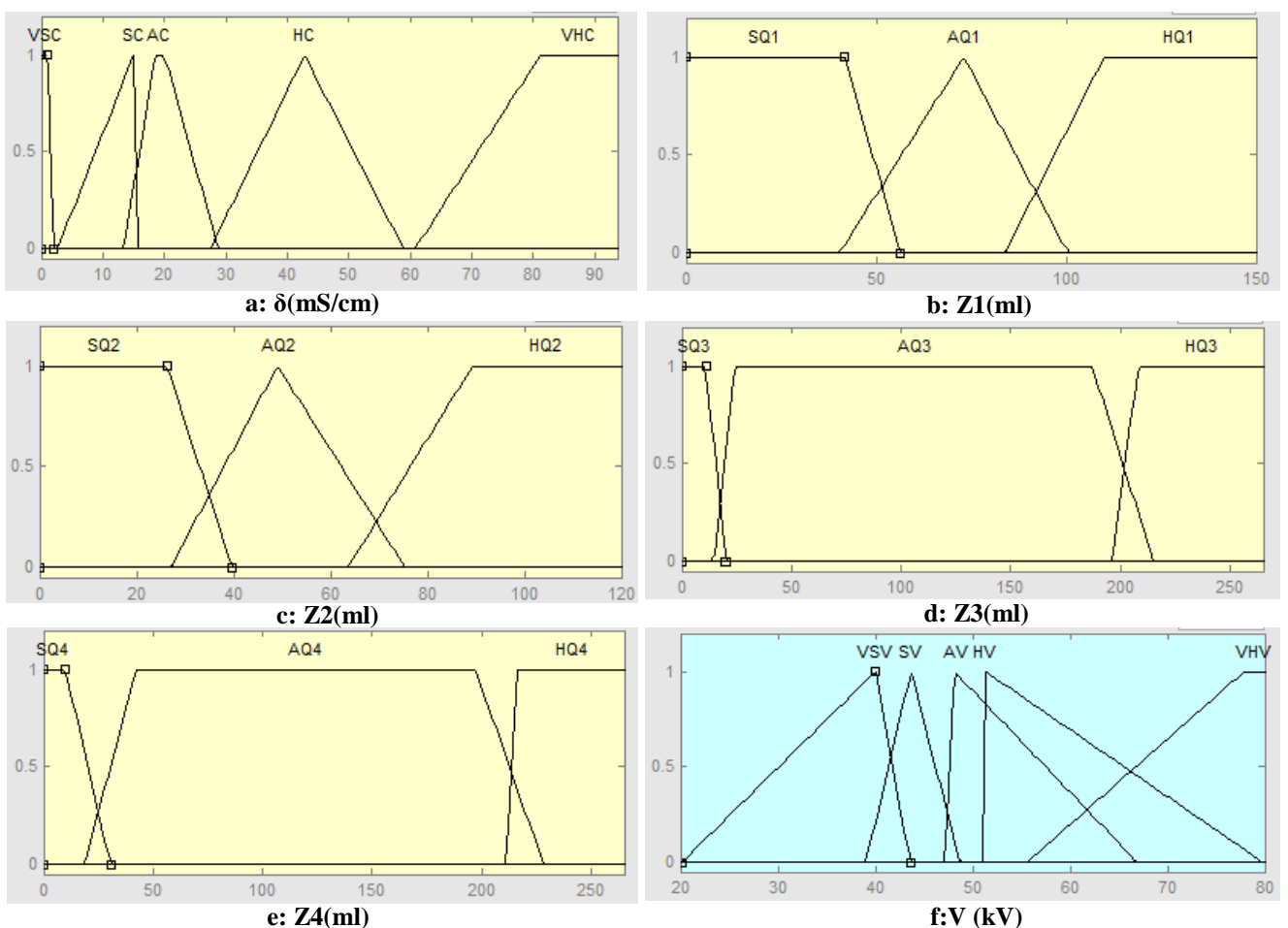


Fig. II.11. Inputs and output under the interface FIS

a,b,c,d,e: Inputs, f: Output.

b. Inference rules

Figure II.12 shows the window used to introduce the fuzzy rules applied in our FIS.

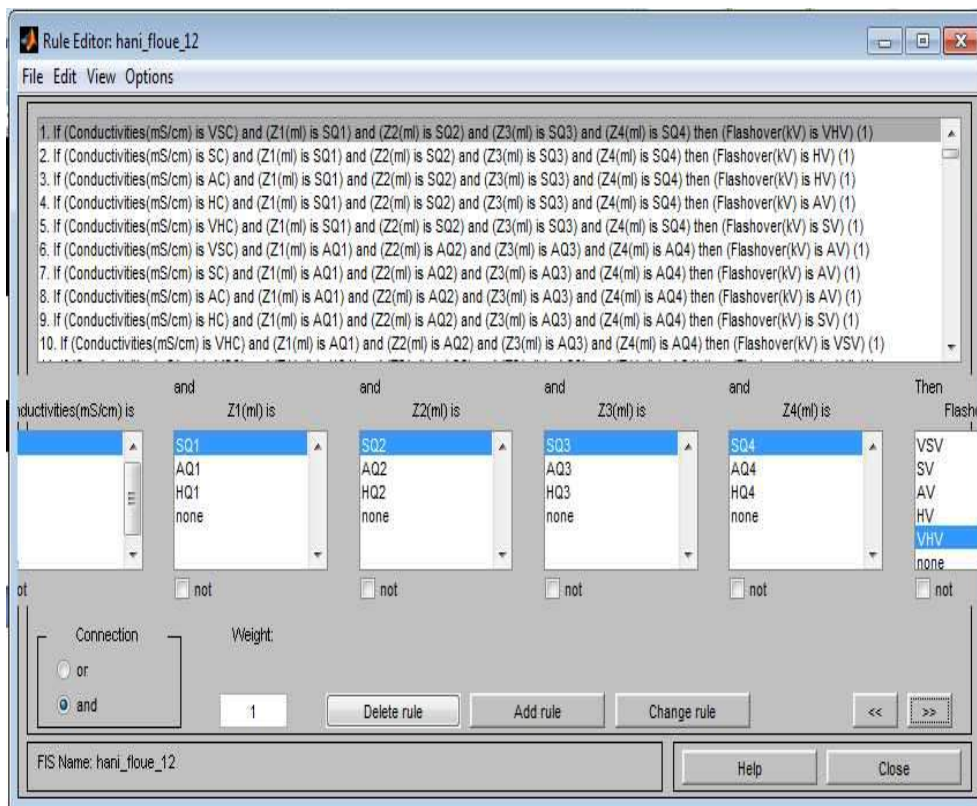


Fig. II.12. Window for visualization fuzzy rules.

- The fuzzification of five input variables is shown in table II.2.
- The appearance functions resulting 135 inference rules can be generated.
- The graphical interface "FIS" makes it possible to introduce and modify the number of rules without exceeding the maximum number. In our work the number resulting maximum 405 rules ($5*3*3*3*3$). Overlooked on the unfavorable case gains in experience, so the maximum number becomes 135 rules.
- The membership functions associated with the inputs by their linguistic terms, defining the output affected by this rule, which is also defined by its associated linguistic term.

The set of the used rules is grouped in table II.3.

c. Defuzzification

The last step to have a fuzzy operational system called the defuzzification is the method most widely used is that of the determination of the gravity centre of the resulting membership function. It is one of the most used methods.

The defuzzification stage occurs in two steps:

- The common linguistic variables should be merged by means of a fuzzy logic operator chosen by the system designer. Therefore, it is a very important step in the inference system since it enables to calculate the value of the final fuzzy output variable on the basis of the fuzzy inputs stemming from fuzzification and from all the basic rules by using an inference method.
- In a second step, we can really begin the delicate part of defuzzification. We have a series of linguistic variables that characterize the unique and same data.

Figure II.13 shows an example of the Matlab defuzzification stages. It shows (a) an example of the 25 rules Matlab defuzzification steps, (b) the same example of 135 rules Matlab defuzzification steps that gave the same results.

Figure II.13 also shows an example of the application of our FIS for the following inputs: $\delta = 3.33$ mS / cm, $Z1 = 30$ ml, $Z2 = 11$ ml, $Z3 = 15$ ml, $Z4 = 15$ ml. The vector [3,33 30 11 15 15] for both cases includes (a) 25 rules, and (b) 135 rules. The value of the calculated (predicted) output after the defuzzification shows the flashover voltage. Both cases gave the same output voltage.

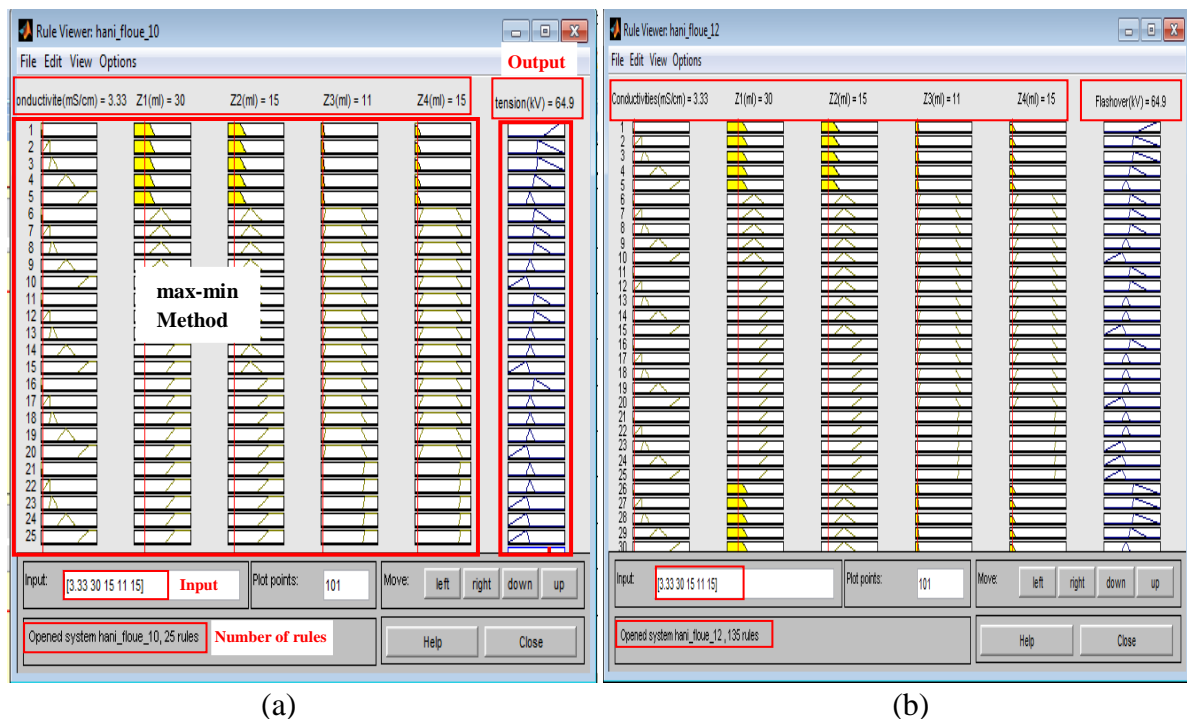


Fig. II.13. Window for visualization fuzzy rules

(a) 25 Rules, (b) 135 Rules.

I apply another example now the clean case; the vector [0 0 0 0 0] or $\delta=0$ mS/cm, $Z1=0$ ml, $Z2=0$ ml, $Z3=0$ ml, $Z4=0$ ml. The output voltage is 72 kV (predicted) for both cases (a) and (b).

II.6.3.2. Tests and validation

The prediction results obtained by the FIS for the various input values [δ , $Z1$, $Z2$, $Z3$ and $Z4$] will be shown in table II.6 and then, will be compared to the practices collected from our laboratory as well as to those obtained by simulation.

- The prediction results obtained by the FIS system under MATLAB were obtained for a trapezoidal and triangular shape (form) of the input and output membership functions.
- According to the following tables, the average error is the order of 7% (6.426%).
- These results enabled us to state that the fuzzy system is valid, efficient and reliable in predicting the flashover voltage tests of the HV 1512L insulator which has been studied and performed in the laboratory. This led us to suggest using the simulated fuzzy system to predict other results for other input values not available in the laboratory.
- The obtained results show that the fuzzy logic has a great power in the study of the flashover voltage prediction.
- The correct choice of the used fuzzy inference system parameters (input and output variables, number, type and shapes of the membership functions, the inference rules, the defuzzification method) produce better results.
- Any changes in the FIS settings may alter the results. In our study, we modified the gates of the different functions of the input and output belonging while keeping their trapezoidal and triangular forms, which helped us improve the results.

such as:

V_exp : Experimental voltage (kV),

V_cal : Calculated voltage (kV),

| Error | : Absolute error = $| V_{exp} - V_{cal} |$ (kV),

Error (%) = $| \text{Error} | * 100 / V_{exp}$ (%),

Li: Level of pollution,

Tab. II.6. Results of tests conducted in the laboratory vs calculated (predicted) our proposed model using FIS.

$\delta=1,823\text{mS/cm}$				$\delta=3,33\text{mS/cm}$			
	State of insulator [V_exp(kV)]	V_cal (kV)	Error (%)		State of insulator [V_exp(kV)]	V_cal (kV)	Error (%)
L1	Flashover	68,2	1,639	L1	Flashover	64,9	1,452
L2	Flashover	56,9	8,521	L2	Flashover	56,8	7,117
L3	Flashover	56,9	1,897	L3	Flashover	56,8	1,248
L4	Flashover	56,9	4,982	L4	Flashover	56,8	9,063
L5	Flashover	56,9	10,916	L5	Flashover	48,4	2,008
L6	Flashover	56,9	14,257	L6	Flashover	43,8	7,548
L7	Flashover	43,7	7,806	L7	Flashover	43,8	3,736
L8	Flashover	43,7	4,585	L8	Flashover	43,8	0,491
(a)				(b)			
$\delta=8,02\text{mS/cm}$				$\delta=12,61\text{mS/cm}$			
	State of insulator [V_exp(kV)]	V_cal (kV)	Error (%)		State of insulator [V_exp(kV)]	V_cal (kV)	Error (%)
L1	Flashover	62,5	2,099	L1	Flashover	61,2	1,608
L2	Flashover	55,2	4,000	L2	Flashover	55,1	0,362
L3	Flashover	55,4	0,727	L3	Flashover	55,4	5,524
L4	Flashover	55,2	8,798	L4	Flashover	54,8	13,693
L5	Flashover	44,9	5,894	L5	Flashover	44,9	0,223
L6	Flashover	43,8	2,719	L6	Flashover	43,8	1,860
L7	Flashover	43,8	0,455	L7	Flashover	43,8	6,311
L8	Flashover	43,8	2,643	L8	Flashover	43,8	10,050
(c)				(d)			
$\delta=16,32\text{mS/cm}$				$\delta=30,5\text{mS/cm}$			
	State of insulator [V_exp(kV)]	V_cal (kV)	Error (%)		State of insulator [V_exp(kV)]	V_cal (kV)	Error (%)
L1	Flashover	61,9	1,223	L1	Flashover	56,2	3,872
L2	Flashover	55,1	4,952	L2	Flashover	53,2	11,502
L3	Flashover	52,7	5,190	L3	Flashover	43,8	0,491
L4	Flashover	43,8	5,538	L4	Flashover	43,8	5,127
L5	Flashover	43,8	4,038	L5	Flashover	43,8	8,631
L6	Flashover	43,8	7,353	L6	Flashover	43,8	11,416
L7	Flashover	33,9	15,216	L7	Flashover	32,6	15,544
L8	Flashover	33,9	11,257	L8	Flashover	32,6	11,892
(e)				(f)			
Clean state							
State of insulator [V_exp(kV)]		V_cal (kV)	Error (%)				
Flashover		72	6,015				
(g)							

$\delta=50,4\text{mS/cm}$				$\delta=93,7\text{mS/cm}$			
	State of insulator [V_exp(kV)]	V_cal (kV)	Error (%)		State of insulator [V_exp(kV)]	V_cal (kV)	Error (%)
L1	Flashover	54,9	0,370	L1	Flashover	43,8	1,245
L2	Flashover	53,6	16,522	L2	Flashover	38,4	4,000
L3	Flashover	43,8	3,458	L3	Flashover	33,3	10,963
L4	Flashover	43,8	7,733	L4	Flashover	33,9	4,775
L5	Flashover	43,8	13,354	L5	Flashover	33,5	2,899
L6	Flashover	43,8	15,567	L6	Flashover	34,3	5,215
L7	Flashover	33,8	7,902	L7	Flashover	34,6	14,570
L8	Flashover	33,8	5,056	L8	Flashover	34,6	20,557
(h)				(i)			

- When analyzing table II.6 on a case-by-case basis, we notice that the maximum error is of the order of 20% for a single case, whereas it is between 10 and 16% for 13 cases and below 10% for the remaining ones.
- In the majority of cases where the error becomes negative, the predicted (calculated) voltage is greater than the measured voltage (experimental results), $V_{cal} > V_{exp}$. In fact, Table II.7 shows the cases where the error is upper (above) than 10%.

Tab. II.7. Error results upper than 10%.

N°	Level of pollution	Conductivities (mS/cm)	Error(%)	State predict with FL
1	L2	30,5	11,502	Flashover
2	L2	50,4	16,522	Flashover
3	L3	93,7	10,963	xxx
4	L4	12,61	13,693	Flashover
5	L5	1,823	10,916	Flashover
6	L5	50,4	13,354	Flashover
7	L6	1,823	14,257	Flashover
8	L6	30,5	11,416	Flashover
9	L6	50,4	15,567	Flashover
10	L7	16,32	15,216	xxx
11	L7	30,5	15,544	xxx
12	L7	93,7	14,570	Flashover
13	L8	12,61	10,050	Flashover
14	L8	16,32	11,257	xxx
15	L8	30,5	11,892	xxx
16	L8	93,7	20,577	Flashover

- If I overlooking the cases where the flashover has been done, then our FIS model to predict that in some cases the flashover is already done so the error equals zero (0%), and the average error becomes 4.080%.

If I apply this remark for all the results obtained by FIS, the average error will become 2.605%.

II.7. Conclusion

One of the advantages of the fuzzy logic is that it does not need the unrequired mathematical model, which makes it easy to interpret and implement.

This chapter describes an MAMDANI type of the fuzzy logic based artificial intelligence approach developed for the prediction of the flashover voltage. Actually, this chapter includes the background necessary for the understanding of the method. Hence, we presented both the use and the concepts of the FL, as a general description of the components of a fuzzy system, then, the concept of the linguistic variable as well as the fuzzy inference system (FIS).

The FL is used to represent the doubtful and imprecise knowledge, which enables us to say that the FL requires the help of an expert, which is very valuable when designing a fuzzy system. A good choice of the different parameters of the system represents the most important phase of the application of the fuzzy logic the parameters of which will be implemented on the basis of the different needed steps.

The results obtained using the FL show their effectiveness in terms of the rate of good predictions and very short calculation time. However, the encountered difficulty in using the fuzzy logic lies in the choice of its parameters. In fact the real difficulties are related to the fuzzification of the input and output variables (form of the membership function, number of fuzzy sets associated with each variable), and the creation of the fuzzy rules that connect the inputs to the output. It can be said here that there are no rules to be followed in choosing the parameters of the fuzzy inference system.

The implementation of the fuzzy inference system "FIS" under the MATLAB environment using interface "Fuzzy Logic" is characterized by its simplicity. This chapter shows the effectiveness of our proposed model to predict the flashover voltage.

Due to the difficult adaptation of our model to the change in the environment, there is no formal method for adjustment. In the next chapter, the technique of artificial intelligence based on neural networks will be used as flashover voltage prediction technique for the same purpose of the current chapter (1512L real insulator).



Chapter III

Prediction of Flashover Voltage Using the Artificial Neural Network (ANN)

III.1. Introduction

The critical flashover voltage of a polluted insulator is a significant parameter for the reliability of power systems. However, the mentioned tests for the study of the insulator behavior under pollution, they are of long duration and the cost of the equipment that is necessary for these experiments is very high. For the above reasons, it seems to be very useful to predict the performance of insulators under pollution conditions using analytical expressions and computer models.

Several approaches have been developed for the estimation of the flashover voltage. In last years, the computational intelligence techniques have been successfully applied in many studies. Several models and techniques are used to improve understanding insulator flashover phenomenon. Among of these methods, artificial neural network (ANN) architectures have been widely used, due to their computational speed, robustness and great efficiency, to study polluted insulators flashover. Some authors have already applied these two techniques in similar area of research.

Artificial neural networks (ANN) can be used in problems requiring function approximation, modeling, pattern recognition and classification, estimation and prediction (calculated), etc.[1]

In the field of high voltage insulators, ANN can be used to estimate the pollution level, [2] to predict a flashover, to analyze surface tracking on polluted insulators, [3] and also to estimate the critical flashover voltage on a polluted insulator. [4]

This last case will be thoroughly examined later.

In this chapter we will use the experimental data in chapter I to construct a model based on ANN architectures that can estimate the flashover voltage on the real model using as inputs some characteristics of the pollution (conductivities (δ) and level of pollution (L_i) or zones of pollution (Z_i)), utilization of interface graphic can help to determinate their parameters as we have applied and explained during our study, and we conclude our chapter with a comparison between the two artificial intelligence methods of Chapter II (FL) and Chapter III (ANN).

III.2. Artificial neural networks

The phrase "artificial neural network" has become the dream of many researchers who want to make better use of the data available to them. This tool is essentially inspired by the process of information processing performed by the human brain. A network of artificial neurons

is a model of calculation the design of which is very schematically inspired by the functioning of biological neurons. [5]

As indicated in its definition, the primary goal of an artificial neural network is to perform a calculation the main asset of which lies in its ability to learn to do it alone through experience.

Artificial neural networks are highly connected by elementary processors operating in parallel. Each elementary processor calculates a single output based on the information it receives. Any hierarchical network structure is obviously a network that tries to simulate the reasoning process of human intelligence and thus be used instead of mathematical functions.

Artificial neural networks are typically specified using the three following factors:

- **Architecture:** it specifies which variables are involved in the network and their relationship with topological purposes. For example, the variables involved in a neural network could be the weights of connections between the neurons and their activities.
- **Activity Rule:** Most of the neural network models have a short dynamic depending on the time scale: the local rules define how the neural activities change. Typically, the rule of an activity depends on the weights (the parameters) that exist in the network.
- **Learning:** The learning rule specifies how the weights of the neural network change over time. This learning is generally expected to take place on a longer time scale than the time of dynamics under the activity rule. Usually, the learning rule depends on the neuron activities as it can also depend on the target values provided by both a teacher and the weight current value.

An artificial neural network is a group of interconnected nodes similar to a large network of neurons in the brain. In figure III.1, each circular node represents an artificial neuron and an arrow represents a link between the outputs of one neuron at the input of another.

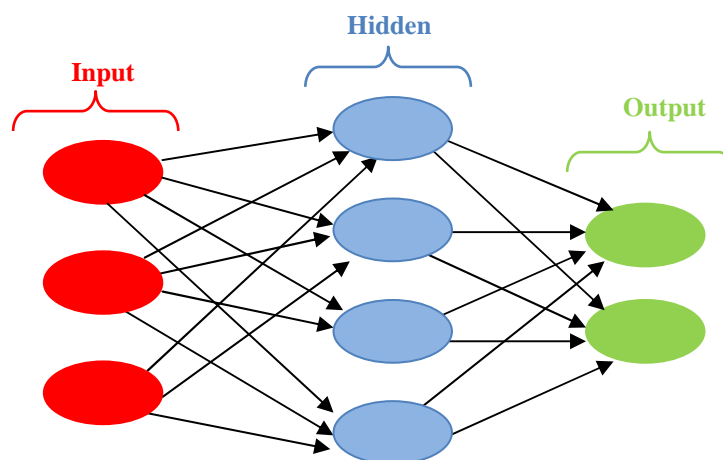


Fig. III.1. Structure of a neuron network.

III.2.1. Mathematical model of a "Formal" or an "Artificial" neuron

The formal neuron model is a very simple mathematical model derived from the analysis of the biological reality the structure of which is given in figure III.2. [6]

Figure III.2 shows the structure of an artificial neuron where each artificial neuron is an elementary processor that receives a variable number of inputs from upstream neurons. Each of these inputs is associated with a weight w , which is a representative of the connection strength. Each elementary processor has a single output which branches out to feed a variable number of downstream neurons where each connection is associated with a weight.

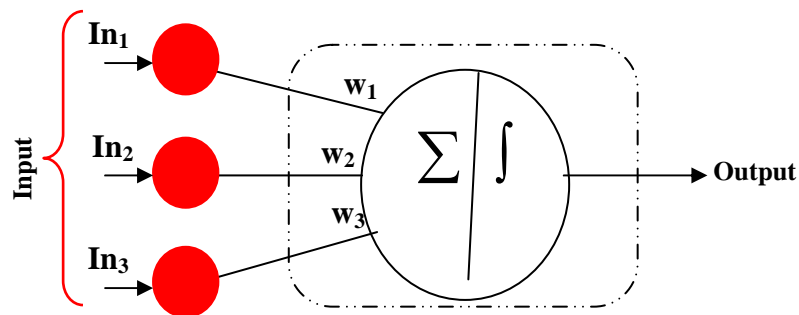


Fig. III.2. General diagram of an artificial neuron.

The mathematical formulation of this neuron is described by the following relation:

$$s = \sum_{j=1}^i (w_j In_j) \quad (\text{III.1})$$

Or:

s : is the output of the neuron

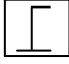
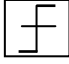
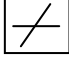

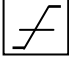
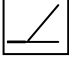


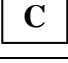
In_i : is the i^{th} input of the neuron, it characterizes the data communicated by the sensor (detection test) or by the expert (diagnosis and basis of facts and knowledge).

f : Activation function (the sigmoid),

w_i : Weight of connections with the inputs.

He five most common activation functions are presented. An activation function performs a mathematical operation on the signal output. All the activation functions described here are also supported by MATLAB. (Table III.1). [7]

Tab. III.1. ANN activation function.[7]

Input / output relationship	Input / output relationship	Icon	Name in Matlab
Threshold	$a = 0$ if $n < 0$ $a = 1$ if $n \geq 0$		hardlim
Symmetrical threshold	$a = -1$ if $n < 0$ $a = 1$ if $n \geq 0$		Hardlims
Symmetrical threshold	$a = n$		Purelin
Linear saturated	$a = 0$ if $n < 0$ $a = n$ if $0 \leq n \leq 1$ $a = 1$ if $n > 1$		Satlin
Linear saturated symmetric	$a = -1$ if $n < -1$ $a = n$ if $-1 \leq n \leq 1$ $a = 1$ if $n > 1$		Satlins
Positive linear	$a = 0$ if $n < 0$ $a = n$ if $n \geq 0$		Poslin
Sigmoid	$a = \frac{1}{1 + \exp^{-n}}$		Logsig
Hyperbolic tangent	$a = \frac{e^n - e^{-n}}{e^n + e^{-n}}$		Tansig
Competitive	$a = 1$ if n maximum $a = 0$ if n other		Compet

III.2.2. Characteristics of the ANN

The basic element of a neural network is of course the artificial neuron. A neuron contains two main elements: (figure III.2)

- A set of weights associated with neuron the connections;
- An activation function.

Neural networks in figure III.3 are generally characterized by:

III.2.2.1. The input layer

The number of neurons in this layer corresponds to that of the inflows (inputs) in the neuron network. This layer consists of passive nodes, that is, that do not participate in the actual signal change but only transmit the signal to the next layer.

III.2.2.2. The hidden layer

This layer has an arbitrary number of layers with an arbitrary number of neurons. The nodes in this layer participate in the modification of the signal, therefore, they are active.

III.2.2.3. The output layer

The number of neurons in the output layer is that of the neuron network outputs. The nodes in this layer are active. (Figure.III.3). [8]

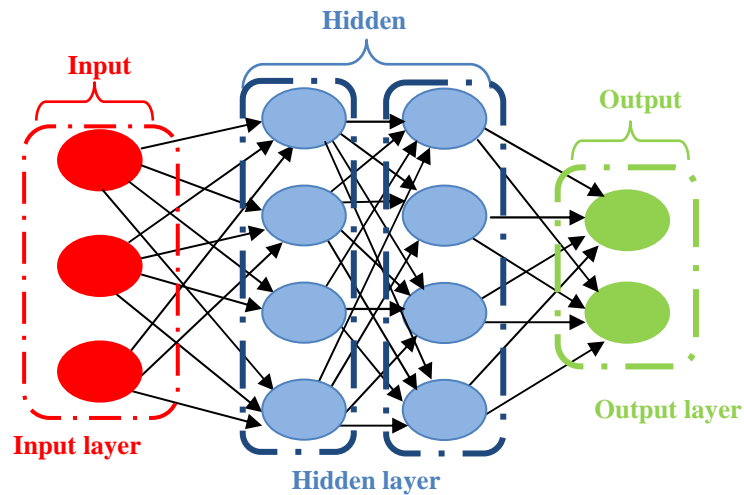


Fig. III.3. General architecture of a neuron network.

III.2.3. Feed-Forward propagation networks

The "back propagation" learning technique is used to train the networks of the architecture neurons of "Feed Forward" type also called unconnected networks. It is a multilayer architecture, which means that the input layer connected to a hidden layer which can, in turn, be connected to another hidden layer or directly connected to the output layer. In general, there is only one layer hidden in this kind of architecture where it is very rare to find more than two layers. Mathematically, this does not change the operation of the network.. In fact, these architectures are the most commonly used.[9]

III.2.3.1. Mono-layer perceptron

Historically, the first ANN, which has been developed by Rosenblatt in the 1950s, is a simple network as it consists only of an input layer and an output layer. In fact, it is basically modeled on the visual system and therefore primarily designed for pattern recognition. Moreover, it can be used to classify and solve simple logical operations (such as "AND" or "OR"), however, its main limitation is that it can solve only separable problems on a straight-line basis. It usually follows a supervised learning according to the error correction rule (or according to Hebb's rule).[10]

The neuron in figure III.4 performs a simple weighted sum of its inputs, compared to the threshold value, and provides a binary output response.

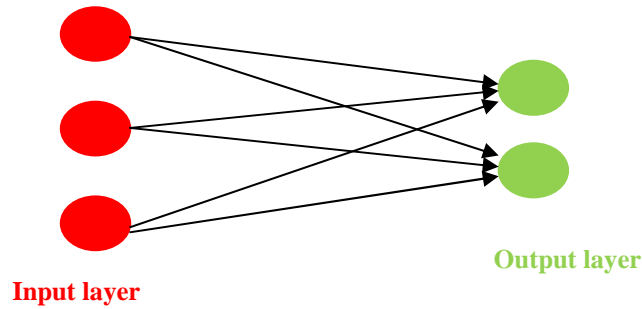


Fig. III.4. Perceptron monolayer type of network: Structure.

III.2.3.2. Multi-layer Perceptron

This perceptron is an extension of the previous one, with one or more hidden layers between the inputs and the outputs. Each neuron in a layer is connected to all the neurons of the previous layer and the next layer (except for the input and output layers), besides, there are no connections between the cells of the same layer. The activation functions used in this type of network are mainly threshold or sigmoid functions. A multilayer perceptron can solve straight line separable problems and more complicated logical problems. It also follows a supervised learning according to the error correction rule.

The choice of the number of hidden layers usually depends on the complexity of the problem to be solved. In theory, a single hidden layer may be enough to solve a given problem, but may have several hidden layers that make it easier to solve a complex problem. [11]. Figure III.5 gives an example of a network containing an input layer, a hidden layer and an output layer.

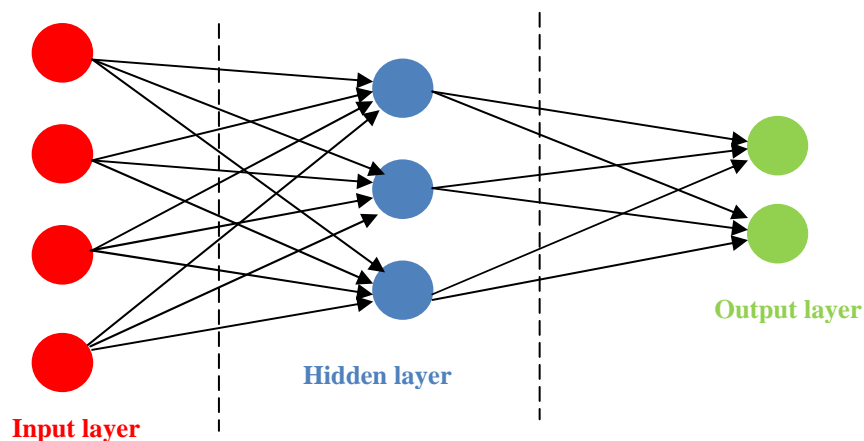


Fig. III.5. Multi-layer perceptron network: Structure.

III.2.4. Learning

Learning is a phase in the development of the neural network during which the neuron weights are calculated so that the outputs of the network can be as close as possible to the desired outputs. In fact, learning involves examples of the behavior of the process to be modeled.

For an artificial neural network (ANN), learning can be considered as the problem of updating the weights of connections within the network in order to succeed in the task that it requires. Learning is the main characteristic of the ANNs, which can be made in different ways and according to different rules.

III.2.4.1. Supervised learning

In this type of learning, the network will be adapted through a comparison between the result it has calculated, on the basis of the provided inputs, and the expected response output. Therefore, the network will change until it finds the right output corresponding to a given input.

III.2.4.2. Strengthening (The reinforcement)

Strengthening is actually a type of supervised learning which is also classified by some authors in the category of supervised modes. According to this approach, the network should know the input/output correlation via an estimate of its error, that is, the failure/success ratio. The network will therefore tend to maximize the performance index called reinforcement (Strengthening) signal, which is provided to it.

In this case, the system is aware of whether the answer it provides is correct or not, but it does not know the correct answer.

III.2.4.3. Unsupervised (or self-organizing) mode

In this case, learning is based on probabilities. The network is going to change depending on the statistical regularities of the input and establish categories by assigning and optimizing a quality value to the recognized categories.

III.2.4.4. Hybrid mode

The hybrid mode is in fact based on the other two approaches since some of the weights will be determined by supervised learning and some by unsupervised learning.

III.2.5. Learning rules

The synaptic weight change strategies are derived from the following general rules:

III.2.5.1. Error correction rule

This rule is part of the supervised learning paradigm, that is to say the case where the network is provided with an input and the corresponding output. If we consider that "y" as the output calculated by the network is the desired output, the principle of this rule is to use the error to change the connections and thus reduce the overall system error.

III.2.5.2. Boltzmann learning

Boltzmann networks are recurring symmetrical networks. They consist of two sub-groups of cells, the first is related to the environment (so-called visible cells) whereas the second is not (so-called hidden cells). This learning rule is stochastic (= which is partially random) and consists in adjusting the weights of the connections so that the state of the visible cells will satisfy a desired probability distribution.

III.2.5.3. The Hebbian theory

This rule, which is based on biological data, models the fact that if, on either side, synapse neurons are synchronically and repeatedly activated, the connection synaptic strength is going to rise. It should be noted that learning is localized, that is to say that the synaptic weight modification of w_{ij} depends only on the activation of i and j neurons.

III.2.5.4. Competitive learning rule

The special feature of this rule is that learning here is about only a single neuron. The principle of this learning consists in grouping the data into categories. This means that the similar patterns will be stored in the same class based on the correlations of the data then will be represented by a single neuron, hence, one speaks about "winner-take-all". In a simple competition network, each output neuron is connected to the neurons of the input layer, to the other cells of the output layer (inhibitory connections) and to themselves (excitatory connection). The output will depend on the competition between the inhibitory and excitatory connections.

III.3. The back-propagation algorithm

The back propagation network refers to the multi-layer neurons that use the back-propagation algorithm for learning. Most often, multilayer feed-forward neural networks are used for the back-propagation algorithm. The back-propagation algorithm is one of the best known algorithms for the prediction of the weights of the neural network. It has been developed by "David Rumelhart", Geoff Hinton and RJ Williams in 1986.[4] It is also one of the most popular learning algorithms given its success in terms of simplicity and applicability.

The algorithm consists of two phases: a learning phase and recall phase (validation & test). In the learning phase, the weights are randomly initialized and the outputs are calculated and compared to the desired outputs. Subsequently, the network error is calculated and used to adjust the weights of the output layer. Similarly, the network error is spread backward and used to update the weights of the previous layers. The learning phase will be completed when the error value is lower than the one set by the supervisor. One of the disadvantages of the back-propagation algorithm is that the learning phase is very long. During the recall phase (validation & testing), the network and the final weights resulting from the learning method are used. The retro-propagation algorithm is the extension of the "delta rule" used in the learning of neural networks (a layer (perceptron)).[6,7]

III.4. Validation

Once the neural network is trained (after learning), it is necessary to test it on a database different from that used for learning. This test allows both to assess the performance of the neural system and to detect the type of data that causes problems. If the performances are not satisfactory, it will be necessary, either to modify the architecture of the network, or to modify the base of learning.[12]

III.5. The strategy followed in this work

The development of a neural network model "feed-forward" raises some problems, the most important of which is the absence of a previous guarantee for the model to behave similarly to the current problem. Several studies have been developed to find out the methods that can lead to the most performing models because there is no theoretical background as to how this architecture will be found. The most typical method followed is the "test and error" process for which a large number of different architectures are examined and compared. However, this process is very long and is mainly based on the previous experience and intuition of the human expert, which may lead to a high level of uncertainty.[13]

In order to understand this problem, it is necessary to examine in detail the characteristics of a "feed-forward" Artificial Neural Network (ANN). In fact, there are four elements that make up the architectures of a feed-forward ANN: [13]

- The number of layers,
- The number of neurons in each layer,
- The activation function of each layer,
- The learning algorithm.

III.5.1. Step of neural network design

Neural networks are often used to solve classification and regression problems in order to design a neural network.[14]

The developing process a neural network always begins with the selection and preparation of data samples (inputs and outputs). Like in the case of data analysis, this step is crucial as it can help the designer to identify the most appropriate type of network to solve our problem. The way in which the sample is presented determines the type of the network, the number of the input and output neurons and the way in which learning, testing and validation will be conducted.[15]

III.5.1.1. Determination of the neural network inputs/outputs.

The inputs and the output are shown in the following figure III.6:

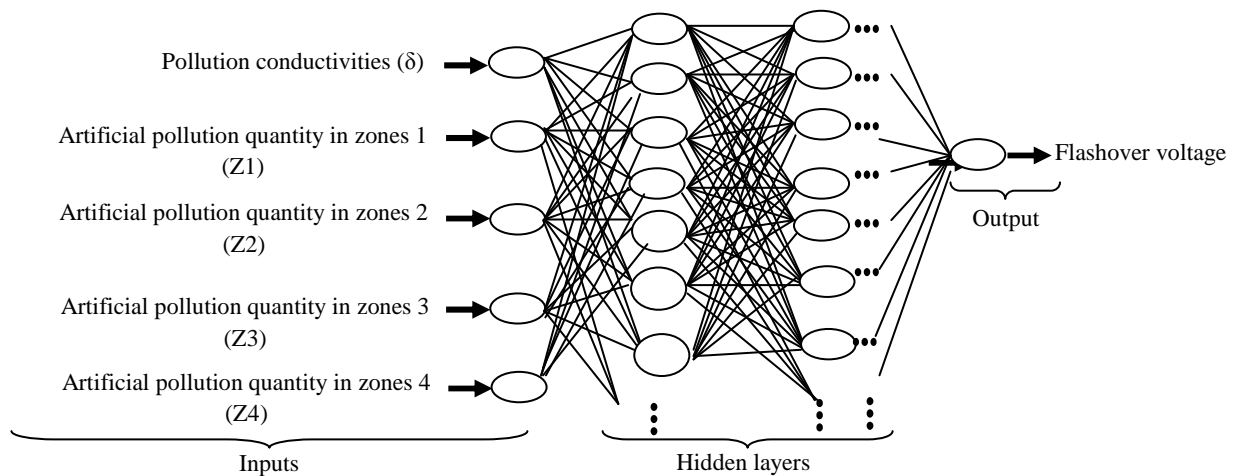


Fig. III.6. Structure of our neural network.

Conductivity as well as the quantities of pollution in 1,2,3,4 zones are considered as inputs with a single output which is the flashover voltage.

III.5.1.2. Elaboration of the network structure

In our work we have used a multi hidden layer to create our ANN architecture. In theory there is no exact method to determine the hidden layers and number of neurons per layer necessary for our ANN application. We have applied a simple method to determine them which will be detailed during this work.

III.5.1.3. Network Learning

Learning consists first in calculating the optimal weights of the different links using a sample. The most used method is the back-propagation. Hence, we include values of the input cells and, depending on the output error, we will correct the weights. This cycle is repeated until

the error curve of the network stops increasing (we must be careful not to over-train a neural network that will become less efficient). [15]

III.5.1.4. Test and validation

While the tests are related the verification of the performance of a non-learning neural network and its generalization ability, validation is sometimes used during the learning process. Actually, once the network is calculated, tests should always be performed to verify that the network is properly responding. In the general, part of the sample is simply dropped out from the training sample and kept for out-of-sample testing. For example, we can use 60% of the sample for learning, 20% for validation and 20% for testing. [14]

III.5.2. Implementation and simulation

The use of simulation within engineering is well recognized. Actually, simulation technology belongs to the set of engineering tools in all the application fields and has been an integral part of the engineering expertise management. Simulation helps reduce the costs, improve the product and system quality, and document and archive the lessons learned. In our work, we use the MATLAB as a tool for predicting the flashover voltage of a high voltage insulator.

III.5.2.1. Software presentation

To predict the flashover voltage, we used the Matlab calculation software in its version 7.9. We have used its inbuilt NNTOOL (neural network tool) package. On the other hand, to build our network, we need a databank that can be directly exported from an excel file after normalization. After exporting the databank by entering the "nntool" command in the command window, a graphical interface appears, (figure III.7), which enables us to create, visualize, train and simulate a network and export the output values.

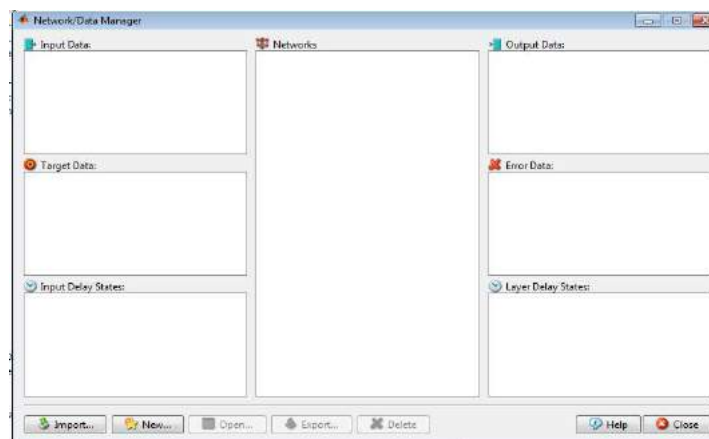


Fig. III.7. Graphical interface "nntool".

III.5.2.2. Data normalization

Actually, neural networks require that their input and output data be normalized to have the same order of magnitude. However, this normalization is very critical for some applications, [6] because it has an influence on the quality of the produced output. Normalization is an important operation because the network learns better with a regularized interval crowded with inputs than with arbitrary values. It is also an important contributing factor in improving the generalization capacity of the network.

Moreover, if sigmoidal or tan-sigmoidal activation functions are used, they are particularly used with a data range falling in the range of $[0, 1]$ and $[-1, 1]$, respectively.[4]

III.5.2.3. Data creation

Before creating a network, we should first introduce the inputs, which are in our case, conductivity, the quantities of pollution in zones 1,2,3,4, and property that must be reached by the network, which is in our case the flashover voltage. Then, by clicking on import (figure III.7), a graphical interface appears in figure III.8, which enables us to introduce the inputs and the value that must be reached by the network.

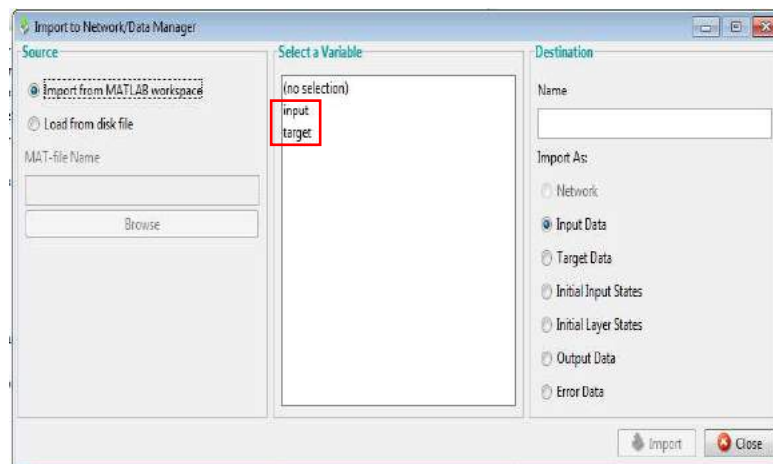


Fig. III.8. Data import window.

III.5.2.4. Performance function

During the network training step, a performance function should be employed to identify the best possible combination of the adjustable parameters that minimize the error between the produced (calculated) results and the values to be achieved (desired) which are relevant throughout the learning process. In fact, the neural network tool enables us to use the following performance features:

- The mean squared error (MSE),

- The MSEREG hybrid method (MSE version with weight moderation),
- The sum of squared errors (SSE).

In our work, we will use the MSE method to evaluate the error at the ANN output.[11]

III.5.2.5. Levenberg–Marquardt algorithm

Once the architecture is chosen, the ANN must undergo a learning phase which consists in calculating the synaptic coefficients so that the neural network outputs will be, for the examples used during the training, as close as possible to the "desired" outputs. These outputs correspond either to the data values of the function that we intend to tackle or to the process output that we try to model.[16,17] Learning from our network will be made with the Levenberg Marquardt algorithm because it has advantages:

- The target error has been reached by this method at a high speed of convergence,
- A large capacity of approximations,

The reason which led us to adopt this algorithm for the continuation of the work is that:

- The Levenberg-Marquardt algorithm is presented as follows [11,18]: Presenting the input vector by propagating (spreading) it to the output and calculating the quadratic error,
- The Jacobian matrix computation J ,

Calculation of ΔW to correct the network weights with the weight correction rule presented as follows:

$$\Delta w = -(J^T J + \mu I)^{-1} J^T e \quad (\text{III.2})$$

Δw : is the adaptation rate of the network weight matrix,

J : The Jacobian matrix of the error derivatives,

μ : is an adaptive coefficient, $\mu \gg$ is the algorithm which is closer to Gradient Descent method. However, if $\mu \ll$ is small, the algorithm is close to the Gauss-Newton method.

e : is the error vector.

- Calculation of the new weights and adjustment of the μ parameter,
- Verification of the convergence towards the required error, which is 10^{-5} in our case.

III.5.2.6. Mean Squared Error (MSE)

MSE is a network performance function. It measures the network's performance according to the mean of squared errors.

If we designate $e_k(n)$ the learning error is associated with a neuron j , then, the instantaneous quadratic error value is defined by $\frac{1}{2}e_k^2$. Similarly, the value of the squared sum of the instantaneous, denoted by $\xi(n)$ is defined by: [11]

$$\xi(n) = \frac{1}{2} \sum_{j=1}^L e_k^2(n) \quad (\text{III.3})$$

It is obtained by adding the terms $\frac{1}{2}e_k^2$ which correspond to all the neurons of the output layer. The expression of the mean of the sum of the quadratic error is given by:

$$MSE(n) = \frac{1}{N} \sum_{n=1}^N \xi(n) \quad (\text{III.4})$$

with N the number of examples representing the learning base. The MSE value is calculated after each iteration (presentation of the learning examples to the network).[11]

III.5.3. Application of the ANN in the prediction of the flashover voltage

Given their performance, artificial intelligence methods are increasingly used to deal with advanced research topics in all the fields, specifically the high voltage one.

III.5.3.1. Neuron network model (Structure of the elaborated ANN)

The table below gives the most important technical data about the established networks.

Tab.III.2. Characteristic of the established neuron network.

Parameters	Choice
Structure of the elaborated ANN	Multi-layer Perceptron (feed-forward)
Input data	Conductivities & quantities of pollution zones
Output data	Flashover voltage
Number input	5 (vectors of 5x65) examples
Number output	1 (vectors of 1x 65) examples
-Learning Algorithm	Learning function Levenberg-Marquardt (TRAINLM)
Adaptation function	LEARNGDM for the adjustment of the weights by the descent of the gradient with momentum with a step of learning and a fixed momentum.
Performance function	Mean square error (MSE)
Activation functions 1 st layer	Tangential sigmoid transfer function (LOGSIG) for hidden layers.
Activation functions 2 nd layer	Linear transfer function (PURELIN) for the output layer.
Number of layers intermediate	2
Number of neurons by hidden layers	6
Number of iterations	1000 epochs

In our work, two databases are used, the first is used to learn the ANN, which consists of (5x45) inputs (δ , Z1, Z2, Z3, Z4), (45) corresponding outputs (flashover voltage) while the second is composed of (5x20) of ((δ , Z1, Z2, Z3, Z4), used to test the ANN for the prediction of the flashover voltage.

III.5.3.2. Creation of the network

To generate a new network, one should click on "New". Hence, a new window appears in figure III.9, and then, the type of preprogrammed network is chosen. The feed-forward Back-propagation designates everything for its convergence properties and approximation capabilities.

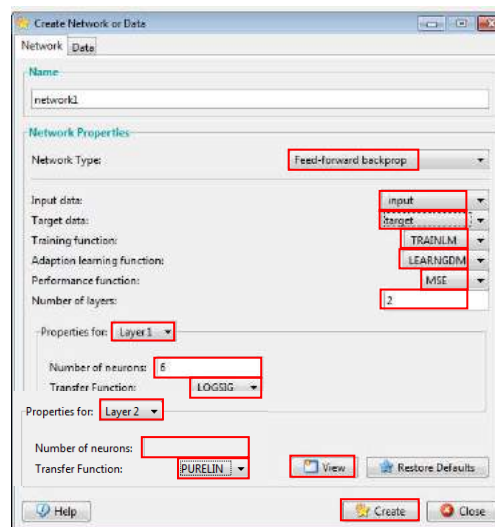


Fig. III.9. Network creation window.

For this reason, the "TRAINLM" training function is chosen as a "LEARNGDM" learning function and the "MSE" as a performance function. In fact, there are two hidden layers, the first consists in activating the "TANSIG" tangential sigmoid, while the second has the role of activating the "PURLIN" linear function.

The only variable that must be incrementally optimized for each network is the number of hidden neurons. After creating the network, it is possible to view it by clicking on "view", therefore, the following window appears in figure III.10.

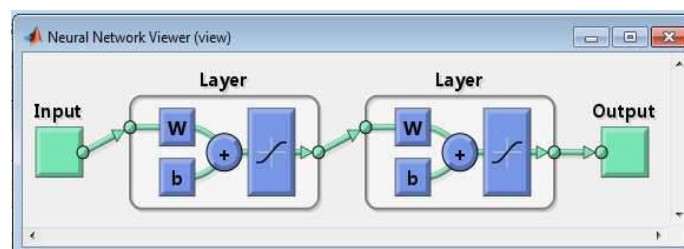


Fig. III.10. Neural network used for the experiment.

III.5.3.3. Determination of the number of hidden layers, number of neurons per hidden layer and number of iteration

The flowchart presented in figure III.11 used for the choice of the number of hidden layers and the number of neurons per layer will be carried after the analysis network performance. In this stage, the architecture is maintained, which has an error and a number of neurons and minimum number of iterations. [11,19]

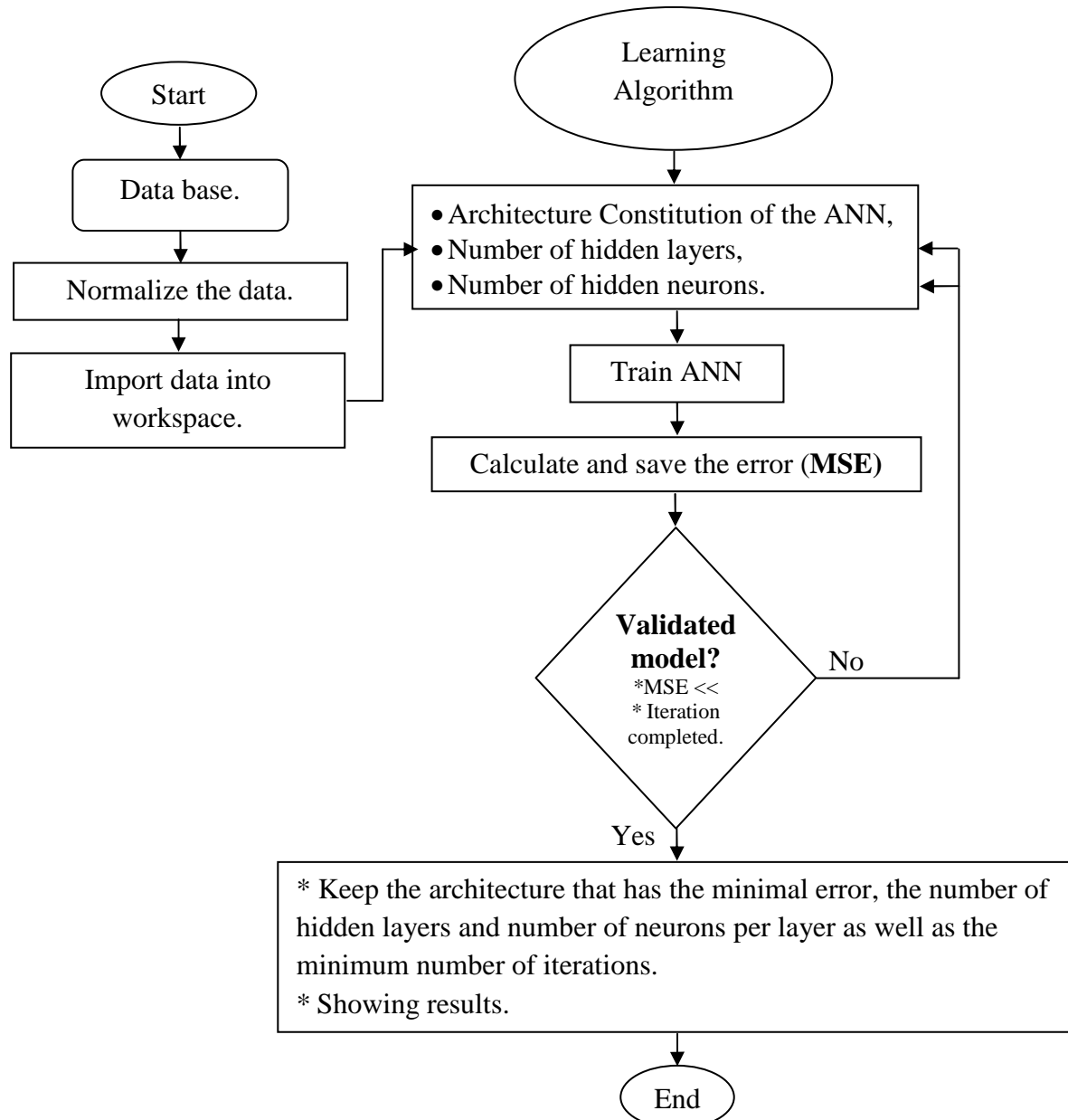


Fig. III.11. Design flowchart of a neural network.

Then, the code is applied as follows:

- The number of hidden layers is provided,
- The number of iterations is given,
- We start with a neuron per hidden layer and we end up with the number of neurons that gave the smallest possible of mean square error (MSE).
- In fact, the same procedure is applied to find out the number of layers as well as that of iterations that gave the smallest possible of MSE.

The test series carried out to better identify the number of hidden neurons and layers as well as that of iterations are shown in the following table.

Tab. III.3. Different ANN parameters tested to optimize the number of hidden layers, neurons per layer so the number of iterations.

Interval of hidden layers	neural interval per hidden layers	Interval of iterations used
[2,3,4]	[2,4,6,8,10,12,14,16,18]	[1000,2000,3000]

III.5.3.4. Implementation of the network

By clicking on "Create" in the network creation interface shown in figure III.9, and on the name of the network "create" in the "network data manager" seen in figure III.12, a new window appears, which enables us to train the network after selecting the appropriate databank, and adjust the parameters, such as the epochs and the desired error.

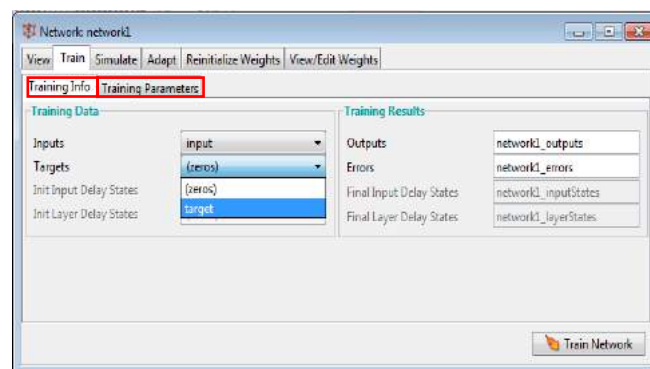


Fig. III.12. Learning window and network simulation.

The most important criteria to stop the learning algorithm are: the performance function, the gradient amplitude of the performance function and the number of failures of the validation (max_fail) called "the maximum number of validation checks ", which is that of successive iterations where the validation of the performance function does not decrease.

Moreover, there are other criteria for stopping the learning algorithm, such as the maximum training time (time), the minimum performance value (0.00001) (goal) and the maximum number iterations (epochs), which can interrupt the training of the ANN.[18,20] In fact, the learning parameters are selected, which causes the learning to stop in two cases, the first when the number of epochs is completed, second when the goal (error) is reached.

III.5.3.5. Choice of the number of neurons per hidden layer/ number of hidden layer and number of iterations

By setting the number of the hidden layers to 2, then, the number of iterations will be 1000. According to table III.4 below, the arrangement which gave the smallest error is the number of 6 neurons in the hidden layer while that of iterations is 1000.

The used function is the logsig.

Tab. III.4. Choice of neuron number per hidden layer.

Number of iterations	Number of hidden layer	Number of neurons per hidden layer	MSE
1000	2	2	0,00038
		4	0,00687
		6	0,00001
		8	0,00001
		10	0,00008
		12	0,00009
		14	0,00002
		16	0,00003
		18	0,00058

Moreover, by setting the number of neurons per hidden layer to 6 as well as the one of iterations to 1000

Tab. III.5. Choice of hidden layer number.

Number of iterations	Number of neurons per hidden layer	Number of hidden layer	MSE
1000	6	2	0,00001
		3	0,00070
		4	0,00004

The best choice for the number of hidden layers is therefore 2.

Then, by setting the number of neurons per hidden layer to 6 as well as hidden layers to 2.

Tab.III.6. Choice of the number of iteration.

Number of hidden layer	Number of neurons per hidden layer	Number of iterations	MSE
2	6	1000	0,00001
		2000	0,00005
		3000	0,00016

Finally, the best choice that gives the optimum of error is: (table III.7)

Tab. III.7. Final parameter of the ANN structure.

Number of hidden layer	Number of neurons per hidden layer	Number of iterations	MSE
2	6	1000	0,00001

III.5.3.6. Result of the number of number of neurons per hidden layer, hidden layer and that of iterations

Finally, if we click on "train network", figure III.12, a graphic appears automatically with the status of learning shown in figure III.13. The latter stop after the number of times reaches the set value.

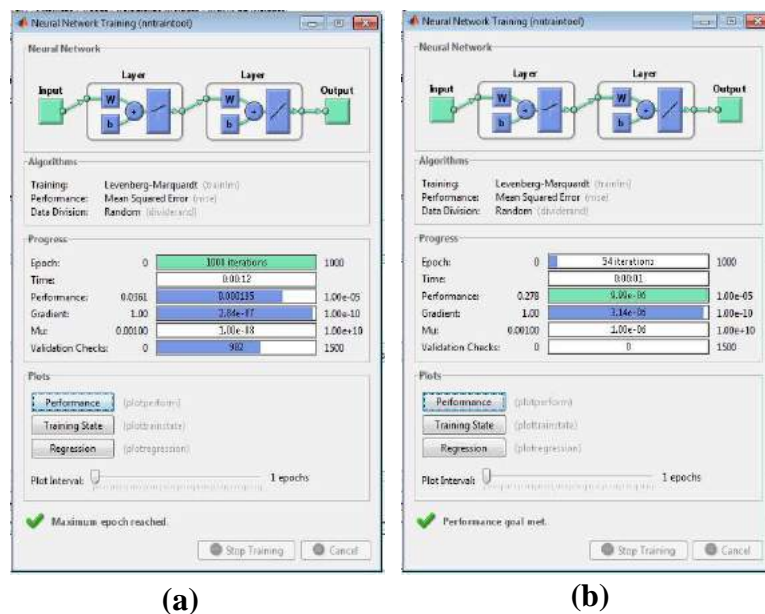


Fig. III.13. Window of the train network in the case:

- (a) two hidden layers and two neurons per layer with a thousand iteration number,
- (b) two hidden layers and six neurons per layer with a thousand iteration number.

Based on the previous figure, it can be said say that:

- Cease of the condition is verified,
- Maximum number of reached iteration.

Based on the analysis of these results, it can be concluded that all of the final parameters of our established ANN are shown in table III.2.

III.5.3.7. Network performance

The training process requires a set of examples of proper network behavior network inputs and target outputs. During training the weights and biases of the network are iteratively adjusted to minimize the network performance function. The default performance function for feedforward networks is mean square error MSE the average squared error between the network outputs and the target outputs.

Figure III.14 gives four curves which represent the correlation between each data type and corresponding desired data. The dash line in each axis represents the ideal result ($R=1$). The solid line represents the best fit linear regression line between outputs and targets data (calculated flashover voltage equal target values). According to figure III.14, the training of our network is perfectly realized since the value of "R" is approximately equal "1" in four regression curve type.

The ordinates of each curve in figure III.14 represent the outputs of the network (calculated "V" values) for the inputs reserved for learning, the entries reserved for validation and the inputs reserved for the test.

- The continuous straight lines (the lines drawn in continuous) of each curve of figure III.14 represent the regression (fitting) of the relationship between the outputs calculated by ANN and the desired one (values of "V" chosen). The dotted lines represent the desired (perfect) reference (regression) approximation (desired outputs = calculated outputs).[20]

When these two lines almost merge or become totally confused, then we speak about a better performance.

- The black circles represent the desired "V" voltage values (targets). Obviously, the more the point cloud is tightly linked to the perfect approximation straight line, the better the performance will be.[11,20]

- The "R" value represents the ratio of the network calculated outputs to the targets. If " $R=1$ ", this implies that the calculated outputs are equal to the targets.[20] In this case, the drawn dotted lines (perfect regression) and the continuous (calculated regression) coincide completely and hence, perfect performance is obtained. Therefore, it can be said say that a better learning gives "R" values very close to "1".

Table III.8 explains the "R" value for each curve (figure III.14 (-a -, - b -, - c -, - d-)).

Tab.III.8. Demonstration of the value of "R" of each curve.

Figures	R	Comments
Figure III.14-a-	0,99961	<ul style="list-style-type: none"> 99.961% of the "V" values calculated at the output of the ANN are the same as those desired for the data reserved for learning.
Figure III.14-b-	0,9904	<ul style="list-style-type: none"> 99.04% of the calculated "V" values are the same as those desired for the data reserved for validation.
Figure III.14-c-	0,99271	<ul style="list-style-type: none"> 99.271% of calculated "V" values are the same as desired data reserved for the test.
Figure III.14-d-	0,99549	<ul style="list-style-type: none"> This means that 99.549% of the desired values of "V" are the same as those calculated from the total database.

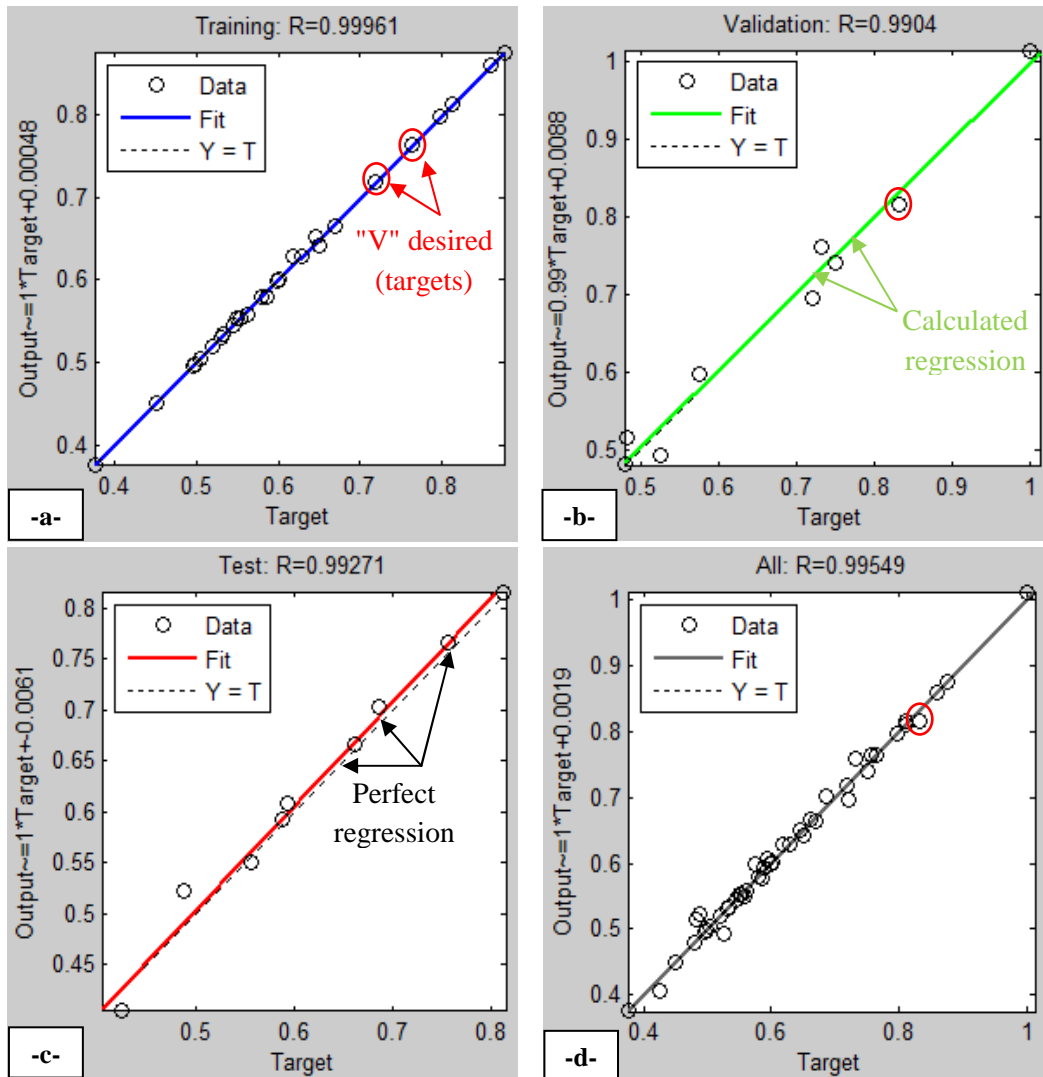


Fig. III.14. Regression curves.

This table shows that all the obtained "R" values are very close to "1", which means that our ANN is well trained, and that the learning task has been successful. It should also be noted that these values are obtained after a several times of restarting the learning until the best "R" values (very close to 1) are obtained.

III.5.3.8. Results and comparison "ANN" & "FL"

Using the graphical interface "nntool" in MATLAB, we can summarize the steps of our work until the result is achieved:

- Select the data current has five variables and one target,
- Use the import option to workspace,
- Type nntool in command window,
- Import input (Input) and target (target),
- Now create the network by clicking New,
 - From network type we can choose the desired network, here I am choosing feed forward with back-propagation,
 - Select the input, output and training and learning algorithms (functions),
- We can see the training, testing, validation and overall data regression oh it is bad fitting until to get good fitting we can train the network,
- Even we can change the weights and retrain the network,
- Again bad results but I won't leave it,
- Even we can change training parameters,
- Now export the network predicted values and other parameters to work space.

Now, tests will be carried out to check the quality of the neural model predictions by presenting new examples of inputs (5x20 of (δ , Z1, Z2, Z3, Z4)) that are not part of the learning set of the collected from literature so that it calculates the corresponding outputs.

For this purpose, we will use the simulation function defined as follows: $s = \text{sim}(\text{Result}, [\delta \ Z1 \ Z2 \ Z3 \ Z4]')$.

s: the "V" output calculated using the network, which is called "Result" in our case.

All the prediction results of the flashover voltage by the ANN are given in table III.8. These results are compared to the ones obtained by FL in chapter II.

Input data							Output data (test)									
		Zones of pollution				Artificial Neural Network (ANN)				Fuzzy Logic (FL)						
		Z1	Z2	Z3	Z4	V_exp	V_cal	Error	Error %	E_av %	V_exp	V_cal	Error	Error %	E_av %	
Conductivities δ (mS/cm)	1,823	L4	120	60	123	123	54,200	54,813	0,613	1,131	1,727	54,200	56,900	2,700	4,982	8,911
	1,823	L7	150	105	229,5	229,5	47,400	47,459	0,059	0,124		47,400	43,700	3,700	47,40	
	3,33	L2	60	30	22	30	61,150	61,363	0,213	0,348		61,152	56,800	4,352	7,117	
	3,33	L4	120	60	123	123	52,080	53,894	1,814	3,483		52,080	56,800	4,720	9,063	
	3,33	L8	150	120	265	265	44,016	44,846	0,83	1,886		44,016	43,800	0,216	0,491	
	8,02	L5	150	75	158,5	158,5	47,712	47,060	0,652	1,367		47,712	44,900	2,812	5,894	
	8,02	L7	150	105	229,5	229,5	44,000	43,781	0,219	0,498		44,000	43,800	0,200	0,455	
	12,61	L3	90	45	87,5	87,5	52,500	52,216	0,284	0,541		52,500	55,400	2,900	5,524	
	12,61	L7	150	105	229,5	229,5	41,200	41,299	0,099	0,240		41,200	43,800	2,600	6,311	
	16,32	L3	90	45	87,5	87,5	50,100	50,033	0,067	0,134		50,100	52,700	2,600	5,190	
	16,32	L4	120	60	123	123	46,368	46,041	0,327	0,705		46,368	43,800	2,568	5,538	
	16,32	L7	150	105	229,5	229,5	39,984	39,591	0,393	0,983		39,984	33,900	6,084	15,216	
	30,5	L2	60	30	22	30	47,712	47,711	0,001	0,002		47,712	53,200	5,488	11,502	
	30,5	L6	150	90	194	194	39,312	39,055	0,257	0,654		39,312	43,800	4,488	11,416	
	50,4	L1	30	15	11	15	55,104	56,567	1,463	2,655		55,104	54,900	0,204	0,370	
	50,4	L5	150	75	158,5	158,5	38,640	38,932	0,292	0,756		38,640	43,800	5,160	13,354	
	50,4	L8	150	120	265	265	35,600	31,762	3,838	10,781		35,600	33,800	1,800	5,056	
93,7	L2	60	30	22	30	40,000	41,476	1,476	3,690	40,000	38,400	1,600	4,00			
93,7	L4	120	60	123	123	35,600	35,623	0,023	0,065	35,600	33,900	1,700	4,775			
93,7	L7	150	105	229,5	229,5	30,200	28,843	1,357	4,493	30,200	34,600	4,400	14,570			
V_exp : Experimental Voltage (kV) V_cal : Calculated Voltage (kV) Error (E): Error between V_exp & V_cal (absolute value) (kV) E_av : Average Error (%) L _i : Level of pollution							Percentage of correct predictions vs. experimental results (%)				Percentage of correct predictions vs. experimental results (%)					
							98.273				91.083					

Tab. III.9. Experimental (practical) data collected and prediction results by "ANN" and "FL".

III.6. Discussion of the results obtained

The prediction results obtained by the ANN for different input values [δ , Z1, Z2, Z3 and Z4] are shown in table III.9. These results will be compared to the practices collected in our laboratory and those obtained by simulation.

- The prediction results obtained by the ANN under MATLAB for different inputs were obtained, our predicted (calculated) result obtained by ANN depend directly on the parameters of the network.
- According to Table III.9, the average error is of the order of 2% (1.727%), for the Neural Network Method (ANN), which means that more than 98% of the results are calculated by the ANN method more efficient and more robust. These results allowed us to judge that the ANN system is valid, efficient and reliable to predict (calculate) the flashover voltage tests of the HV 1512L insulator studied in our thesis.
- The results obtained also show that the neural network has a very great power in the study of the flashover voltage.
- The simulations carried out for the determination of the number of hidden layers, number of neurons by layer as well as the number of iterations necessary for a satisfactory prediction, so the number of layer chosen is 2, the number of neurons by layer is 6 with 1000 of iterations that gives the minimal MSE error, this clearly shows that the resolution of our problem requires more than one hidden layer, more than one neuron by hidden layer and 1000 iterations.
- By comparison, improved prediction results by ANN compared to that of the previous chapter (FL).
- It is clear from the results obtained that fuzzy logic (FL) has great power in the study of the prediction of the flashover voltage, the average error is of the order of 9% (8.911%) , for the fuzzy logic method, which means that more than 91% of the calculated results are correct.

The good choice of the parameters of the used fuzzy inference system (input and output variables, number and type and forms of the membership functions, inference rules, defuzzification method) leads to better results.

- Regarding the use of Artificial Neural Networks, the rate of the correct predictions of the of the carried out tests is the highest in all the methods used (studied).

III.7. Conclusion

Among the advantages of the mentioned neural networks is the speed and efficiency as well as a very low error rate compared to other artificial intelligence methods. Neural networks

do not require the use of very complex mathematical models for their operation. Indeed, thanks to their learning capacity, they are mainly based on the data models to be processed.

This chapter describes a neural approach (ANN) developed for the prediction of flashover voltage. The ANN approach, which is a supervised learning network, has been applied using the electro-geometric constraints (δ , Z1, Z2, Z3, Z4) of the insulator as input variables and the flashover voltage (V) as an output variable.

An ANN based algorithm has also been used for the same purpose of chapter II. In fact, we have presented the use of neural networks as an artificial intelligence technique to predict the flashover voltage of the 1512L cap and pin insulator.

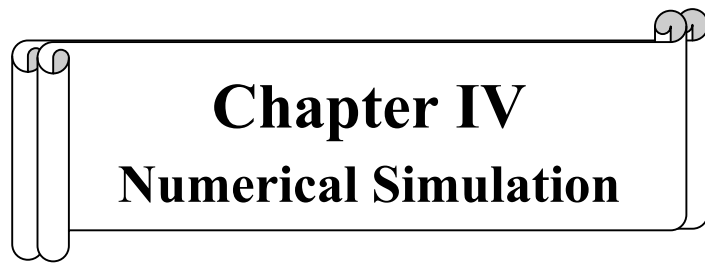
Regarding the Artificial Neural Networks (ANN), the difficulties encountered during their implementation lie in the choice of the type of the ANN to be used, its architecture (number of hidden layers, number of neurons by layer and number of iterations), the learning method and its optimization, the stopping criterion (performance function) without forgetting the choice of the database used for learning.

The implementation of ANNs in the MATLAB environment using the graphical interface is mainly characterized by its simplicity in creating ANNs, however, learning can diverge.

The obtained results showed that the ANNs are efficient in terms of high percentage of good predictions (more than 98%) and a very short calculation time. The used practical (experimental) data to conduct this work are collected especially from the validation of the two techniques (ANN & FL) used, are collected from our high voltage laboratory at the university of Biskra.

The results obtained by the multilayer perceptron neural network approach (ANN) were compared with those obtained by fuzzy logic (FL). We found that the results obtained by the ANN approach are more efficient compared to those found by the FL. The most important step in such an artificial intelligence study, in particular FL and ANN, is to manage to collect the necessary databases. Unlike conventional modeling methods, where many parameters must be considered that influence the behavior of the phenomenon studied.

Finally, it can be said that the application of the artificial intelligence techniques proposed in this study for the prediction of the flashover voltage of the various electro-geometric parameters is efficient and simple. You have only to choose the different parameters of each technique.

A decorative border resembling a scroll, with rounded ends and a slight shadow effect, framing the chapter title.

Chapter IV
Numerical Simulation

IV.1. Introduction

The knowledge of the distribution of the electric field within and around high voltage equipment is a crucial aspect of the design, performance and exploitation of high voltage insulators. It could be useful for the detection of defects in insulators.[1,2]

Computer simulation has become an essential part of science and engineering, the simulation methods give the possibility to examine the behaviour of models with very complex geometry without using analytical methods or experiments numerical. it is a complementary means of investigations, interesting in its flexibility and speed [3]. It is an approach that gives researchers the possibility to analyze the behavior of several phenomena which, because of their complexity, are beyond the scope of classical calculus [4]. For this reason, COMSOL Multiphysics® can serve as a powerful and interactive way to solve complex problems using the finite element method.

COMSOL Multiphysics® is a widely used tool in various fields of scientific research. It amply facilitates the modeling steps. The Finite Element Method (FEM) is most well-situated for calculate the electric field and potential distribution in high voltage insulator, because it is one of the more successful numerical methods to solve electrostatic problems (using the discretization of the domain) [5]. Hence, it is a method flexible and led to relatively simple techniques allowing to estimate the fields at the surface of the electrode thin and highly curve with various dielectric materials, which is well adapted to problems of complicated geometry [6-9].

In this chapter, the model with two dimensions of finite element method (FEM) developed by real geometrical dimension, and it is implemented to calculate the electric field and the potential distribution of insulator. The main objective is to study the electrical field and potential distribution of clean and dry insulator under discontinuous uniformly polluted. Electric field and potential distribution along a cap and pin insulator (1512L) has been calculated in COMSOL Multiphysics®. Level of pollution layer has been fixed (L1: Level of discontinuous pollution) and with various conductivities to investigate effect of pollution on electric field and potential distribution.

The objective of this work is predicting the behavior of polluted insulator under AC voltage. For thus, the distribution of the potential and the electric field along high voltage insulator is investigated using a numerical method. The commercial Comsol Multiphysics proved to be one of the best software used in 2D modeling. The potential and the electric field distributions along this insulator are simulated under various conditions: the two cases: clean

and polluted insulators and applying different conductivity values. We used electrostatic 2D simulations in the AC/DC module. The results are auspicious and promising.

IV.2. Modeling on the comsol software

Numerical simulations essentially consist of integrating differential equations, minimizing the impact of numerical defects on the simulated physical situation. COMSOL Multiphysics® is a powerful interactive environment for modeling and solving all kinds of scientific and engineering problems based on partial differential equations (PDEs). [5,8-9]

COMSOL Multiphysics® software is above all a tool for solving finite element partial differential equations. It now has its own graphical environment allowing both the drawing of geometries and the display of results in post-processing. Its specificity is also to allow the coupling of different EDPs, so as to describe multiphysical phenomena. It has been chosen for the following reasons:

- Specializes in solving electromagnetic problems,
- Possible to take into account the presence of several dielectrics,
- Possible to model a thin conductive surface (layer of pollution),
- Work in static or quasi-static mode (50 Hz)
- Finally, it allows a quick modeling of the problem. This software uses the F.E.M.

In our case the modeling and simulation of the insulator can be shown in figure IV.1

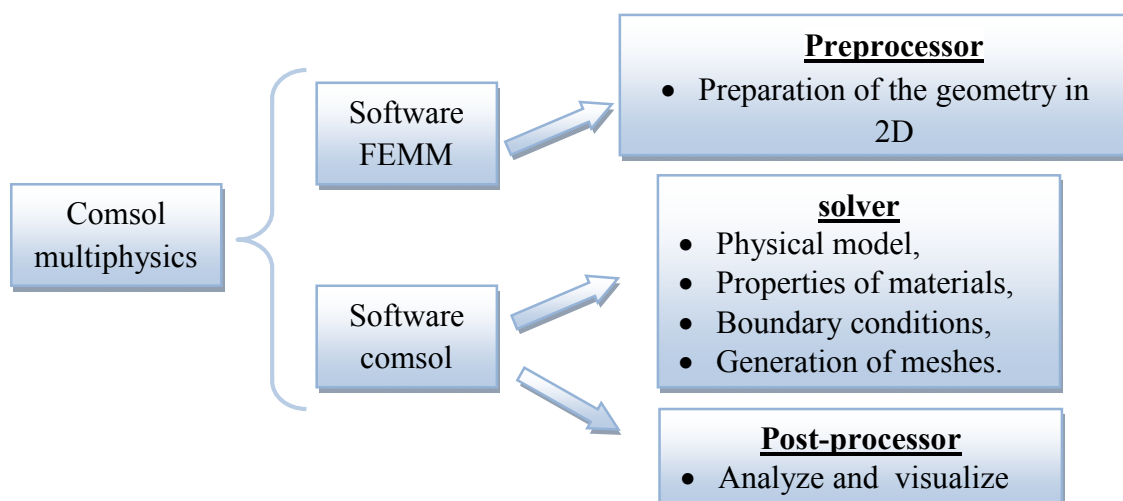


Fig. IV.1. Basic structure of the software Comsol Multiphysics

The basic structure can be summarized in five successive steps:

- The first step is to define the entire model geometry the isolator through a graphical design interface,
- The second step concerns the definition of the electrical properties of the materials present. This involves defining the relative permittivities and the conductivities of each domain. In addition, it is necessary to choose the type of analysis, that is to say either static or quasi-static,
- In the third stage, we define the boundary conditions which are translated by the potential imposed on each electrode and determine the boundaries of the electrical insulation, (the boundaries where the electric field can be considered as zero),
- The fourth step is to solve the problem by applying the numerical method,
- The last step consists in displaying the results obtained, among which the equipotential, the norm of the electric field and its normal and tangential components, etc.

IV.3. Method of the simulation

Cap and pin insulators have four major components. It constituted of an insulating block carrying to its upper part a cap sealed out of malleable pig iron and inside a steel stem, with grooves and whose conical head is also sealed in glass. The lower end of this stem is round and has dimensions wanted to penetrate in the cap of the following element and to be maintained by a pin there.

The symmetry of the insulator has been exploited when creating the Finite Element Model in two dimensional (2D). The insulator, which is simulated, is shown in figure. IV.2. In this part, an insulator made of the glass material is considered for the simulation dimensions of the 220 kV insulation. Figure IV.2 and table IV.1 shown the real insulator used for the simulation study. So, the FEM model of the real insulator used in this work has been shown in figure IV.3. We examine the electric field and potential distribution of glass insulator in two different surface conditions. The first, clean model and the second, under discontinuous pollution for different conductivities. The properties of the materials of the various domains of the insulator (cap, pin, glass..etc.) are shown in table IV.2. The level of discontinuous pollution (L1) has been kept constant in our chapter.

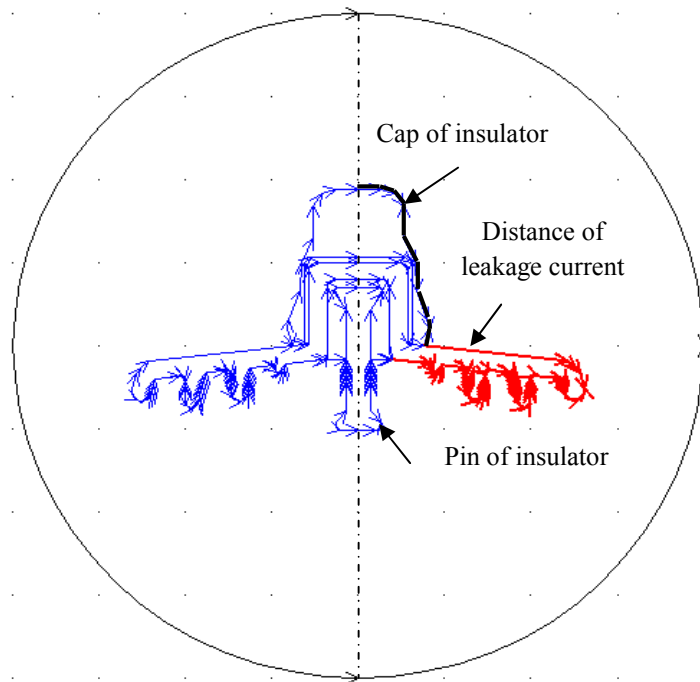


Fig. IV.2. Parameters of cap and pin insulator 1512L.

Tab. IV.1. Geometrical parameter of cap and pin 1512L insulator.

Parameters	Size (mm)
Distance of leakage current	292
Cap of insulator	244
Pin of insulator	125

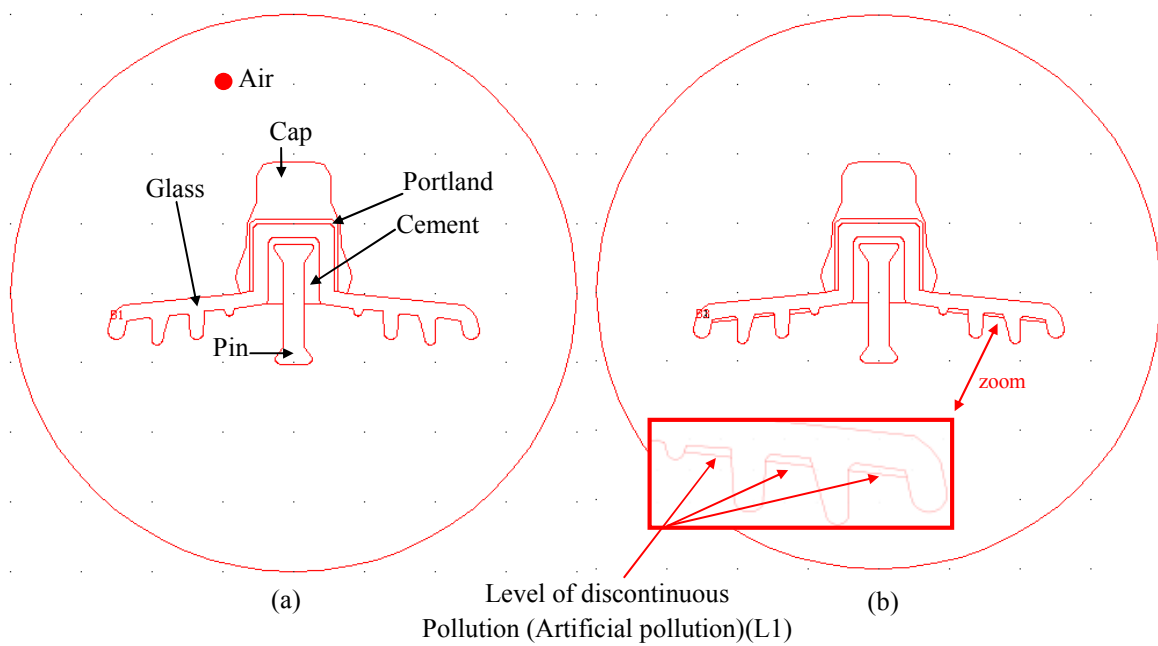


Fig. IV.3. FEM model in the software of 220kV insulator
 (a) Clean model, (b) Discontinuous uniformly polluted model.

Tab. IV.2. Material properties of FEM model of cap and pin 1512L insulator.

Properties	Cap & pin	Glass	Portland & Cement	Air	Artificial pollution
Relative permittivity (ϵ_r)	10^6	6	5	1.0005	80
Conductivities ($\mu s / cm$)	10^6	$1.e^{-12}$	$1.e^{-12}$	$1.e^{-14}$	0,70,700,1200,3000

IV.4. Mathematical Model

Electrostatic problems consider the behavior of electric field intensity: E , and electric flux density (alternatively electric displacement): D . There are two conditions that these quantities must obey. The first condition is the differential form of Gauss Law, which says that the flux out of any closed volume is equal to the charge contained within the volume [10-11]. The basic equations used to calculate the potential (electric field) are Maxwell's equations:

For the electrostatic model, the following equations are used:

$$\text{div} \vec{D} = \rho \quad (\text{IV.1})$$

$$\vec{D} = \epsilon \vec{E} \quad (\text{IV.2})$$

$$\vec{E} = -\overrightarrow{\text{grad}} V \quad (\text{IV.3})$$

The combination of these three equations gives:

$$\text{div} \epsilon (-\overrightarrow{\text{grad}} V) = \rho \quad (\text{IV.4})$$

$$\text{div} \epsilon \overrightarrow{\text{grad}} V = -\rho \quad (\text{IV.5})$$

This expression (IV.4, IV.5) is called the Poisson equation.

So the Laplace's equation can be obtained by making space charge $\rho = 0$.

In our case, in high-voltage equipment, space charges are not present or negligible ($\rho = 0$)

and therefore the equation to be solved for the dielectric media is [11-13]:

Hence the preceding equation becomes (IV.4):

$$\text{div} \epsilon (-\overrightarrow{\text{grad}} V) = 0 \quad (\text{IV.6})$$

The program solves (IV.6) for voltage (potential) distribution V over a user-defined domain with user-defined sources and boundary conditions.

For conductive media in stationary mode, it comes, since $\text{div} \vec{j} = 0$ et $\vec{j} = \sigma \vec{E}$:

$$\text{div} (\sigma (-\overrightarrow{\text{grad}} V)) = 0 \quad (\text{IV.7})$$

The equation of the place in Cartesian coordinates is:

$$\operatorname{div} \overrightarrow{\operatorname{grad}} V = \frac{\partial^2 V}{\partial^2 x} + \frac{\partial^2 V}{\partial^2 y} + \frac{\partial^2 V}{\partial^2 z} \quad (\text{IV.8})$$

The calculation software determines the electrical potential to obtain the field distribution by solving the following partial differential equation for two dimensions [14].

$$-\operatorname{div} \varepsilon \overrightarrow{\operatorname{grad}} V - \operatorname{div} \sigma \overrightarrow{\operatorname{grad}} V = 0 \quad (\text{IV.9})$$

For resolution steps in Comsol Multiphysics can be summarized in the following four successive steps:

- The first step is to define the two-dimensional (2D) geometry of the 1512L insulator in the Comsol (software).
- The second step concerns the definition of the electrical properties of the materials present. It consists of defining the relative permittivities ε and the conductivities σ for each part of the insulator. Also, it is necessary to define the boundary conditions which translate into the potential imposed on each electrode (Dirichlet conditions).
- The third step is devoted to solving the problem by applying the numerical method and by the construction of the system of equations ($-\operatorname{div} \varepsilon \overrightarrow{\operatorname{grad}} V - \operatorname{div} \sigma \overrightarrow{\operatorname{grad}} V = 0$), and this by introducing the factors of each part of the equation.
- The final step is to solve the problem and display the simulation results as the potential distribution and electric field.

The simulation algorithm flowchart computer for COMSOL has shown in figure IV.4.

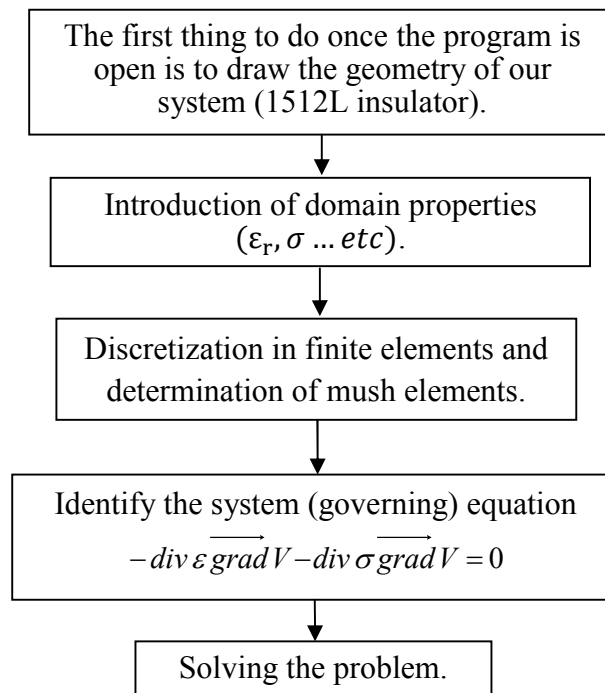


Fig. IV.4. Resolution Steps in COMSOL

IV.5. Results and Discussion

Electric field distribution and voltage distribution mainly depends on applied voltage, properties of materials used in insulator and surrounding or environmental condition. Pollution effect plays an important role in determining the potential distribution and the electric field along the insulator. To demonstrate this effect, several values of the conductivities of the pollution layer were used. The clean case has been also introduced for reference; we suppose that the Finite Elements Method has been best suited to the constraints imposed by the problem. Also, this method has been successfully applied in calculating the electrical field and potential distribution around the insulators. We introduced presented our model with all its specifications in table IV.2 to this software. Due to the complexity of our real model, we have drawn the model in the FEMM software; then we call the model in the software comsol, we followed all the steps as shown by figure IV.4. We fixed the applied voltage of the active electrode with 30 kV.

Numerical results for different meshing presented by figure IV.5. In fact, the type of the mesh has been changed based on the elements number. For thus, two meshes have been tested. The first case corresponds to a coarse mesh composed of 15668 elements (see figure IV.5(a)). The second case corresponds to 62672 elements after refining (see figure IV.5(b)). The corresponding time calculation and the number of nodes and all characteristics of meshing are presented in table IV.3.

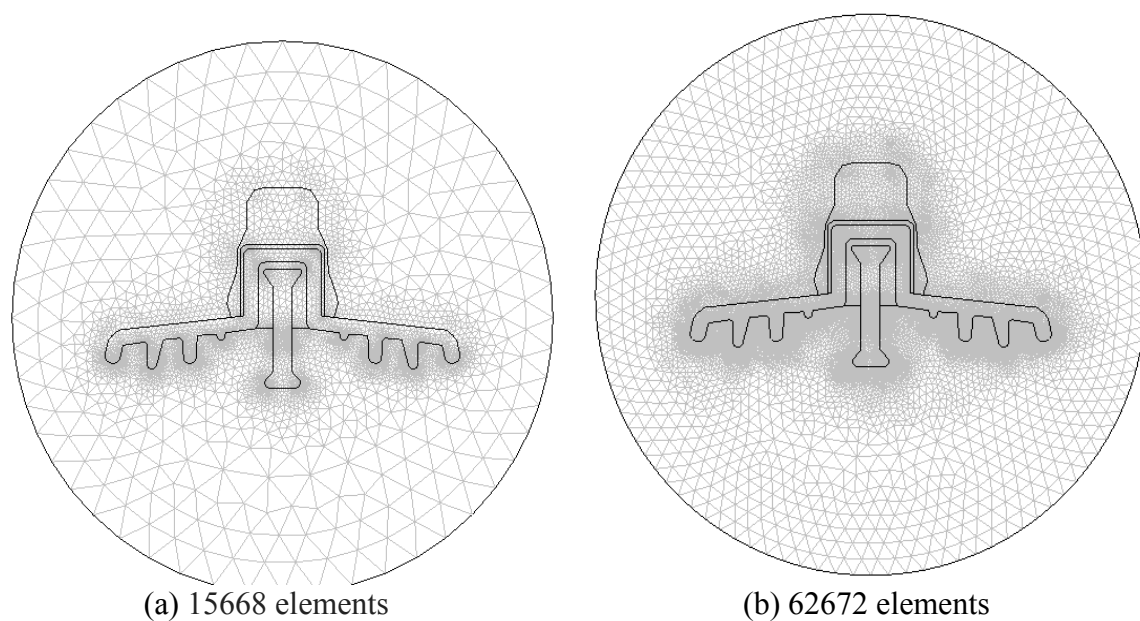


Fig IV.5. Discretization in finite elements and determination of mesh elements of the insulator 1512L.Multiphysics.

Tab. IV.3. Characteristic of the meshing.

		Triangular elements	Number of nodes	Number of boundary elements	Time calculation (s)
Number of elements	15668	15668	7860	912	3.025
Number of elements after the first refining	62672	62672	31387	1824	7.285

IV.5.1. Electric potential distribution

This first part is devoted to the study of the distribution of the electrical potential on the insulator 1512L.

IV.5.1.1. Influence of the conductivities

We were interested in determining the potential distribution on the 1512L. We have introduced in the software, values of the conductivities $\sigma = 0, 70, 1200, 3000 \mu\text{S}/\text{cm}$. The applied voltage of the line has been fixed to 30 kV. It helps to simulate the behavior of the insulators of high voltage (220 kV).

Figure IV.6 to figure IV.8 shows, the potential distribution of the insulator, electrical potential distribution for different conductivities and the variation of the potential along the distance of leakage current for different conductivities respectively.

The maximum voltage is achieved at the insulator pin of the line end unit whereas the minimum voltage is achieved at the insulator cap.

The potential is very important to the high voltage electrode and then decreases as one move away from the ground electrode. In the case of the clean and polluted model, 30kV is the maximum value of the voltage, shown around the active electrode, and then decreases as it moves away from this electrode to the grounding electrode where the potential is canceled. For a $\sigma = 0, 70, 1200, 3000 \mu\text{S}/\text{cm}$ the curves of the potential are confused. In the clean state, the curves of the potential are closer to that of $\sigma = 0, 70, 1200, 3000 \mu\text{S}/\text{cm}$.

We note that the variation of the conductivity of the polluted layer a slight difference can be observed between the results when the insulator is cleaned and when its polluted. The distribution of the voltage along the insulator is not uniform, the part of the insulator nearer the conductor being more highly stressed. Also, the insulator is higher stressed under pollution conditions.

It concluded that the voltage distribution is non-linear and non-uniform along the surface of insulator because of stray capacitance.

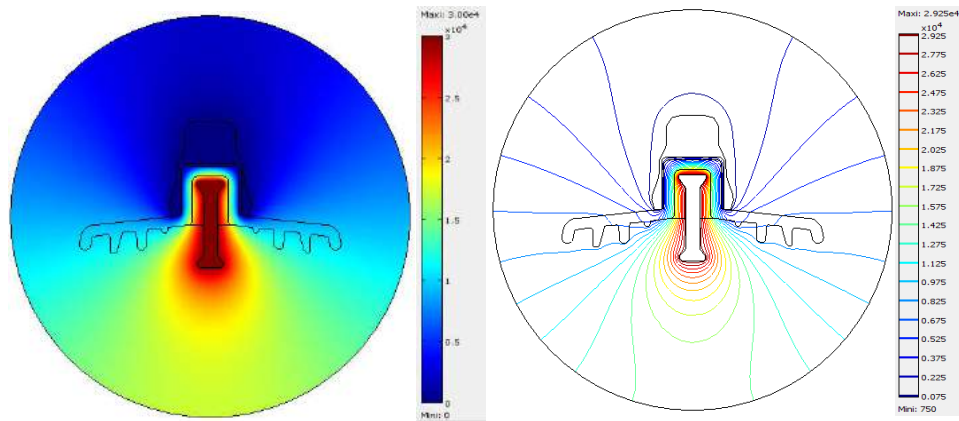


Fig. IV.6. Potential distribution and equipotential lines (clean model).

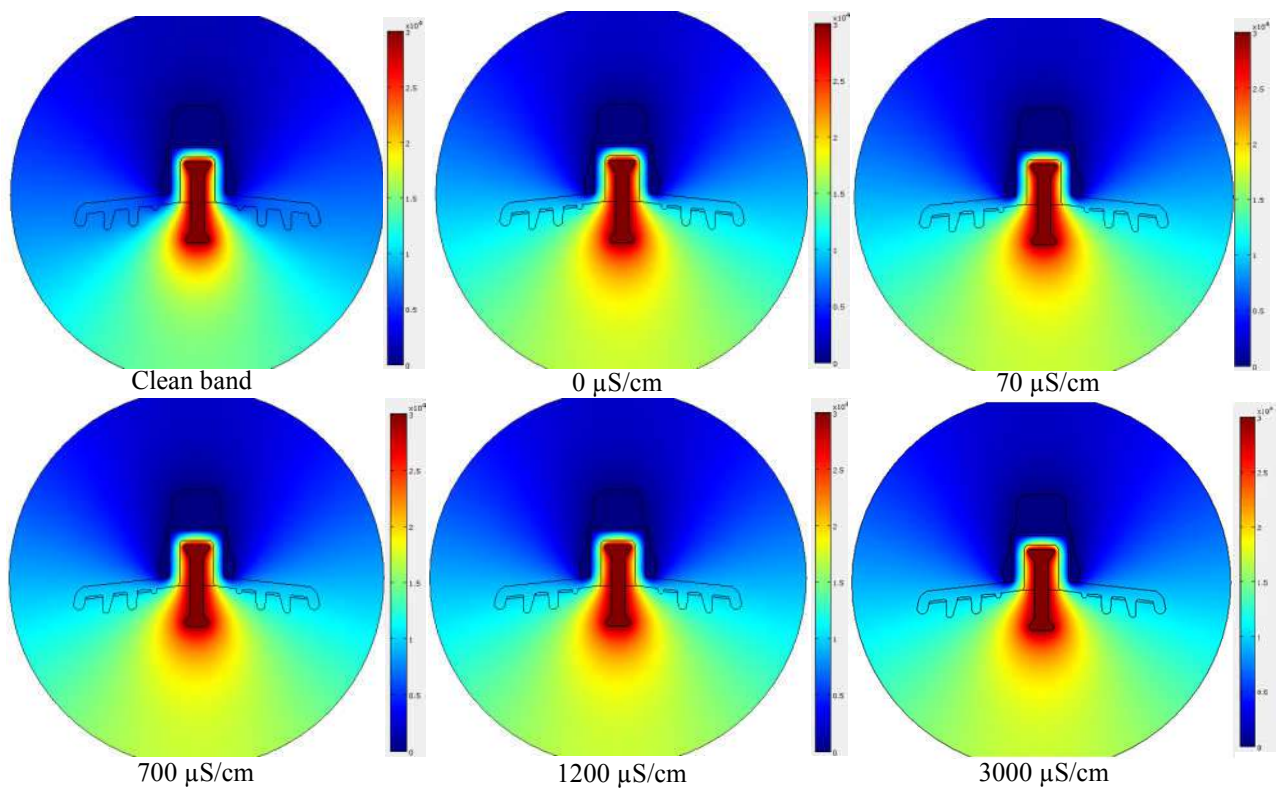


Fig. IV.7. Electrical potential distribution for different conductivities.

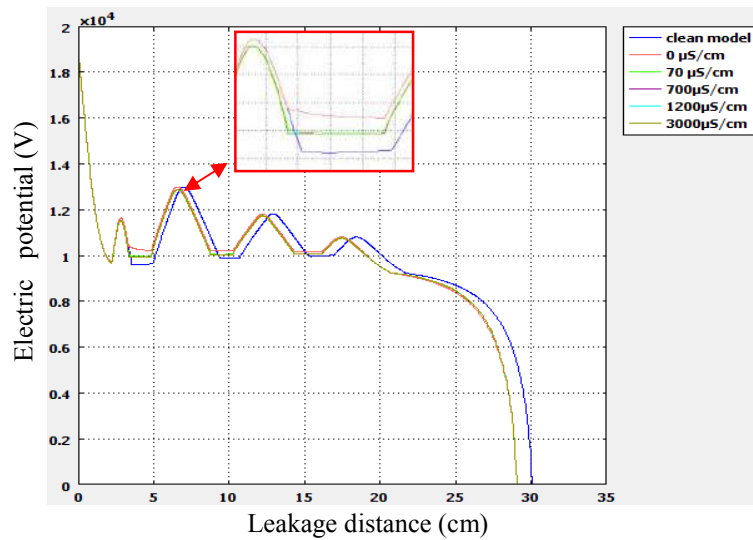


Fig. IV.8. Electric potential-leakage distance for different conductivities.

IV.5.1.2. Influence of the applied voltage of the line

Figure IV.9 presents the distribution of potential depending on the leakage distance for different applied voltage. Shows that in function of the applied voltage of the line, only the values of applied voltage change, the shape is the same. The cap and the pin being the metallic parts. The voltage to their levels remains constant; they are the parts equipotential (active electrode (HV) and ground electrode). The variation of the potential depending on the leakage distance for different applied voltage.

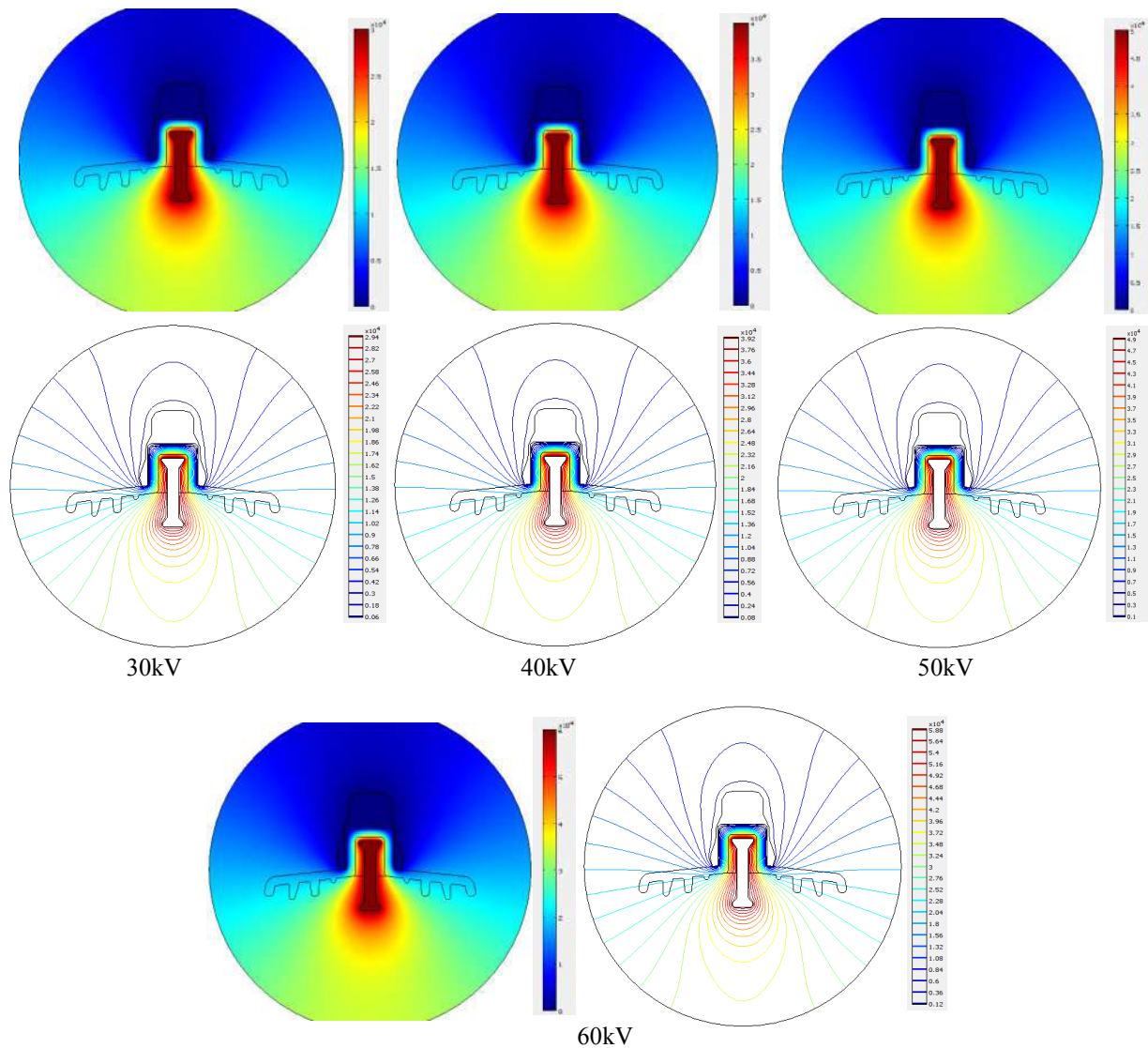


Fig. IV.9. Electrical potential distribution for different applied voltage of the line.

Given in figure IV.10 four levels of applied voltage were considered. We in function of the applied voltage of the line, the potential are distributed equitably along the leakage distance. The three curves are passing equally by three regions where the potential remains constant. It has to do with the metallic parts of the insulator.

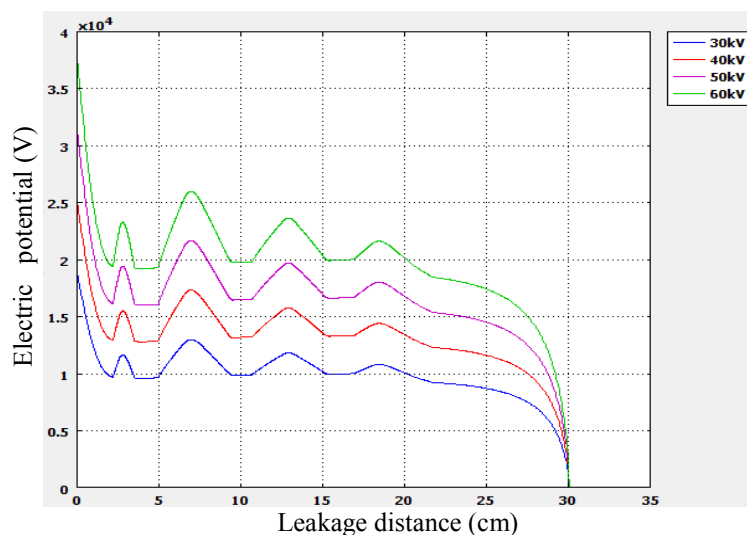


Fig. IV.10. Electric potential-leakage distance for different applied voltage of the line.

IV.5.2. Electric field distribution

For the outdoor high voltage transmission line applications, the insulator strings are exposed not only to the atmosphere but also to the different type of pollutant conditions. Electric field stress at any point along the insulator surface is considered to be responsible for corona and dry band arcing under certain conditions. Non-uniform electric field distribution along the insulator surface can affect their flashover characteristics and can damage the insulator in long term due to corona discharges. [2]

Investigations of the electric field have been studied by many researchers [1-2, 7-10, 10-12, 16-20, 22-23]. In the case of the clean model, (figure IV.11).

We concluded the following:

Within the two electrodes (active and ground electrodes), the electric field is practically zero, because the two electrodes are conductive, the vectors of the electrical fields emerge from the activated electrode to ground electrode. The vectors shown in figure IV.11 are a tangent, we see that the electric field is more significant with the internal dimensions of the electrodes.

The electric fields vectors emerge from the activated electrode to ground electrode. The vectors (tangent) shown in figure IV.11 are stronger at the junction of insulator pin-cement- verre. The electric field vectors are scattered throughout the specified region. We see that the electric field is more significant with the internal dimensions of the electrodes.

We noted that the electric field intensity is higher at those points which are closer to energized end (insulator pin) than those points which are closer to the grounded end (insulator

cap). Also it is observed that, the magnitude of electric field has higher values at the junction of (air-cap-glass).

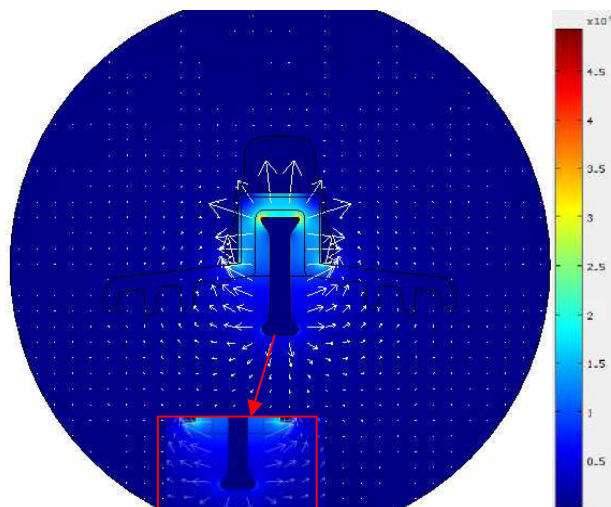


Fig. IV.11. Electrical (electric) field distribution for a clean model.

IV.5.2.1. Influence of the conductivities

For a constant voltage of 30kV, figure IV.12 presents the variations of the intensity of electric field along of the leakage distance of the insulator. The intensity electric field is very high notably when the model is polluted, in the cap of insulator (ground).

Electric field investigated in literature that corona and dry band arcing are closely related with the ageing, degradation of insulator surface [24]. Electric field distribution along a 1512L insulator has been investigated under contamination conditions to evaluate the effect of pollution on electric field stress along the insulator surface and the possibility of corona and dry band arcing initiation.

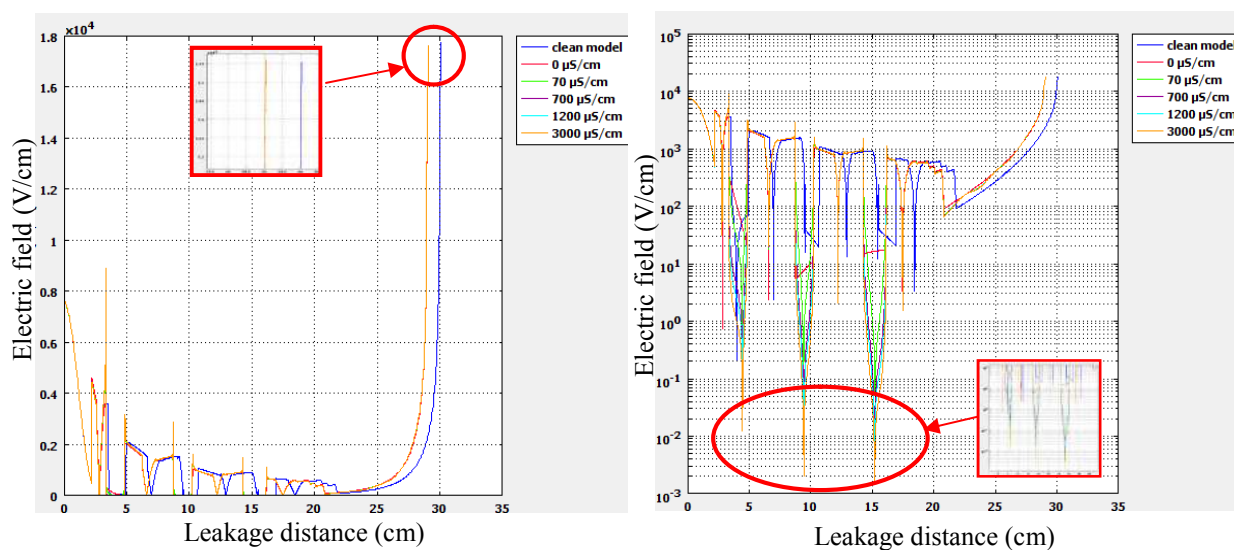


Fig. IV.12. Electric field-leakage distance for different conductivities.

In the clean layers on the surface of the insulator, the electric field is more intense, which explains experimentally, the appearance of the electric arcs at the levels of the clean layers before the flashover of the insulator. Indeed, the electric arcs were observed in experimental studies by many researchers [16,22,25-29]. The electric fields lines diverge from the active electrode (oriented from the HV electrode to the ends of the insulator and converge towards the ground electrode) and the system becomes less rigid and the conductivity of the surface of the insulator increases. In the near of the active electrode, the electric field is intense and decreases as it moves away from the active electrode and closer to the ground electrode. Also, the electric field vectors diverge (from the HV (active) electrode to the ground electrode). In the near area of the active electrode, the electric field is important, and zero in the clean zones (figure IV.12 (a)). figure IV.12 (b) on the logarithmic scale shows that in the dielectric material, the electric fields is never canceled, but takes values close to zero, (The field does not disappear in the insulator but gives a very low value).

Otherwise, figure.IV.13 shows that the increase in the conductivity of the layer of pollution generates an increase in the current density and consequently the electric field. The influence of the pollution severity on the distribution of the electric field has been presented in [30], and it has been shown that the intensity of the electric field increases with the increase of the conductivities of the pollution.

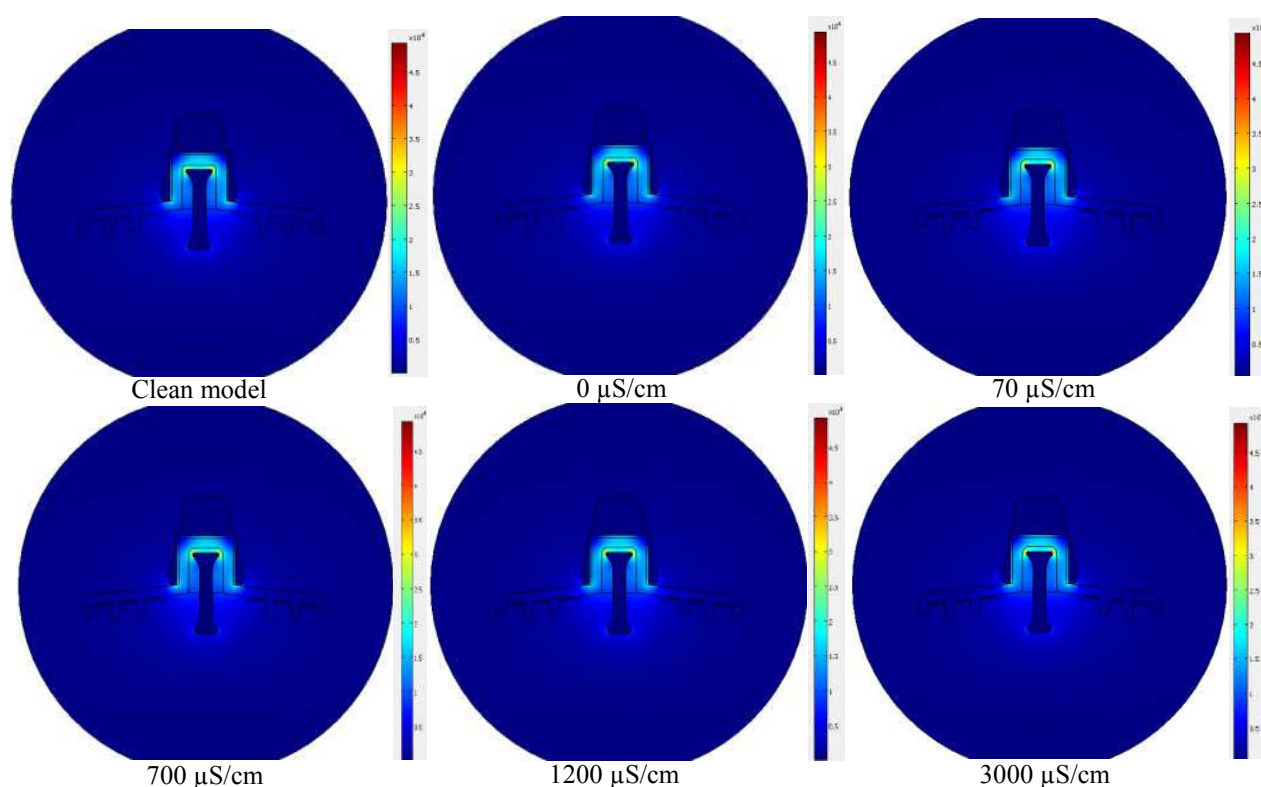


Fig. IV.13. Electric field distribution for different conductivities.

IV.5.2.2. Influence of the applied voltage of the line

For a clean model, we present in the figure IV.14 electric field along the leakage distance for different applied voltage, (a) simple scale & (b) logarithmic scale.

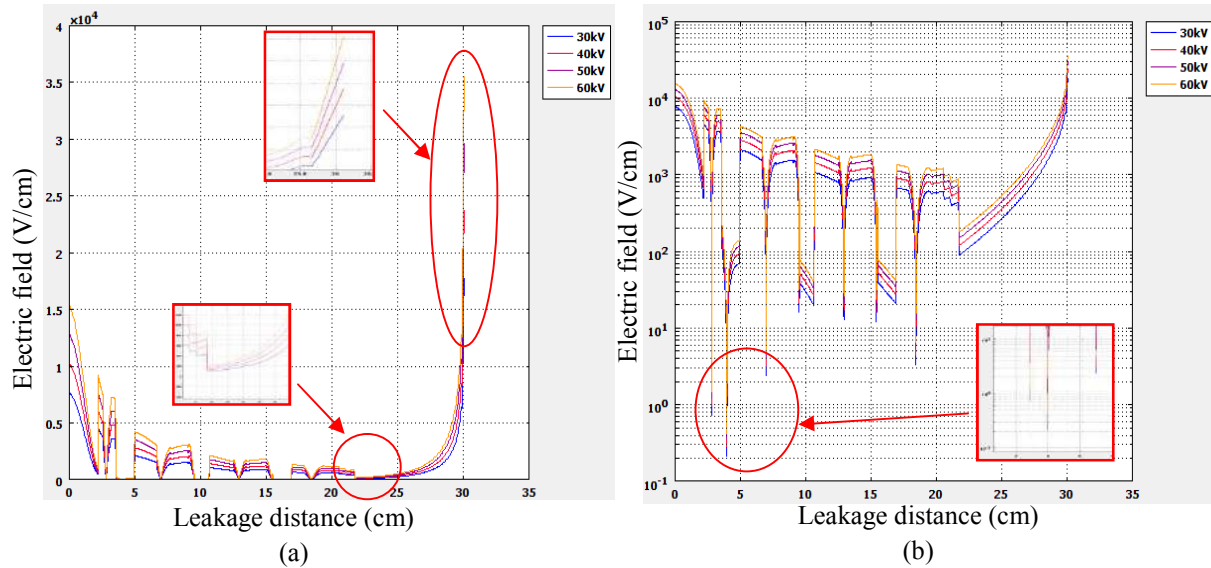


Fig. IV.14. Electric field-leakage distance for different applied voltage.
 (a) Simple scale (b) Logarithmic scale.

The increase of the applied voltage of the line increases the intensity of the electric field (Figure IV.14 (a)). Also, the insulator becomes less rigid, which explains exactly in the experiment that the increase in the applied voltage causes the flashover of the insulator.

We also note that electric field gets maximal values at the extremities of the insulator (cap and pin of the insulator). Obviously, as shown, that the electric field never vanishes in the dielectric materials (glass), but gives a very small value (figure IV.14 (b)). Figure IV.15 presents the electric field distribution for different applied voltage of the line, the increase of the applied voltage leads to the increase of the intensity of the electric field.

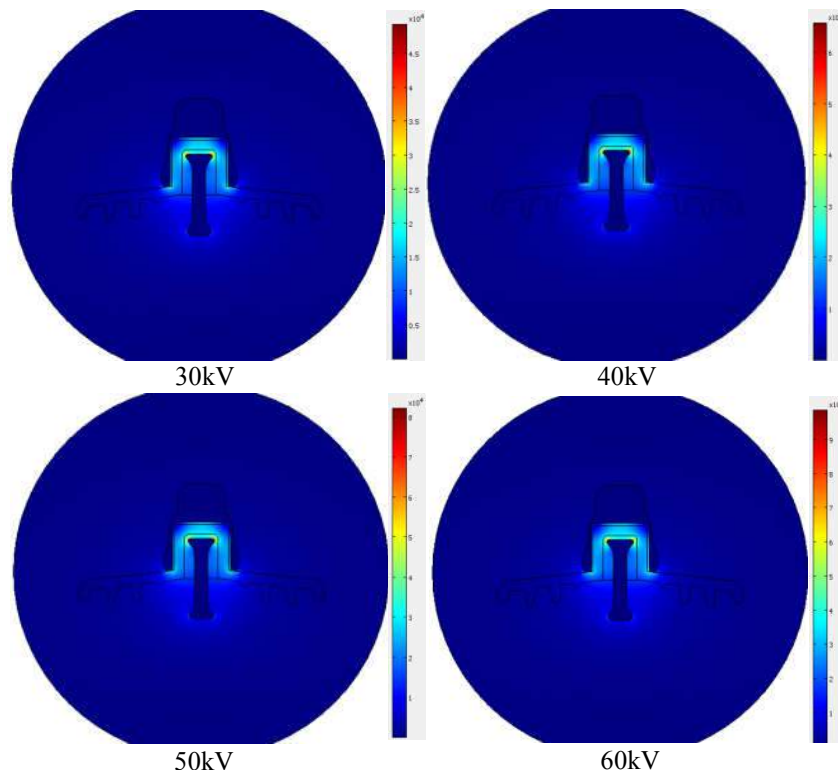


Fig. IV.15. Electric field distribution for different applied voltage.

IV.5.3. Influence of the rib width of the insulator

In this part we have been able to find, if possible, the model with the same leakage distance, the same surface and practically the same shape (form) as the real model, but with a better distribution of the field. This leads us to assume that the real model can be improved. Always our system studied has been mentioned previously in figure .IV.2 having the characteristics presented in table IV.1.

Our work is to change the geometry of the real insulator (1512L) by changing the length of leakage distance and keeping the same radius (R). The results of the field thus obtained will be compared with those obtained by the real model. In order to see the influence of the width of the ribs ($x_{1,2,3,4}$) of the cap and pin insulator, to determine the distribution of the electric field on this insulator model, which is mentioned in figure IV.16.

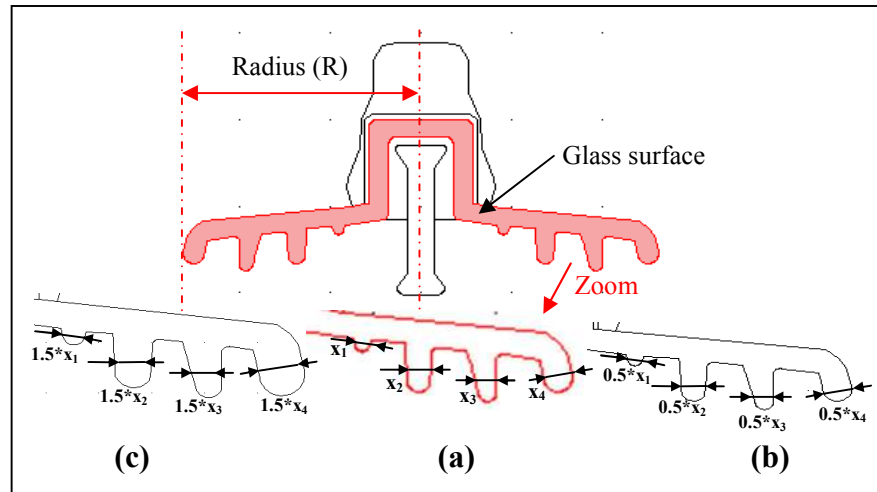


Fig. IV.16. Dimensioning of the ribs of the insulator 1512L.

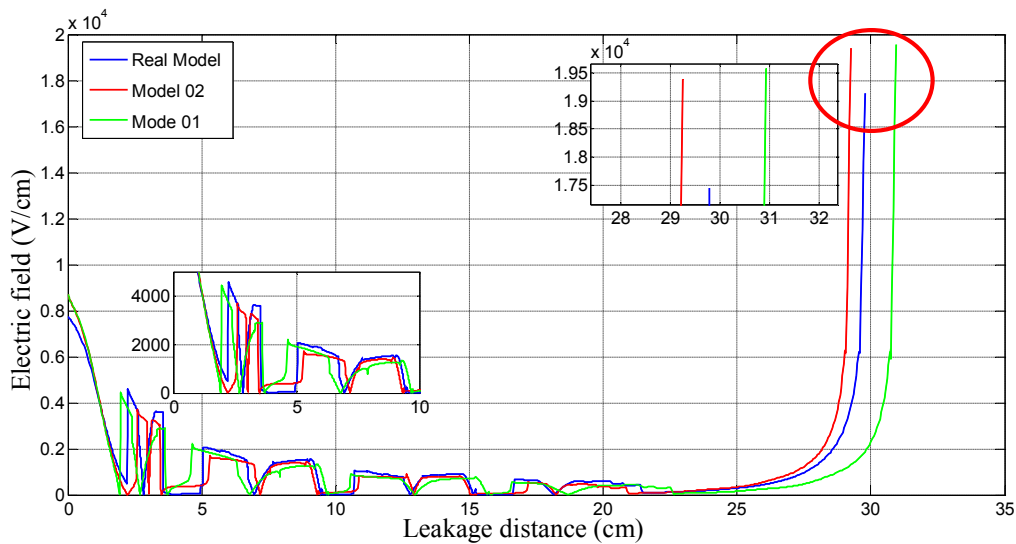
(a)Real Model, (b) Model_02, (c) Model_01.

- **Real_Model** (a) keeping our real dimensions of the cap and pin insulator 1512L, with a surface of 47.949cm².
- **Model_02** (b) by decreasing the width of the ribs by 0.5 of its real width, but keeping the same radius (R) as the real model, with a surface of 42.7028 cm².
- **Model_01** (c) by increasing the width of the ribs by 1.5 of its actual width, but keeping the same radius (R) as the real model, with a surface of 53.873 cm².
- Changes in the real model, are made in a hazardous way in (figure IV.16 a, b, c), table IV.4.

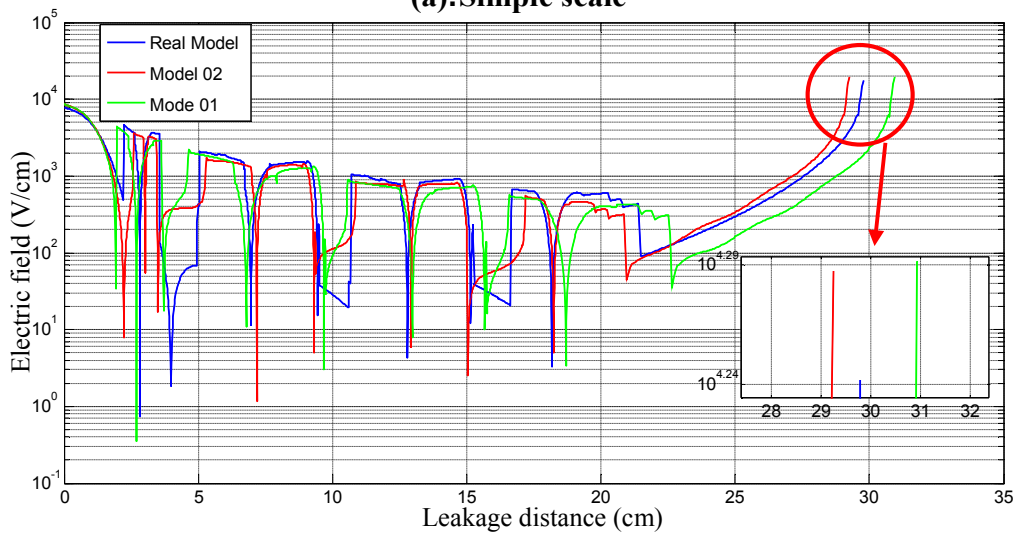
Tab. IV.4. Sizing of proposed HV insulator.

Model study	Dimension	Radius	Glass surface (cm ²)
Real model	$x'' = x = [x_1, x_2, x_3, x_4]$ (fig.IV.15.-a-)	R	47.949
Model_02	$x'' = 0.5 * x = 0.5 * [x_1, x_2, x_3, x_4]$ (fig.IV.15.-b-)	R	42.7028
Model_01	$x'' = 1.5 * x = 1.5 * [x_1, x_2, x_3, x_4]$ (fig.IV.15.-c-)	R	53.873

Figure IV.17 ((a) simple scale, (b) logarithmic scale), shows respectively the distribution of the normal tangential component of the electric field on the insulator on the leakage distance for the three cases studied (real model, model_01, model_02), for the models indicated in table IV. 4. We apply a voltage of 30 kV in the case of the insulator.



(a). Simple scale



(b) Logarithmic scale

Fig. IV.17. Electric field-leakage distance for three studied cases (real model, model_01, model_02). (a) Simple scale, (b) Logarithmic scale.

The results cited above demonstrate the importance and influence of the geometric shape of the insulator on its dielectric behavior.

We notice that the electric field fluctuates between the cap and the pin of the insulator, it presents several local maximums. These local fluctuations and local maximums explain the appearance of localized arcs on the surface of the insulator.

We also note that the distribution of the field on the leakage distance follows the same variations of the real model with a spatial shift due to the difference of the leakage distance lengths. In general, the shape of the field distribution is similar for all models studied. Since the changes made are done in a hazardous manner, the chance of achieving a good result is very small.

From the results that we have come up the real model is the model optimize, the value of the electric field to the cap of the real insulator is optimal with compared the other two models.

IV.5.4. Performance of a destroyed insulator

The insulator during its service is under several constraints: mechanical, electrical and environmental.

These constraints can affect the performance in several ways such that the destruction of the ribs due to mechanical force acts on the insulator.

For this we change the geometry of the insulator 1512L so as to reduce the line of leakage distance of the insulator and keeping the same radius (R).

The changes made to the real model are shown in figure IV.18. Two cases studied:

- One for a broken of the four ribs of the insulator,
- The other for broken only two ribs in the middle.

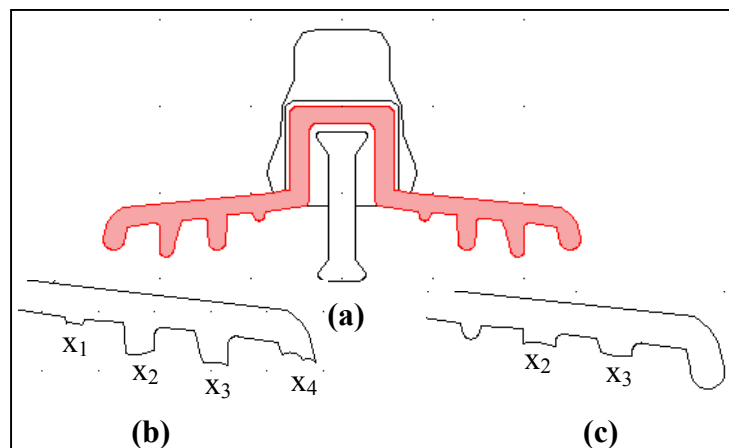


Fig. IV.18. Insulator destroyed for two cases

(a) Real model

(b) Broken ribs $x_{1,2,3,4}$

(c) Partially broken (the two internal ribs $x_{2,3}$)

Figure IV.19 ((a) Simple scale (b) Logarithmic scale), represents respectively the distribution of the normal tangential component of the electric field on the line of leakage distance of the insulator for the three cases studied (real model, broken ribs, partial broken ribs), you can see that the distribution of the electric field on the leakage distance takes the same form of a real model, with a spatial shift due to the decrease of the leakage distance.

So we can say that this figure IV.18 confirms that the decrease of the leakage distance with maintaining the constant radius, leads to a change in the geometric shape of the insulator lead the increase of the electric field, which could reduce the flashover voltage.

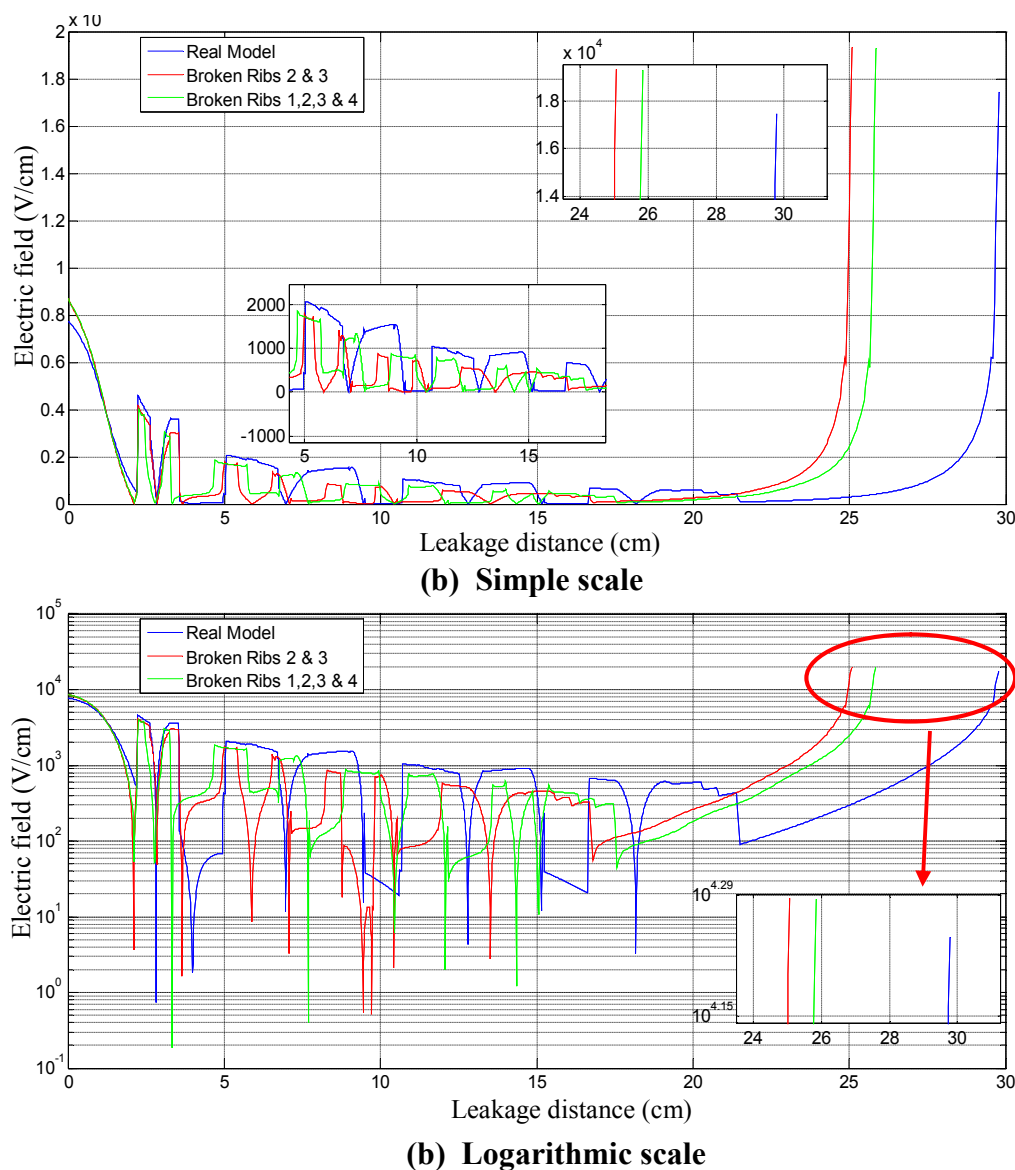


Fig. IV.19. Electric field-leakage distance for three studied cases (real model, broken ribs, partial broken ribs). (a) Simple scale, (b) Logarithmic scale.

IV.6. Conclusion

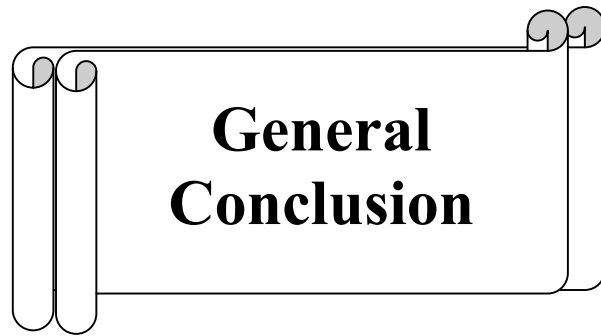
In this work, we have studied the electric field and electric potential distribution artificially polluted of cap and pin insulator (1512L) largely used by Algerian Society for Electricity and Gas (SONELGAZ). It has been analyzed using COMSOL multiphysics based on the finite element method (FEM), for different electro-geometric parameters such as the influence of conductivity and applied voltage of the line under AC voltage.

The surface state which affects the distribution of the potential and the electric field. Indeed, the potential distribution is practically equitable since all the elements of the insulator will receive a very close potential difference. Moreover, the parts near the active electrode are most exposed to the electric constraints, namely, the potential difference and the electric field. The metal parts of the insulator, in this case, the cap and the pin, are equipotential and the value of the potential is always fixed. We also noted that potential and the electric field increases with the applied voltage. However, the form (shape) of the electric field and potential remain the same. In other words, the difference is in the magnitudes and not in the form. We have noted that the potential and the electric field increase with the increase in applied voltage.

The maximum value of the electric field is obtained when the insulator is polluted (3000 $\mu\text{S}/\text{cm}$). On the other hand, the effect of the surface state and the conductivity of the pollution is very negligible on the potential distribution. The performance study of a real insulator has the advantage of taking into account all the complexity of the real model for a good analysis of the physical phenomena.

The modification of the geometric shape of the insulator generates an increase in the electric field, then a reduction of the flashover voltage.

Finally, in this chapter, it has been shown how Comsol Multiphysics have been used to calculate the electric field, and potential distribution for electrostatics problems have been achieved.



**General
Conclusion**

General Conclusion

The presence of a pollution layer on the surface of an insulator completely changes the behavior of the high voltage insulator. This study allowed us, first of all, to acquire knowledge about the phenomena of conduction and electric discharge on contaminated insulating surfaces, and to contribute, afterwards, to the study of the behavior of polluted insulators.

As part of this thesis, we studied the flashover phenomenon of polluted insulators of high voltage. In particular, Our research work is a contribution to the study of the behavior of an insulator 1512L of HV in the conditions of pollution under electro-geometric stress when an AC voltage is applied to it.

In a first place, we made a comparative experimental study between the real model and our proposed model based on the experimental tests. However our model facilitates the observations and the measurements necessary for a good (functional) analysis of the physical phenomena of flashover.

The original idea in this part that the sophisticated (complex) form of the insulator has been replaced by a developed model also called circular model. The advantage of the latter is that it gives the opportunity to see and better understand the phenomenon of flashover retaining the same characteristics of the real model, especially the distance of leakage current.

The following results have been reported:

- During the development of the arc, the leakage current increases.
- The flashover of polluted insulators is initiated with lower leakage current.
- The value of the minimum flashover voltage is obtained for higher conductivity and pollution level ($L8$ and $\delta = 93.7$ mS/cm).
- The flashover of polluted insulators depends on the conductivity as well as the level of pollution that is applied to the surface of the insulators.
- The leakage current increases with the applied voltage, the conductivity and the level of pollution.
- The insulator has a capacitive character in the proper case, this is explained by the domination of clean areas compared to polluted ones and takes the resistive case in the polluted case where the insulator becomes less rigid.
- Pollution on the surface of insulators creates a non-uniform distribution of voltage along the length of the leakage distance.

The prediction of flashover voltage using two artificial intelligence methods "LF" also referred to as fuzzy inference system "FIS" based on human expertise, and the "ANN" neuron network.

The results obtained by the ANN method are more efficient compared to those found by the fuzzy logic "FL". This is justified by the coefficient of determination (error%) making it possible to evaluate the performance of the artificial intelligence method between the estimated values (calculated) and the experimental values of the flashover voltage. The percentage of correct predictions relative to the experimental results obtained by the fuzzy logic is 91.083%.

The coefficient of determination R obtained by the ANN approach is 99.271% of the calculated "V" values are the same as the desired data reserved for the test, it is very acceptable and superior to that found by FL. It should be noted that the maximum value of R is 1. The percentage of correct predictions compared to the experimental results obtained by the neuron network is 98.273%. Although ANNs demonstrate good efficiency and attractive performance in some areas, an appropriate definition of their parameters, in advance, remains a crucial task to ensure their smooth operation.

The original idea in this is the involvement of artificial intelligence " FL & ANN " to predict the flashover voltage of an insulator of HV. The results from the validation show that the ANN method is more efficient in predicting the flashover voltage than the fuzzy method "FL", these results also show the importance and interest of ANN neuron network in the improved performance of the estimate (calculate).

The validation of two proposed ANN & FL methods has been justified by the evaluation indices. The average error (E_{av} (%)), the absolute error $|\text{Error}|$ and in percentage (Error%), the coefficient of determination (R) thus the rate of correct predictions compared to the experimental results in (%).

We can also say that apart from its originality, its potential and universality of application, the ANN and FL approach could be considered as a step further in the field of research of the phenomenon of flashover of polluted insulators, particularly the prediction of the flashover voltage. About the use of artificial neural networks, the rate of correct predictions of the tests carried out is the highest in all the methods used (studied).

The difficulty we have encountered in the use of artificial intelligence techniques (ANN and LF) lies in the choice of their parameters. Let's start with the fuzzy logic, the difficulties concerns, the fuzzification of the input variables and the output (a form of the membership

function, number of fuzzy sets associated for each variable) and the creation of the fuzzy rules that connect the inputs to the output. We can say here that there are no rules for choosing fuzzy inference system parameters.

The implementation of the fuzzy inference system "SIF" in the MATLAB environment using the graphical interface "SIF" is characterized by its simplicity. The choice of the various system parameters is the most crucial phase of the application of the fuzzy logic, then implement it according to the different necessary steps.

Finally and with the aim of studying the performances of a real insulator of HV by the finite element method "FEM" with the advantage of taking into account all the complexity of the model for functional (good) analysis of the physical phenomena based on the Comsol Multiphysics environment.

As primary results, we can say that the conductivity of the polluting layer has practically no effect (no observed) on the distributions of the potential and the electric field. On the other hand, it is the surface state of the insulator which influences the distribution of the electric field.

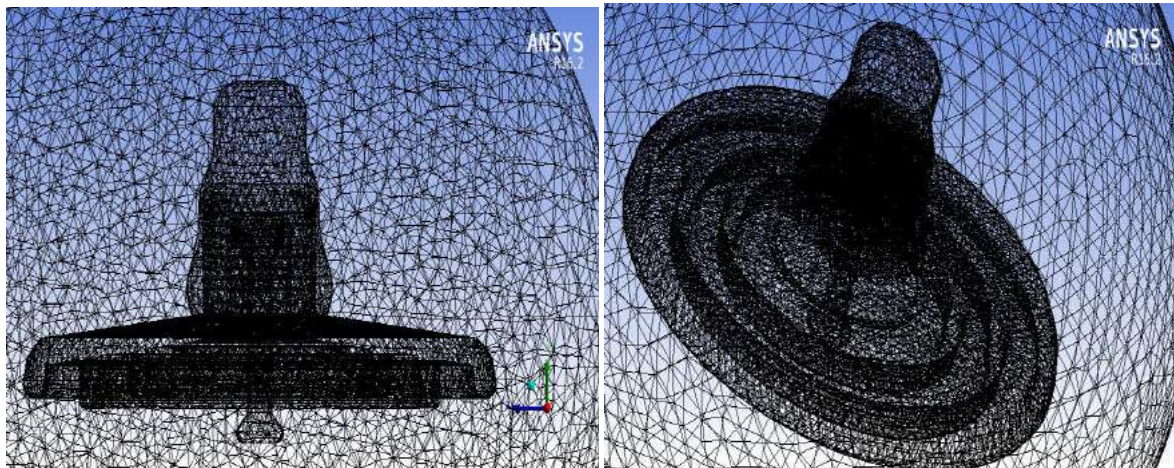
The maximum field is reached at the pin whatever they are of the dimensions of the insulator, so the field remains relatively high at the cap.

The electric field increases with the applied voltage. However, the shape (form) of the field and the electrical potential remain the same. In other words, the difference is in the values and not in the form.

To get better performance of the insulator, keeping us the same rayon of the real insulator but we play on the dimensioning of the ribs randomly leads to a change in the geometric shape (form) of the insulator and increases the electric field, which could lead to a reduction in the flashover voltage.

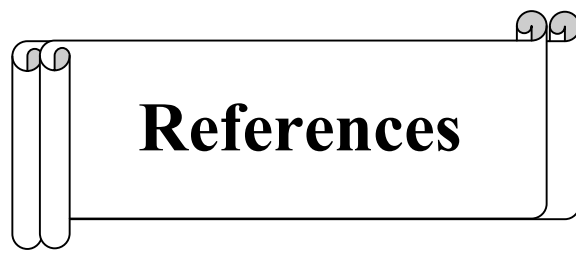
The modification of the geometrical shape of the insulator generates an increase of the electric field, then a reduction of the flashover voltage.

The followed approach and results presented in this work open to multiple perspectives as an experimental point of view than a view of modeling and numerical simulation of physical phenomena occurring on insulators for transmission lines and distribution of electrical energy in humid conditions (rain, dew ...) with an aim of optimization of the real model by using ANSYS in the response surface window.



1512L insulator in ANSYS.

We hope to humbly contribute, by this thesis, to see the behavior of insulators exposed to pollution under AC voltage.



References



References

Ref_General Introduction

- [1] H. Terrab, A. Bayadi. "Experimental study using design of experiment of pollution layer effect on insulator performance taking into account the presence of dry bands". IEEE Transactions on Dielectrics and Electrical Insulation. 21 (2014) 2486-2495.
- [2] El Bahi Azzag. "Problèmes de contournement et perforation des isolateurs de haute tension". PhD, Thesis, Annaba University, Algeria, 2007.
- [3] V. M.Rutsky. "Prediction of discharge characteristics of external high-voltage insulation near industrial enterprises, polluting the atmosphere". 9^{ème} international symposium on high voltage engineering, rapport 3247, Autriche, 28 Aout-1^{er} September 1995.
- [4] G. Houlgate, P.J. Lambeth, W.J. Roberts. "Performances des isolateurs en milieu maritime en très haute et ultra haute tension". CIGRE, Rapport 33-01, 1982.
- [5] Keller-Jacobsen, Aa. Pederson, J.K. Rasmussen, A. Henriksen, C. Lindqvist, S. Smedsfelt. "Essais au laboratoire et en plein air pour dimensionner correctement les isolateurs exposés a la pollution saline". CIGRE, rapport 33-11,1978.
- [6] M.A.B El-Koshairy, El Sayed A.H Aly, A.E Abdullah, Ahmed M. El-Arbaty, E.A.A Mansour, S. El Debeiky. "Comportement des isolateurs en résine époxy pour lignes de transport à haute tension dans les conditions de pollution rencontrées dans le désert". CIGRE, rapport 15-12, 1978.
- [6] A. El-Arbaty, A.Nosseir, S. El-debeiky, E. Nasser, A. El-Sarky. "Choix d'isolateurs utilisables dans des ambiances polluées et notamment dans des régions désertiques". CIGRE, Rapport 33-11, 1980.
- [7] M.A.B El-Koshairy, E. El-Sharkawi, M.M. Awad, H.E.M Zarzoura, M.M. Khalifa, A. Nosseir."Performances de chaines d'isolateurs haute tension soumises à la pollution du désert". CIGRE, Rapport 33-09, 1982.
- [8] J. Li, Z. Guang, L. Wang, H. Yang. "An Experimental Study of AC Arc Propagation over a Contaminated Surface". IEEE Transactions on Dielectrics and Electrical Insulation. 19 (4) (2012) 1360-1368.
- [9] F. Obenaus. "Contamination flashover and creepage path length". Dtsch. Elektrotechnik 1958, 12, 135–136.
- [10] F. A. M. Rizk. "Mathematical Models for Pollution Flashover". Electra. 78 (1981) 71-103.
- [11] R. Wilkins. "Flashover of high voltage insulators with uniform surface pollution films". IEE Proceedings - Generation, Transmission and Distribution. 116 (1969) 457–465.
- [12] S.Gopal, Y.N. Rao. "Flashover phenomena of polluted insulators". IEE Proceedings. 131 (3)(1984) 140–143.

- [13] N.Dhahbi-Megrache, A . Beroual. "Flashover Dynamic model of polluted insulators under AC voltage". IEEE Transactions on Electrical Insulation. 7 (2000) 283–289.
- [14] M. Khalifa, M. Abou-Seda, H. El-Ghazaly. "Laboratory simulation of desert pollution flashover of high voltage insulators. Proc Fourth Int Symp on HV Engineering1983. pp. 5-7.
- [15] A.G. Kanashiro, G.F. Burani. "Leakage current monitoring of insulators exposed to marine and industrial pollution". Electrical Insulation, 1996, Conference Record of the 1996 IEEE International Symposium on. IEEE1996. pp. 271-274.
- [16] A. Loannis, Stathopulos. "Relation between pollution flashover voltage and maximum leakage current" 7^{eme} international symposium on high voltage engineering, Dresden, Rapport 43-20, 26-30 Aout 1991.
- [17] F. Bouchelga, R. Boudissa. "Effect of the development of electrical parallel discharges on performance of polluted insulators under DC voltage". IEEE Transactions on Dielectrics and Electrical Insulation. 22 (2015) 2224-233.
- [18] F. Aouabed, A. Bayadi, R. Boudissa. "Flashover voltage of silicone insulating surface covered by water droplets under AC voltage". Electric Power Systems Research. 143 (2017) 66-72.
- [19] M.E.-A. Slama, A. Beroual, H. Hadi. "Influence of the linear non-uniformity of pollution layer on the insulator flashover under impulse voltage-estimation of the effective pollution thickness". IEEE Transactions on Dielectrics and Electrical insulation. 18 (2011) 384-392.
- [20] Z. Zhang, X. Jiang, Y. Chao, L. Chen, C. Sun, J. Hu. "Study on DC pollution flashover performance of various types of long string insulators under low atmospheric pressure conditions". IEEE Transactions on Power Delivery. 25 (2010) 2132-2142.
- [21] R. Matsuoka, K. Kondo, K. Naito, M. Ishii. "Influence of nonsoluble contaminants on the flashover voltages of artificially contaminated insulators". IEEE Transactions on Power Delivery. 11 (1996) 420-430.
- [22] R. Matsuoka, S. Ito, K. Sakanishi, K. Naito. "Flashover on contaminated insulators with different diameters". IEEE transactions on electrical insulation. 26 (1991) 1140-1146.
- [23] L. Bo, R. S. Gorur . "Modeling Flashover of AC Outdoor Insulators under Contaminated Conditions with Dry Band Formation and Arcing". IEEE Transactions on Dielectrics and Electrical Insulation. 19(3) (2012) 1037-1043.
- [24] A. Farag. "Estimation of polluted insulators flashover time using artificial neural networks". AFRICON, 1996, IEEE AFRICON 4th. pp. 226-234.
- [25] V. Kontargyri, A. Giaketsi, G. Tsekouras, I. Gonos, I. Stathopulos. "Design of an artificial neural network for the estimation of the flashover voltage on insulators". Electric Power Systems Research. 77 (2007) 1532-1540.

- [26] G. Asimakopoulou, V. Kontargyri, G. Tsekouras, C.N. Elias, F. Asimakopoulou, I. Stathopoulos. "A fuzzy logic optimization methodology for the estimation of the critical flashover voltage on insulators". *Electric Power Systems Research*. 81 (2011) 580-588.
- [27] G. Asimakopoulou, V. Kontargyri, G. Tsekouras, F. Asimakopoulou, I. Gonos, I. Stathopoulos. "Artificial neural network optimisation methodology for the estimation of the critical flashover voltage on insulators". *IET Science, Measurement & Technology*. 3 (2009) 90-104.
- [28] V. Kontargyri, A. Gialketsi, G. Tsekouras, I. Gonos, I. Stathopoulos. "Design of an artificial neural network for the estimation of the flashover voltage on insulators". *Electric Power Systems Research*. 77 (2007) 1532-1540.
- [29] M. Gençoğlu, M. Cebeci. "Investigation of pollution flashover on high voltage insulators using artificial neural network". *Expert Systems with Applications*. 36 (2009) 7338-7345.
- [30] M. Cirstea, A. Dinu, M. McCormick, J.G. Khor. "Neural and fuzzy logic control of drives and power systems". *Livre elseiver*, 2002.
- [31] Y. Bourek, L. Mokhnache, S. Nait, R. Kattan. "Study of discharge in Point-Plane air interval using fuzzy logic". *Journal of Electrical Engineering and Technology*. 4 (2009) 410-417.
- [32] G. Asimakopoulou, V. Kontargyri, G. Tsekouras, C.N. Elias, F. Asimakopoulou, I. Stathopoulos. "A fuzzy logic optimization methodology for the estimation of the critical flashover voltage on insulators". *Electric Power Systems Research*. 81 (2011) 580-588.
- [33] J. S. Roger Jang, N. Gulley. "MATLAB Fuzzy Logic. Toolbox- User's Guide Fuzzy Logic".
- [34] C. Volat, F. Meghnefi, M. Farzaneh, H. Ezzaidi. "Monitoring leakage current of ice-covered station post insulators using artificial neural networks". *IEEE Transactions on dielectrics and Electrical insulation*. 17 (2010) 443-450.
- [35] H.O. de Lima, S.C. Oliveira, E. Fontana. "Flashover risk prediction on polluted insulators strings of high voltage transmission lines". *Intelligent Systems Design and Applications (ISDA), 2011 11th International Conference on. IEEE2011*. pp. 397-401.
- [36] H.O. de Lima, S.C. Oliveira, E. Fontana. "Fuzzy inference system for risk classification on polluted insulator strings of high voltage transmission lines". *Microwave & Optoelectronics Conference (IMOC), 2011 SBMO/IEEE MTT-S International. IEEE2011*. pp. 117-120.
- [37] N.A. Al-geelani, M.A.M. Piah, R.Q. Shaddad. "Characterization of acoustic signals due to surface discharges on HV glass insulators using wavelet radial basis function neural networks". *Applied Soft Computing*. 12 (2012) 1239-1246.
- [38] M. Savaghebi, A. Gholami, A. Jalilian, H. Hooshyar. "A neuro-fuzzy approach for estimation of time-to-flashover characteristic of polluted insulators". *Power and Energy Conference, 2008 PECon 2008 IEEE 2nd International. IEEE2008*. pp. 1485-1487.

- [39] J.-L. Rasolonjanahary, L. Krahenbuhl, A. Nicolas. "Computation of electric fields and potential on polluted insulators using a boundary element method". IEEE Transactions on Magnetics. 28 (1992) 1473-1476.
- [40] S.A Bessedik. "Contournement des isolateurs pollués". Ph.D. thesis in Sciences, Department of Electrical Engineering, University of oran,Oran, Algeria, june 28, 2015.
- [41] R. Hartings. "Electric fields along a post insulator: AC-measurements and calculations". IEEE transactions on power delivery. 9 (1994) 912-918.
- [42] H. El-Kishky, R. Gorur. "Electric potential and field computation along ac HV insulators". IEEE Transactions on Dielectrics and Electrical Insulation. 1 (1994) 982-990.
- [43] C. Volat, M. Farzaneh. "Three-dimensional modeling of potential and electric-field distributions along an EHV ceramic post insulator covered with ice-part I: simulations of a melting period". IEEE Transactions on Power Delivery. 20 (2005) 2006-2013.
- [44] A.J. Phillips, J. Kuffel, A. Baker, J. Burnham, A. Carreira, E. Cherney, et al. "Electric fields on AC composite transmission line insulators". IEEE Transactions on Power Delivery. 23 (2008) 823-830.
- [45] B. M'hamdi, M. Teguar, A. Mekhaldi. "Potential and electric field distributions on HV insulators string used in the 400 kV novel transmission line in Algeria". Solid Dielectrics (ICSD), 2013 IEEE International Conference on. IEEE2013. pp. 190-183.
- [46] Z. Aydogmus, M. Cebeci. "A new flashover dynamic model of polluted HV insulators". IEEE Transactions on Dielectrics and Electrical Insulation. 11 (2004) 577-584.
- [47] W. Sima, Q. Yang, C. Sun, F. Guo. "Potential and electric-field calculation along an ice-covered composite insulator with finite-element method". IEE Proceedings-Generation, Transmission and Distribution. 153 (2006) 343-349.
- [48] Arora R, Mosch W. "High voltage insulation engineering". Wiley-IEEE press series on power engineering. First Edition. Institute of Electrical and Electronics Engineers. Published by John Wiley & Sons, Inc. 2011.
- [49] Z. Guan, L. Wang, B. Yang, X. Liang, Z. Li. "Electric field analysis of water drop corona". IEEE Transactions on power delivery. 20 (2005) 964-969.
- [50] Y. Gu, J. Li. "Finite element analysis of the instep fatigue trauma in the high-heeled gait". World J Model Simul World Journal of Modelling and Simulation. 1(2) (2005) 117-122.
- [51] Y. Liu, C. Yu, X. Sun, J. Wang. " 3D FE model reconstruction and numerical simulation of airflow for the upper airway". Journal of Modelling and Simulation. 2 (2006) 190-195.

Ref_Chapter_I

- [1] A. Banik, S. Dalai, B. Chatterjee. "Studies the effect of equivalent salt deposit density on leakage current and flashover voltage of artificially contaminated disc insulators". Power,

Dielectric and Energy Management at NERIST (ICPDEN), 2015 1st Conference on. IEEE2015. pp. 1-5.

[2] W.H. Schwardt, J.P. Holtzhausen, W.L. Vosloo. "A comparison between measured leakage current and surface conductivity during salt fog tests [power line insulator applications] ". AFRICON, 2004 7th AFRICON Conference in Africa. IEEE2004. pp. 597-600.

[3] K. Naito. "A study on the characteristics of various conductive contaminants accumulated on high voltage insulators". IEEE Transactions on Power Delivery. 8 (1993) 1842-1850.

[4] A.S. Sidthik, L. Kalaivani, M.W. Iruthayarajan. "Evaluation and prediction of contamination level in coastal region insulators based on leakage current characteristics". Circuits, Power and Computing Technologies (ICCPCT), 2013 International Conference on. IEEE 2013. pp. 132-137.

[5] K. Naito. "A study on the characteristics of various conductive contaminants accumulated on high voltage insulators". IEEE Transactions on Power Delivery. 8 (1993) 1842-1850.

[6] Z.-j. Zhang, X. Jiang, C. Sun, J.-h. Yuan, Y.-J. Zhang. "Comparison of the AC pollution flashover characteristics of insulators under two different polluting manners". Zhongguo Dianji Gongcheng Xuebao (Proceedings of the Chinese Society of Electrical Engineering) 2006. pp. 124-127.

[7] X. Jiang, J. Hu, Y. Liang, L. Shu, S. Xie. "Pollution flashover performance of short sample for 750 kV composite insulators". Electrical Insulation, 2004 Conference Record of the 2004 IEEE International Symposium on. IEEE2004. pp. 312-315.

[8] R. Matsuoka, H. Shinokubo, K. Kondo, Y. Mizuno, K. Naito, T. Fujimura, et al. "Assessment of basic contamination withstand voltage characteristics of polymer insulators". IEEE transactions on power delivery. 11 (1996) 1895-900.

[9] H. Mohseni, A.N. Jahromi, M. Sanaye-Pasand, S.H. Jayaram, A.S. Akmal. "A method of increment short-circuit current in test of ceramic and composite polluted insulators". IEEE Transactions on Power Delivery. 22 (2007) 977-985.

[10] K.L. Chrzan, W.L. Vosloo, J.P. Holtzhausen. "Leakage current on porcelain and silicone insulators under sea or light industrial pollution". IEEE Transactions on Power Delivery. 26 (2011) 2051-2052.

[11] **H. Benguesmia**, N. M'ziou, A. Boubakeur. "AC Flashover: An analysis with influence of the pollution, potential and electric field distribution on high voltage insulator". Multiphysics Modelling and Simulation for Systems Design and Monitoring. Springer2015. pp. 269-279.

[12] N. M'ziou, **H. Bengasmia**, T. Guia. "Influence of the pollution on the flashover of high voltage insulator". Word Academy of Science Engineering and Technology, Dubai, United Arab Emirates (UAE), (2012) 1595–1597.

[13] N. M'ziou, **H. Bengasmia**, A. Boubakeur. " Influence of discontinuous pollution on the tension of flashover of an insulator of high voltage". In : 7th International Conference on Electrical Engineering. Batna, Alegria, 2012, 556–558.

- [14] N. M'ziou, **H. Bengasmia**, A. Boubakeur. "Influence of pollution of the flashover of an high voltage insulator". In : The International Conference on Electronics & Oil: from Theory to Applications. Ouargla, Algeria, (2013) pp51.
- [15] **H. Benguesmia**, N. M'ziou, A. Boubakeur. "Pollution discontinue et le contournement d'un isolateur de haute tension sous tension alternative". 1er Workshop sur la Pollution des Isolateurs des Réseaux Electriques,(POLIREL 2013), 29 avril, USTO-MB, Oran, Algérie, (2013) pp13.
- [16] **H. Benguesmia**, N. M'ziou, A. Boubakeur. "The pollution flashover on high voltage Insulators under alternatif current". The 3rd International conference on information processing and electrical engineering (ICPEE'14-ID87), 24-25 November, Tebessa, Algeria, 2014.
- [17] **H. Benguesmia**, N. M'ziou, A. Chouchou, L. Rachdi. "Experimental Study of the various pollution and simulation of potential and electric field distribution using FEMM at a high voltage insulator under alternative current". International Symposium on Computational and Experimental Investigations of Fluid and Structure Dynamics, (CEFSD2015-94), March 16-18, Hammamet, Tunisia (2015) pp144.
- [18] **H. Benguesmia**, N. M'ziou, A. Boubakeur. "Study of The pollution effect on the high voltage of the cap and pin (1512L) insulator using Comsol Multiphysics". International Conference on Mechanics and Energy, (ICME2016-114), December 22-24, Hammamet, Tunisia, (2016) pp 138.
- [19] **H. Benguesmia**, N.M'ziou, Y.Bourek, A. Kara, I.N. El ghouli. "Experimental study and simulation with COMSOL Multiphysics influence of pollution on HV insulator under AC Voltage". International Conference on Mechanics and Energy, (ICME2017-46), December 18-20, Sousse, Tunisia, (2017) pp 109.

Ref_Chapter_II

- [1] M. Sallak, F. Aguirre, W. Schon. "Incertitudes aléatoires et épistémiques, comment les distinguer et les manipuler dans les études de fiabilité? "., QUALITA, Université de Technologie de Compiègne, hal.archives-ouvertes.fr, 2013.
- [2] E.H. Mamdani, S. Assilian. "An experiment in linguistic synthesis with a fuzzy logic controller". International journal of man-machine studies. 7 (1975) 1-13.
- [3] L. Zadeh. "A Fuzzy sets. Information and control". 8(1965) 338-353.
- [4] S. Ayouni. "Etude et extraction de regles graduelles floues: définition d'algorithmes efficaces". These de doctorat, Université Montpellier. 2 (2012).
- [5] F.Dernoncourt. "Introduction to fuzzy logic". Massachusetts Institute of Technology. (2013).
- [6] P.Benoit. "la logique floue". Equipe de recherche en ingénierie des connaissances (ERICAE), Université laval, decembre (2002).

- [7] L. Baghli. "Contribution à la commande de la machine asynchrone, utilisation de la logique floue, des réseaux de neurones et des algorithmes génétiques". Université Henri Poincaré-Nancy I (1999).
- [8] C.-C. Lee. "Fuzzy logic in control systems: fuzzy logic controller. I". IEEE Transactions on systems, man, and cybernetics. 20 (1990) 404-418.
- [9] F. Chevrier, F. Guely. "Fuzzy Logic: Schneider-Electri Cahier Techniques No. 191". France: Schneider. (1998).
- [10] C. C. Lee. "Fuzzy Logic in Control Systems : Fuzzy Logic Controller, part II". IEEE Transactions on Systems, Man, and Cybernetics March/April 20 (1990) 419-435.
- [11] B.-M. Bernadette. "Logique floue, principes, aide à la décision". Lavoisier 2003.
- [12] J. Godjevac. "Idées nettes sur la logique floue". PPUR presses polytechniques 1999.
- [13] M. Sugeno, G. Kang. "Structure identification of fuzzy model". Fuzzy sets and systems. 28 (1988) 15-33.
- [14] A. Kaufmann. "Introduction à la logique floue. Ed ". Techniques Ingénieur (1999) 1-9.
- [15] Z. Abdehafid. "Etude de l'implémentation d'un contrôleur à logique floue sur une carte FPGA". International conference on systems and processing information May 12-14, Guelma, Algeria 2013.
- [16] N. Tkouti. "Optimisation des systèmes photovoltaïques connectés au réseau par la logique floue". Thèse de doctorat, Université Mohamed Khider-Biskra 2004.
- [17] O. Guenounou. "Méthodologie de conception de contrôleurs intelligents par l'approche génétique: application à un bioprocédé". Université de Toulouse III-Paul Sabatier, 2009.
- [18] N. Martaj, M. Mokhtari. "Contrôle par logique floue". MATLAB R2009, SIMULINK et STATEFLOW pour Ingénieurs, Chercheurs et Etudiants. Springer, 2010. pp. 747-805.
- [19] D. Mokeddem. "Contrôle flou des processus biotechnologiques à base d'algorithmes génétiques". Thèse de doctorat. Université de Setif 2014.
- [20] E.B. Huerta. "Logique floue et algorithmes génétiques pour le pré-traitement de données de biopuces et la sélection de gènes ". Thèse de doctorat, Université d'Angers 2008.
- [21] J.-S. Jang. "ANFIS: adaptive-network-based fuzzy inference system". IEEE transactions on systems, man, and cybernetics. 23 (1993) 665-685.
- [22] W. Wu. "Synthèse d'un contrôleur flou par algorithme génétique: application au réglage dynamique des paramètres d'un système". Thèse de doctorat, Université de Lille 1998.
- [23] B. Mohammed. "Sûreté de fonctionnement d'un système d'inférence floue avec une architecture redondante un parmi deux avec diagnostic (1oo2D) à base de FPGA". Thèse de doctorat, Université abdelmalek essaadi, Tanger, (2013).

- [24] M. Sugeno. "Industrial applications of fuzzy control". Elsevier Science Inc.1985.
- [25] T. Takagi, M. Sugeno. "Fuzzy identification of systems and its applications to modeling and control". IEEE transactions on systems, man, and cybernetics. (1985) 116-132.
- [26] M. Sugeno, G. Kang. "Structure identification of fuzzy model". Fuzzy sets and systems. 28 (1988) 15-33.
- [27] J.-S. Jang. "ANFIS: adaptive-network-based fuzzy inference system". IEEE transactions on systems, man, and cybernetics. 23 (1993) 665-685.
- [28] A. Bouzidi. "Diagnostic du cancer du sein a laide du classification fuzzy-FLR". These de doctorat, Universite de tlemcen, 2015.
- [29] S.A. Bessedik, H. Hadi. "Prediction of flashover voltage of insulators using adaptive neuro-fuzzy inference system". JEE Journal of Electric Engineering. 13 (2013).
- [30] G. Asimakopoulou, V. Kontargyri, G. Tsekouras, C.N. Elias, F. Asimakopoulou, I. Stathopoulos. "A fuzzy logic optimization methodology for the estimation of the critical flashover voltage on insulators". Electric power systems research. 81 (2011) 580-588.
- [31] K. Erenturk. "Adaptive-network-based fuzzy inference system application to estimate the flashover voltage on insulator". Instrumentation Science and Technology. 37 (2009) 446-461.
- [32] **H. Benguesmia**, N. M'Ziou, A. Boubakeur. "Experimental study of pollution effect on the behavior of high voltage insulators under alternative current". Frontiers in Energy. (2017) 1-9.
- [33] Y. Bourek. "Etude de la decharge electrique par l'intelligence artificielle". These dde doctorat, Université de Batna2, 2016.
- [34] Y. Bourek, L. Mokhnache, N.N. Said, R. Kattan. "Determination of ionization conditions characterizing the breakdown threshold of a point-plane air interval using fuzzy logic". Electric Power Systems Research. 81 (2011) 2038-2047.

Ref_Chapter_III

- [1] S. Haykin. "Neural networks: a comprehensive foundation". No.Book, Publisher: New York, Macmilan(Prentice Hall PTR) 1994.
- [2] A.S. Ahmad, P. Ghosh, S.S. Ahmed, S.A.K. Aljunid. "Assessment of ESDD on high-voltage insulators using artificial neural network". Electric Power Systems Research. 72 (2004) 131-136.
- [3] M. Ugur, D. Auckland, B. Varlow, Z. Emin. "Neural networks to analyze surface tracking on solid insulators". IEEE transactions on dielectrics and electrical insulation. 4 (1997) 763-766.
- [4] V. Kontargyri, A. Gialketsi, G. Tsekouras, I. Gonos, I. Stathopoulos. "Design of an artificial neural network for the estimation of the flashover voltage on insulators". Electric Power Systems Research. 77 (2007) 1532-1540.

- [5] F. Elie. "Conception et réalisation d'un système utilisant des réseaux de neurones pour l'identification et la caractérisation à bord de satellites de signaux transitoires de type sifflement". Thèse de doctorat, Orléans, 1997.
- [6] M. Nezar. "Diagnostic des associations convertisseurs statiques–machine asynchrone en utilisant les techniques de l'intelligence artificielle". Thèse de doctorat, Université de Batna, 2006.
- [7] Y.H. Hu, J.-N. Hwang. "Handbook of neural network signal processing". Livre ASA 2002.
- [8] M. Parizeau. "Réseaux de neurones". Cour d'université de Laval, Canada, Hiver 2006.
- [9] J. Heaton. "Introduction to neural networks with Java". 1st Edition' Heaton Research, Inc. (book), 2008.
- [10] D. Djarah. "Application des réseaux de neurones pour la gestion d'un système de perception pour un robot mobile d'intérieur". Thèse de doctorat, Université de Batna2, 2006.
- [11] Y. Bourek. "Etude de la décharge électrique par l'intelligence artificielle". Thèse de doctorat, Université de Batna2, 2016.
- [12] G. Dreyfus, J.-M. Martinez, M. Samuelides, M.B. Gordon, F. Badran, S. Thiria, et al. "Réseaux de neurones-méthodologie et applications". 2002.
- [13] A. Azadeh. "The effect of neural network parameters on the performance of neural network forecasting. Industrial Informatics". 2008 INDIN 2008 6th IEEE International Conference on. IEEE2008. pp. 1498-1505.
- [14] T. M. Hagan, H. Demuth, M. Beale. "Neural network design". Pws publishing company, Boston, vol.20, 1995.
- [15] J. Moody, C.J. Darken. "Fast learning in networks of locally-tuned processing units". Neural computation. 1 (1989) 281-294.
- [16] D. Barman, N. Chowdhury. "A method of movie business prediction using back-propagation neural network". International Journal of Information Technology and Computer Science (IJITCS). 4 (2012) 67-73.
- [17] A. Singh, P. Saxena, S. Lalwani. "A study of various training algorithms on neural network for angle based triangular problem". International Journal of Computer Applications. 71 (2013).
- [18] L. Baghli. "Contribution à la commande de la machine asynchrone, utilisation de la logique floue, des réseaux de neurones et des algorithmes génétiques". Université Henri Poincaré-Nancy I, 1999.
- [19] M.Y. Ammar. "Mise en œuvre de réseaux de neurones pour la modélisation de cinétiques réactionnelles en vue de la transposition batch/continu". Thèse de doctorat, Institut national polytechnique de Toulouse, 2007.

[20] N. Gökçe, M. Eminli. "Model-based test case prioritization using neural network classification". *Computer Science & Engineering*. 4 (2014) pp.15.

Ref_Chapter_IV

[1] **H. Benguesmia**, N. M'ziou, A. Boubakeur. "Simulation of the potential and electric field distribution on high voltage insulator using the finite element method". *Diagnostyka*. 19 (2018) 11-17.

[2] A.N. Arshad, S. McMeekin, M. Farzaneh. "Effect of pollution layer conductivity and thickness on electric field distribution along a polymeric insulator". *Comsol conference Grenoble*, 2015.

[3] V.T. Kontargyri, I.F. Gonos, I.A. Stathopoulos. "Measurement and simulation of the electric field of high voltage suspension insulators". *International Transactions on Electrical Energy Systems*. 19 (2009) 509-517.

[4] S.A. Bessedik. "Contournement des isolateurs pollués". Ph.D. thesis, Department of Electrical Engineering, University of sciences and technology in Oran, 2015.

[5] W. Sima, Q. Yang, C. Sun, F. Guo. "Potential and electric-field calculation along an ice-covered composite insulator with finite-element method". *IEE Proceedings-Generation, Transmission and Distribution*. 153 (2006) 343-349.

[6] R. Arora, W. Mosch. "High voltage and electrical insulation engineering". (book), John Wiley & Sons, vol.69, 2011.

[7] Z. Guan, L. Wang, B. Yang, X. Liang, Z. Li. "Electric field analysis of water drop corona". *IEEE Transactions on power delivery*. 20 (2005) 964-969.

[8] Y. Gu, J. Li. "Finite element analysis of the instep fatigue trauma in the high-heeled gait". *World of Journal of Modelling and Simulation*. 2 (2005) 117-122.

[9] Y. Liu, C. Yu, X. Sun, J. Wang. "3D FE model reconstruction and numerical simulation of airflow for the upper airway". *Journal of Modelling and Simulation*. 2 (2006) 190-195.

[10] C. Muniraj, S. Chandrasekar. "Finite element modeling for electric field and voltage distribution along the polluted polymeric insulator". *Journal of Modelling and Simulation*. 8(2012) 310-320.

[11] D.Meeker. "Finite element method magnetics--". *Version 4.2 User's Manual*, September 22. (2006).

[12] E. Nicolopoulou, E. Gralista, V. Kontargyri, I. Gonos, I. Stathopoulos. "Electric field and voltage distribution around composite insulators". *XVII International Symposium on High Voltage Engineering*, Hannover, Germany, 2011.

[13] B. M'hamdi. "Amelioration des performances des chaînes d'isolateurs de haute tension". Ph.D. thesis in Sciences, Department of Electrical Engineering, Ecole Nationale Polytechnique, Algiers, 2016.

- [14] C. Volat, M. Farzaneh. "Three-dimensional modeling of potential and electric-field distributions along an EHV ceramic post insulator covered with ice-part I: simulations of a melting period". IEEE Transactions on Power Delivery. 20 (2005) 2006-2013.
- [15] S. Bessedik, H. Hadi. "Dynamic arc model of the flashover of the polluted insulators". Electrical Insulation and Dielectric Phenomena (CEIDP), 2011 Annual Report Conference on. IEEE2011. pp. 550-554.
- [16] **H. Benguesmia**, N. M'ziou, A. Boubakeur. "Study of the pollution effect on the high voltage of the cap and pin (1512L) insulator using Comsol Multiphysics". International Conference on Mechanics and Energy, (ICME2016-114), December 22-24, Hammamet, Tunisia, (2016) pp. 138.
- [17] H. Terrab, A. Bayadi. "Experimental study using design of experiment of pollution layer effect on insulator performance taking into account the presence of dry bands". IEEE Transactions on Dielectrics and Electrical Insulation. 21 (2014) 2486-2495.
- [18] H. El-Kishky, R. Gorur. "Electric potential and field computation along ac HV insulators". IEEE Transactions on Dielectrics and Electrical Insulation. 1 (1994) 982-990.
- [19] J. Andrew, A.J. Phillips, J. Kuffel, A. Baker, J. Burnham, A. Carreira, E. Cherney, et al. "Electric fields on AC composite transmission line insulators". IEEE Transactions on Power Delivery. 23 (2008) 823-830.
- [20] B. M'hamdi, M. Teguvar, A. Mekhaldi. "Potential and electric field distributions on HV insulators string used in the 400 kV novel transmission line in Algeria". Solid Dielectrics (ICSD), 2013 IEEE International Conference on. IEEE2013. pp. 190-193.
- [21] **H. Benguesmia**, N. M'ziou, A. Boubakeur. "AC Flashover: An analysis with influence of the pollution, potential and electric field distribution on high voltage insulator". Multiphysics Modelling and Simulation for Systems Design and Monitoring. Springer2015. pp. 269-279.
- [22] **H. Benguesmia**, N. M'ziou, A.M. Chouchou, L. Rachdi. "Experimental study of the various pollution and simulation of potential and electric field distribution using FEMM at a high voltage insulator under alternative current". International Symposium on Computational and Experimental Investigations of Fluid and Structure Dynamics, (CEFSD2015-94), Hammamet, Tunisia, March 16-18, (2015) pp144.
- [23] E.-S.M. El-Refaie, M.A. Elrahman, M.K. Mohamed. "Electric field distribution of optimized composite insulator profiles under different pollution conditions". Ain Shams Engineering Journal, (2016).
- [24] V. Moreno, R. Gorur. "Impact of corona on the long-term performance of nonceramic insulators". IEEE transactions on dielectrics and electrical insulation. 10 (2003) 80-95.
- [25] N. M'ziou, **H. Bengasmia**, T. Guia. "Influence of the pollution on the flashover of high voltage insulator". Word Academy of Science Engineering and Technology, Dubai, January (2012)1595-1597.

- [26] **H. Benguesmia**, N. M'ziou, A. Boubakeur. "Influence de la pollution discontinue sur la tension de contournement d'un isolateur de haute tension". 7th International Conference on Electrical Engineering, Batna, Alegria, October, 8- 10. (2012) pp 556-558.
- [27] **H. Benguesmia**, N. M'ziou, A. Boubakeur. "Influence de la pollution sur le contournement d'un isolateur de haute tension". The International Conference on Electronics & Oil: from Theory to Applications, Ouargla, Algeria, proceeding, March (2013) pp 51.
- [28] N. M'ziou, **H. Benguesmia**, A. kara, H. Rahali, I.N. EL ghouli. "Simulation of an insulator model of HV using COMSOL Multiphysics software under alternative current". International Conference on Mechanics and Energy, (ICME2017-45), December 18-20, Sousse, Tunisia, (2017) pp 108.
- [29] **H. Benguesmia**, N.M'ziou, Y.Bourek, A. Kara, I.N. El ghouli. "Experimental study and simulation with COMSOL Multiphysics influence of pollution on HV insulator under AC voltage". International Conference on Mechanics and Energy, (ICME2017-46), December 18-20, Sousse, Tunisia, (2017) pp 109.
- [30] A. Nekahi, S. McMeekin, M. Farzaneh. "Effect of pollution severity on electric field distribution along a polymeric insulator". Properties and Applications of Dielectric Materials (ICPADM), 2015 IEEE 11th International Conference on the. IEEE2015. pp. 612-615.